THE QUARTERLY JOURNAL OF MECHANICS AND APPLIED MATHEMATICS

VOLUME IV
1951

OXFORD
AT THE CLARENDON PRESS

Oxford University Press, Amen House, London E.C. 4
GLASGOW NEW YORK TORONTO MELBOURNE WELLINGTON
BOMBAY CALCUTTA MADRAS CAPE TOWN
Geoffrey Cumberlege, Publisher to the University

PRINTED IN GREAT BRITAIN
AT THE UNIVERSITY PRESS, OXFORD
BY CHARLES BATEY, PRINTER TO THE UNIVERSITY

RR

THE QUARTERLY JOURNAL OF MECHANICS AND APPLIED MATHEMATICS

VOLUME IV PART 1

MARCH 1951

OXFORD
AT THE CLARENDON PRESS
1951

Price 12*s*. 6*d*. *net*

PRINTED IN GREAT BRITAIN BY CHARLES BATEY AT THE UNIVERSITY PRESS, OXFORD

THE QUARTERLY JOURNAL OF MECHANICS AND APPLIED MATHEMATICS

THE QUARTERLY JOURNAL OF MECHANICS AND APPLIED MATHEMATICS is published at 12*s.* 6*d.* net for a single number with an annual subscription (for four numbers) of 40*s.* post free.

NOTICE TO CONTRIBUTORS

1. *Communication.* Papers should be communicated to one or other of the Executive Editors, by name, at King's College, Strand, London, W.C. 2.

2. *Presentation.* Manuscripts should preferably be typewritten, and each paper should be preceded by a summary not exceeding 300 words in length. References to literature should be given in standard order, *author, title of journal, volume number, date, page.* These should be placed at the end of the paper and arranged according to the order of reference in the paper.

3. *Diagrams.* The number of diagrams should be kept to the minimum consistent with clarity. The lines of the figures should be drawn in ink either on draughtsman's paper or on good quality white paper. Each individual line in the figure should bear reducing to one-half of the size of the original, and great care should be exercised to see that the lines are regular in thickness, especially where they meet. Lettering of the figure should be in pencil and should be sufficient to define clearly the lines and curves in it. The writing of formulae or of explanations on the diagram itself should be avoided. All explanations of symbols, etc., should be given in underline. Contributors should indicate on their manuscripts where figures should be inserted.

4. *Tables.* Tables should preferably be arranged so that they can be printed with the columns parallel to the longer edge of the page.

5. *Notation.* All single letters used to denote vectors in the manuscript should be marked by underlining with a wavy line. Scalar and vector products should be denoted by $\underset{\sim}{a}.\underset{\sim}{b}$ and $\underset{\sim}{a} \wedge \underset{\sim}{b}$ respectively. Real and imaginary parts of complex quantities should be denoted by re and im respectively.

6 *Offprints.* Authors of papers will be entitled to 25 free offprints. This number is available for sharing between authors of joint papers.

7. All correspondence other than that dealing with contributions should be addressed to the Publisher:

GEOFFREY CUMBERLEGE
OXFORD UNIVERSITY PRESS
AMEN HOUSE, LONDON, E.C. 4

S

is
on

ve

ld
re
ve.
of

th
er
ng
he
ld
he
All
li-

he

ld
be
es

is

ed

(Ph

Th
bour
on th
it is
the l
nam
first
valu

1. I

Som
effe
by e
infir
He
aero
simp
ing
com
for
touc
tion
mon
and
0·09
valu
thar
denc
the

Th
from

† T
not p

[Qu
50

THE LIFT AND MOMENT ACTING ON A CIRCULAR-ARC AEROFOIL IN A STREAM BOUNDED BY A PLANE WALL†

By S. TOMOTIKA, K. TAMADA, *and* H. UMEMOTO
(*Physical Institute, Faculty of Science, University of Kyoto, Kyoto, Japan*)

[Received 25 July 1950]

SUMMARY

The lift and moment of an aerofoil in the form of a circular arc placed in a stream bounded by a plane wall are discussed. The earlier work of Green (**1**) and Hudimoto (**7**) on this problem is reviewed and by adopting a method similar to that of Hudimoto it is found that when the camber of the aerofoil is small the effect of the wall on the lift and moment is similar to that for an aerofoil in the form of a flat plate, namely, as the arc-aerofoil approaches the wall the lift and moment coefficients first decrease and then increase to values which are greater than the corresponding values for an arc-aerofoil in an unlimited stream.

1. Introduction

Some years ago, Green (**1**) investigated the manner in which the ground effect upon the lift and moment of an aerofoil is modified by its camber, by evaluating the forces acting on a circular-arc aerofoil placed in a semi-infinitely extended stream in any position near the bounding plane wall. He performed a few numerical calculations for a particular circular-arc aerofoil with camber approximately equal to 0·097 in the comparatively simple cases when the centre of the circular-arc aerofoil lies on the bounding wall and when the circle on which the arc lies touches the wall. By combining his results with the previous results obtained by one of us (**2**, **3**) for a limiting case in which the trailing edge of the circular-arc aerofoil touches the wall, Green has indicated the general nature of the modification introduced by the camber on the ground effect upon the lift and moment forces acting on an aerofoil. He was led to suppose that the lift and moment coefficients of a circular-arc aerofoil (with camber equal to 0·097) are probably always decreased by the presence of the wall for all values of the ratio l/H and for all values of the angle of incidence α less than 85° (including the small values which occur in practice), where l denotes the chord of the aerofoil and H the distance of the midpoint of the chord from the wall.

These results differ from those for a flat plate (plane aerofoil) and also from experiment (except when the distance of the aerofoil from the ground

† This paper was completed by the end of March 1942. Publication at that time was not possible, however.

is large). In previous papers (**4**, **5**, **6**), one of the present writers has shown that for small values of the angle of incidence α (e.g. $\alpha = 5^\circ$, 10°), as the flat plate approaches the wall, the lift coefficient first decreases and then increases to values which are greater than the values for a flat plate in an unlimited stream and that similar results also hold for the moment coefficient.

A flat plate is evidently the limiting form of a circular-arc aerofoil whose camber tends to zero. It seems therefore probable that the results for an aerofoil in the form of a circular arc with a camber smaller than that considered by Green will differ from his results, but will be somewhat similar to those for a flat plate. Thus, in order to determine the true nature of the effect of the wall upon the lift and moment acting on a circular-arc aerofoil, it is desirable to extend the investigation to cases of aerofoils with fairly small camber; and the principal object of the present paper is to present the results of our detailed numerical calculations.

We have reinvestigated the problem *ab initio* by employing suitable conformal transformations, which are somewhat different from those used by Green. The analysis we have developed is similar to that given in a paper by Hudimoto (**7**), who has also discussed the effect of the ground upon the lift and moment of a circular-arc aerofoil. His results for one special case† are similar to Green's, namely that the lift coefficient of the circular-arc aerofoil is decreased by the presence of the ground.‡

The final expressions obtained by Hudimoto for the lift and moment are unfortunately inelegant and complicated. However, we have been able to obtain the general formulae for the lift and moment in fairly elegant forms, as in Green's paper, although we have employed a method of analysis similar to Hudimoto's.

We have carried out detailed numerical calculations for three circular-arc aerofoils, the cambers of which are respectively 0·022, 0·053, and 0·097 approximately, the value of the angle of incidence α being taken to be 5° in all cases, and for values of the ratio l/H between 0 and 22·95.§

Thus it has been found that when the camber is sufficiently small and the angle of incidence is also fairly small, as in practice, the manner in which the lift and moment coefficients of a circular-arc aerofoil are affected by the presence of the wall is similar to that for the case of a flat plate: namely, as the circular-arc aerofoil approaches the wall, the lift coefficient first decreases and then increases to values which are greater than the

† In his numerical calculations a circular-arc aerofoil with camber equal to 0·115 was placed at an angle of incidence $17^\circ\ 2{\cdot}28'$ and the value of the ratio l/H was 0·885.

‡ No numerical discussions on the moment have been made by Hudimoto.

§ The latter value 22·95 corresponds to the limiting case when the trailing edge of the arc touches the wall.

values for the circular-arc aerofoil in an unlimited stream. Similar results hold also for the moment coefficient.

2. The conformal transformations

Taking the plane of the fluid motion (assumed to be two-dimensional) as the z-plane, we consider a steady irrotational flow of an incompressible inviscid fluid past a circular-arc aerofoil, AA', placed in any position near an infinite plane wall HH', and such that the circle on which the arc

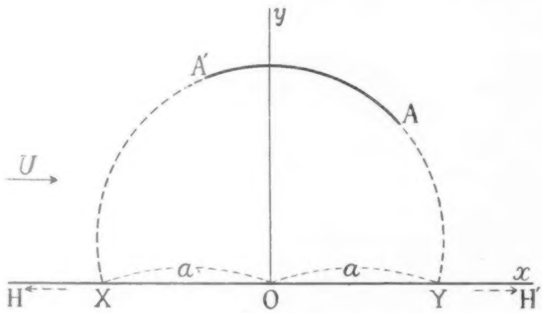

FIG. 1.

aerofoil AA' lies intersects the bounding wall at two real points X and Y (Fig. 1).

The complex velocity potential for the flow under discussion will be determined by using certain conformal transformations introduced by Hudimoto. We take the origin O of the z-plane to be the midpoint of the join of the intersections X and Y, and we take the real x-axis along the wall HH', while the arc-aerofoil is assumed to lie in the upper half of the z-plane.

Denoting by a the length of OX and OY, we transform the z-plane on to an f-plane by the transformation

$$f = \log\frac{z-a}{z+a}. \tag{1}$$

The upper half of the z-plane is then transformed into an infinitely long strip of breadth π parallel to the real axis of the f-plane, one side of the strip coinciding with the real axis of the f-plane. The points X and Y in the z-plane correspond to the point at infinity in the f-plane, while the point at infinity in the z-plane is transformed into the origin of the f-plane. Further, the circular arc AA' is transformed into a straight line-segment denoted as AA' parallel to the real axis. The f-plane is shown in Fig. 2.

Next, by making a cut along $CGG'C'$, as shown in Fig. 2, where both CG and $C'G'$ pass through the midpoint M of AA' and are perpendicular

to the real axis, we transform the f-plane on to the upper half of a t-plane (Fig. 3) by the method of Schwarz–Christoffel. The transformation is

$$\frac{df}{dt} = M\frac{t^2-b^2}{(t^2-h^2)\sqrt{\{(t^2-c^2)(t^2-g^2)\}}}, \tag{2}$$

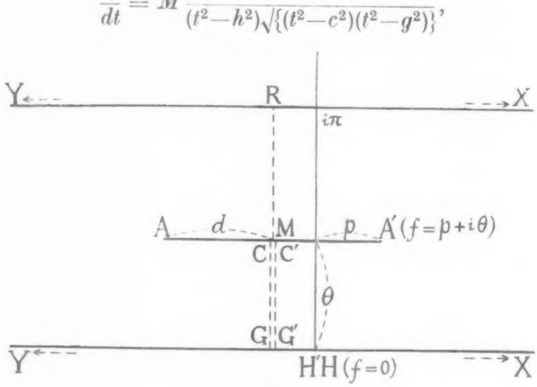

FIG. 2. f-plane.

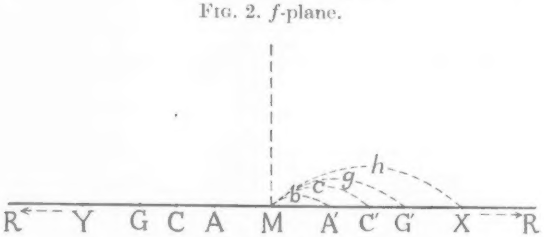

FIG. 3. t-plane.

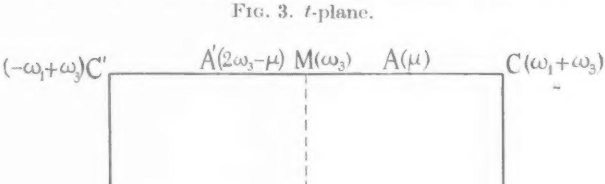

FIG. 4. s-plane.

where M is a certain constant which will be determined presently, while b, c, g, h are all real constants and the points $t = b$, $-b$, c, $-c$, g, $-g$, h, and $-h$ correspond to A', A, C', C, G', G, X, and Y respectively.

Lastly, by introducing Weierstrass's $\wp$ function with periods $2\omega_1$, $2\omega_3$, where ω_1 and ω_3/i are real and positive, we conformally transform the

upper half of the t-plane into a rectangle of sides $2\omega_1$ and ω_3/i in an s-plane by the relation

$$t^2 = \wp(s)-e_3. \tag{3}$$

The points $A, A', C, C', G, G', X, Y, M, R$ now correspond to $s = \mu, -\bar{\mu}, \omega_1+\omega_3, -\omega_1+\omega_3, \omega_1, -\omega_1, -\nu, \nu, \omega_3, 0$ respectively, while both the points H, H' correspond to the same point $s = s_0$, say (Fig. 4).

3. Now, from (2) and (3) we have

$$\begin{aligned}\frac{df}{ds} &= M\frac{\wp(s)-\wp(\mu)}{\wp(s)-\wp(\nu)}\\ &= M\frac{\wp(\nu)-\wp(\mu)}{\wp'(\nu)}[\zeta(\mu+\nu)-\zeta(\mu-\nu)-\zeta(s+\nu)+\zeta(s-\nu)].\end{aligned} \tag{4}$$

This differential equation can be integrated to give

$$f = M\frac{\wp(\nu)-\wp(\mu)}{\wp'(\nu)}\left[\{\zeta(\mu+\nu)-\zeta(\mu-\nu)\}s-\log\frac{\sigma(s+\nu)}{\sigma(s-\nu)}+C\right], \tag{5}$$

where C is an integration constant to be determined presently, and $\sigma(s)$ is the Weierstrass sigma function.

Since the function f is continuous along the cut $CGG'C'$ artificially made in Fig. 2, it must necessarily have a period $2\omega_1$; thus the function f must satisfy the relation $f(s+2\omega_1) = f(s)$, and this condition gives immediately a relation between the constants μ and ν in the form:

$$\zeta(\mu+\nu)-\zeta(\mu-\nu) = 2\eta_1\nu/\omega_1, \tag{6}$$

where, as usual, $\eta_1 = \zeta(\omega_1)$.

Again, since the values of f at R ($s = 0$) and at G ($s = \omega_1$) differ by $i\pi$, we have

$$f_G-f_R = f(\omega_1)-f(0) = \int_0^{\omega_1}(df/ds)\,ds = -i\pi.$$

Thus, integrating the function df/ds from $s = 0$ to $s = \omega_1$, bearing in mind that the point $s = \nu$ is a simple pole of the function df/ds and taking (6) into account, we get

$$M = \frac{\wp'(\nu)}{\wp(\nu)-\wp(\mu)}. \tag{7}$$

Combining this result with (6), the expression for f can be written in the form

$$f = \frac{2\eta_1\nu}{\omega_1}s-\log\frac{\sigma(s+\nu)}{\sigma(s-\nu)}+C. \tag{8}$$

The constant C on the right-hand side can be determined by the condition that the points H, H' correspond to $f = 0$ in the f-plane and to $s = s_0$ in the s-plane. We thus have

$$C = -\frac{2\eta_1\nu}{\omega_1}s_0+\log\frac{\sigma(s_0+\nu)}{\sigma(s_0-\nu)},$$

and on substituting this value of C in (8), we have ultimately the expression for f in the form

$$f = \frac{2\eta_1\nu}{\omega_1}(s-s_0) - \log\frac{\sigma(s+\nu)\sigma(s_0-\nu)}{\sigma(s-\nu)\sigma(s_0+\nu)}$$

$$= \log\frac{\vartheta_1\{\frac{1}{2}(s-\nu)/\omega_1\}\vartheta_1\{\frac{1}{2}(s_0+\nu)/\omega_1\}}{\vartheta_1\{\frac{1}{2}(s+\nu)/\omega_1\}\vartheta_1\{\frac{1}{2}(s_0-\nu)/\omega_1\}}. \tag{9}$$

4. Denote by θ the angle which the chord XY subtends at any point of the arc AA' in Fig. 1. Then the complex coordinate of the point A' in the f-plane may be written as $f_{A'} = p+i\theta$, where p denotes the distance of A' from the imaginary axis of the f-plane (see Fig. 2). Also, we denote by $2d$ the distance between the two points A and A'. These three quantities θ, p, and d can be expressed in terms of μ, ν, and s_0 as follows.

Firstly, since the values of f at C ($s = \omega_1+\omega_3$) and at G ($s = \omega_1$) differ by $i\theta$, we have

$$f_C - f_G = f(\omega_1+\omega_3) - f(\omega_1) = i\theta,$$

and when use is made of the second expression for f in (9), this condition gives immediately

$$\theta = \pi\nu/\omega_1. \tag{10}$$

Next, since the distance between the points A and A' is equal to $2d$ and M is the midpoint of the segment AA', the values of f at $s = \omega_3$ and at $s = \mu$ evidently differ by d. We therefore have

$$f_M - f_A = f(\omega_3) - f(\mu) = d,$$

and this condition gives

$$d = \log\frac{\vartheta_1(\frac{1}{2}\tau - \frac{1}{2}\nu/\omega_1)\vartheta_1\{\frac{1}{2}(\mu+\nu)/\omega_1\}}{\vartheta_1(\frac{1}{2}\tau + \frac{1}{2}\nu/\omega_1)\vartheta_1\{\frac{1}{2}(\mu-\nu)/\omega_1\}}, \tag{11}$$

where, as usual, $\tau = \omega_3/\omega_1$.

This expression for d can be greatly simplified, however, if we make use of the well-known properties of theta functions. In fact, putting

$$\mu = m+\omega_3, \tag{12}$$

where m is real, we have

$$d = \log\frac{\vartheta_4\{\frac{1}{2}(m+\nu)/\omega_1\}}{\vartheta_4\{\frac{1}{2}(m-\nu)/\omega_1\}}. \tag{13}$$

Also, bearing in mind that the value of f at the point A', which corresponds to $s = -\bar{\mu}$ in the s-plane, is given by $f_{A'} = p+i\theta$ we have from (10), (12), and (13),

$$p+i\theta = \log\frac{\vartheta_1\{\frac{1}{2}\tau - \frac{1}{2}(m+\nu)/\omega_1\}\vartheta_1\{\frac{1}{2}(s_0+\nu)/\omega_1\}}{\vartheta_1\{\frac{1}{2}\tau - \frac{1}{2}(m-\nu)/\omega_1\}\vartheta_1\{\frac{1}{2}(s_0-\nu)/\omega_1\}}$$

$$= i\theta + d + \log\frac{\vartheta_1\{\frac{1}{2}(s_0+\nu)/\omega_1\}}{\vartheta_1\{\frac{1}{2}(s_0-\nu)/\omega_1\}},$$

from which we obtain

$$p-d = \log\frac{\vartheta_1\{\frac{1}{2}(s_0+\nu)/\omega_1\}}{\vartheta_1\{\frac{1}{2}(s_0-\nu)/\omega_1\}}. \tag{14}$$

Further, for convenience we shall rewrite the relation (6) in terms of theta functions, using (12). We then have

$$\frac{\vartheta_4'\{\frac{1}{2}(m+\nu)/\omega_1\}}{\vartheta_4\{\frac{1}{2}(m+\nu)/\omega_1\}} = \frac{\vartheta_4'\{\frac{1}{2}(m-\nu)/\omega_1\}}{\vartheta_4\{\frac{1}{2}(m-\nu)/\omega_1\}}. \tag{15}$$

From the given geometrical properties of the circular-arc aerofoil AA', we first calculate the values of the three quantities θ, p, and d, using certain relations which connect these three quantities with geometrical parameters defining the circular arc. This will be discussed subsequently. The values of the three quantities m, ν, and s_0 can then be found by solving equations (10), (13), and (14), while equation (15) determines the value of the parameter q $(= \exp(\tau\pi i))$ for the elliptic functions as well as for the theta functions used here.

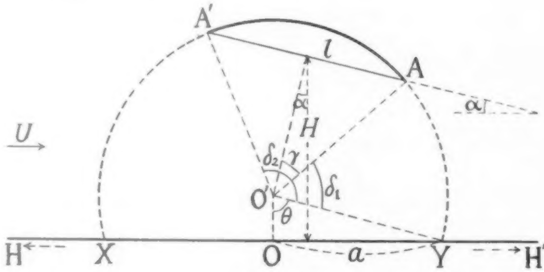

FIG. 5.

5. Geometrical parameters defining the circular-arc aerofoil

We are now in a position to consider the geometrical parameters defining the circular-arc aerofoil AA'. Referring to Fig. 5, let l be the length of the chord AA', R the radius of the arc AA', 2γ the angle which the arc AA' subtends at its centre O', and H the distance of the midpoint of the chord AA' from the bounding wall. Further, let α be the acute angle which the chord AA' of the aerofoil makes with the wall. Then α is the angle of incidence of the aerofoil when the fluid flows in the positive direction of the x-axis. Since θ denotes the angle which the chord XY subtends at any point on the arc AA', both the angles $XO'O$ and $YO'O$ are evidently equal to θ.

Further, remembering that $OX = OY = a$, we have the following obvious relations:

$$R\sin\theta = a, \qquad R\sin\gamma = \tfrac{1}{2}l.$$

from which we get

$$a = \tfrac{1}{2}l\frac{\sin\theta}{\sin\gamma}, \qquad R = \frac{a}{\sin\theta} = \tfrac{1}{2}l\frac{1}{\sin\gamma}. \tag{16}$$

Also, it is easily seen that

$$H = R(\cos\theta+\cos\alpha\cos\gamma), \tag{17}$$

and the maximum height of the circular arc AA' is equal to $R(1-\cos\gamma)$.

Thus, the so-called camber σ of the arc-aerofoil, which is defined as usual by the ratio of its maximum height to the chord length l, is given by

$$\sigma = \frac{R(1-\cos\gamma)}{l} = \frac{1-\cos\gamma}{2\sin\gamma} = \tfrac{1}{2}\tan\tfrac{1}{2}\gamma, \tag{18}$$

and the ratio l/H becomes

$$\frac{l}{H} = \frac{2\sin\gamma}{\cos\theta+\cos\alpha\cos\gamma}. \tag{19}$$

Next, consider the expression for the distance $2d$ between the two points A and A' in the f-plane. Let the complex coordinates of these points be denoted, as before, by f_A and $f_{A'}$ respectively, and let those of the corresponding points in the z-plane be denoted by z_A and $z_{A'}$ respectively. Then, bearing in mind that the f- and z-planes are connected by the relation (1), we have

$$2d = f_{A'}-f_A = \log\frac{(z_A+a)(z_{A'}-a)}{(z_A-a)(z_{A'}+a)},$$

and after some reduction we have ultimately

$$d = \tfrac{1}{2}\log\frac{\cos\alpha+\cos(\theta-\gamma)}{\cos\alpha+\cos(\theta+\gamma)}. \tag{20}$$

Further, since $f_{A'} = p+i\theta$, we have

$$p = f_{A'}-i\theta = \log\frac{z_{A'}-a}{z_{A'}+a}-i\theta,$$

and therefore
$$p-d = \tfrac{1}{2}\log\frac{(z_A-a)(z_{A'}-a)}{(z_A+a)(z_{A'}+a)}-i\theta.$$

After some reductions we get the expression for $p-d$ in the form:

$$p-d = \tfrac{1}{2}\log\frac{\cos\gamma+\cos(\theta+\alpha)}{\cos\gamma+\cos(\theta-\alpha)}. \tag{21}$$

Combining (20) and (21) with (13) and (14) we have ultimately

$$\left.\begin{aligned}\frac{\vartheta_4\{\frac{1}{2}(m+\nu)/\omega_1\}}{\vartheta_4\{\frac{1}{2}(m-\nu)/\omega_1\}} &= \left\{\frac{\cos\alpha+\cos(\theta-\gamma)}{\cos\alpha+\cos(\theta+\gamma)}\right\}^{\frac{1}{2}},\\ \frac{\vartheta_1\{\frac{1}{2}(s_0+\nu)/\omega_1\}}{\vartheta_1\{\frac{1}{2}(s_0-\nu)/\omega_1\}} &= \left\{\frac{\cos\gamma+\cos(\theta+\alpha)}{\cos\gamma+\cos(\theta-\alpha)}\right\}^{\frac{1}{2}},\end{aligned}\right\} \tag{22}$$

and if the values of α, γ, and l/H (or θ) are given, then these two equations, together with equations (10) and (15), determine the values of m, ν, s_0, and q.

6. The complex velocity potential

We shall now obtain the complex velocity potential for a steady irrotational continuous flow of an incompressible inviscid fluid past the circular-arc aerofoil AA' placed in the neighbourhood of the wall HH' (Fig. 1). We assume that the fluid at infinity flows with constant velocity U from left

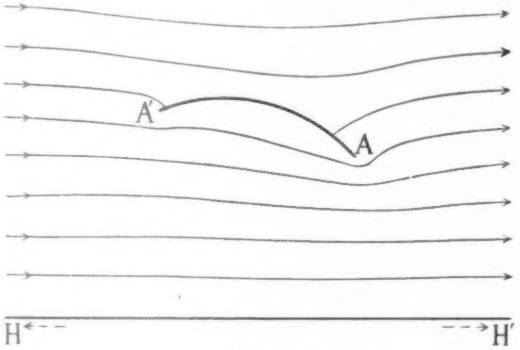

FIG. 6.

to right, i.e. in the positive direction of the x-axis. Also, we assume for the present that the circulation round the aerofoil is zero. Then the flow pattern will become as shown schematically in Fig. 6.

Let w_1 be the complex velocity potential for the flow under consideration. Then, in the z-plane the conjugate complex velocity dw_1/dz is everywhere finite except at the two edges A and A' of the arc, where, as will be seen later, it becomes infinite.

If now we transform the z-plane on to the f-plane (Fig. 2), then as we have seen the point $z = \infty$ is transformed to the origin of the f-plane, and on taking account of the obvious relation

$$dw_1/df = (dw_1/dz)(dz/df),$$

together with an expansion

$$dz/df = 2a/f^2 + \text{positive integral powers of } f,$$

(which follows immediately from (1) on assuming f to be very small) it is readily seen that the origin $f = 0$ becomes a singular point of the flow in the f-plane.

On the other hand, the two poles at the leading and trailing edges of the arc-aerofoil are transformed respectively to the ends A' and A of the line-segment AA' of the f-plane, and it can easily be shown that these points are still the poles of the function dw_1/df.

Also, it is readily seen from (1) that $(dz/df)_{z=\pm a}=0$, and remembering also that $f=\infty$ corresponds to the points X $(z=-a)$ and Y $(z=a)$ in the z-plane, we have $(dw_1/df)_{f=\infty}=0$. The flow pattern in the f-plane is shown schematically in Fig. 7.

If we further transform the f-plane on to the s-plane, the pole at $f=0$ (H, H') is transformed to the point $s=s_0$. However, since it is readily seen from (4) that $df/ds=0$ when $s=\mu$ and $s=-\bar{\mu}$, the function dw_1/ds has no longer poles at the points A and A', but is rather finite and

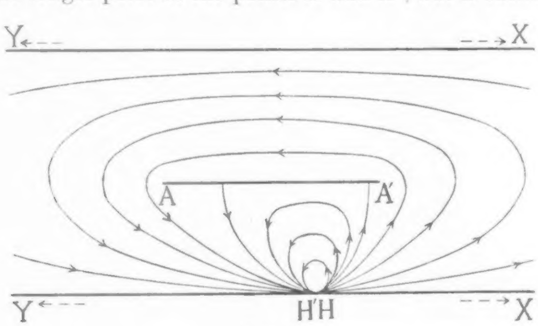

FIG. 7.

regular there. Furthermore, in spite of the fact that $(dw_1/df)_{f=\infty}=0$, dw_1/ds is finite and regular at the points X and Y, since $(df/ds)_{s=\pm\nu}=\infty$ as will be seen from (4).

Thus the conjugate complex velocity dw_1/ds in the s-plane is everywhere finite inside the rectangle except at the point $s=s_0$ where it has a pole of certain order.

We shall now consider the order of a single pole at $s=s_0$ of the function dw_1/ds. First, we have

$$\frac{dw_1}{ds}=\frac{dw_1}{dz}\frac{dz}{df}\frac{df}{ds}=\frac{dw_1}{dz}\frac{dz}{df}\left(\frac{df}{ds}\right)^2\frac{ds}{df}.$$

Since the velocity of the undisturbed uniform flow at infinity in the z-plane has been denoted by U, we have $(dw_1/dz)_{z=\infty}=U$. Also, as shown previously, we have

$$dz/df=2a/f^2+\text{positive integral powers of } f,$$

while equation (9) gives immediately

$$f=\alpha(s-s_0)+\beta(s-s_0)^2+\ldots\quad(\alpha\neq0).$$

Therefore, remembering that $z=\infty$ corresponds to $f=0$ as well as to $s=s_0$, we have

$$\frac{dz}{df}\left(\frac{df}{ds}\right)^2=2a\left(\frac{1}{f}\frac{df}{ds}\right)^2+\ldots=\frac{2a}{(s-s_0)^2}+\ldots,$$

and consequently, when s tends to s_0,

$$\frac{dw_1}{ds} = \frac{2aU}{(s-s_0)^2}\left(\frac{ds}{df}\right)_{s=s_0} + \text{positive integral powers of } (s-s_0). \tag{23}$$

Since, however, $(ds/df)_{s=s_0}$ is finite, we find ultimately that the function dw_1/ds has a pole of the second order at $s = s_0$.

Further, dw_1/ds must be real on both the lower and upper sides (GG' and CC') of the rectangle in the s-plane, which correspond respectively to the rigid plane wall and the arc aerofoil in the z-plane. Hence, it is seen, by Schwarz's principle of reflection, that dw_1/ds must have a period $2\omega_3$. Moreover, it is readily seen that the said function dw_1/ds must have one more period $2\omega_1$, since it takes the same values at any corresponding points on the two sides CG and $C'G'$.

Thus we find that dw_1/ds is a doubly-periodic function with periods $2\omega_1$, $2\omega_3$ having a pole of the second order at the point $s = s_0$. Such a function can, however, be uniquely expressed by using Weierstrass's $\wp$ function with periods $2\omega_1$, $2\omega_3$ having a pole at $s = s_0$. We thus have

$$dw_1/ds = w_s\,\wp(s-s_0)+C_1, \tag{24}$$

where w_s and C_1 are constants which can be determined as follows.

Firstly, the constant C_1 can be determined from the condition of no circulation round the aerofoil, which can be expressed in the form

$$\int_{-\omega_1+\omega_3}^{\omega_1+\omega_3} (dw_1/ds)\,ds = 0.$$

Inserting the expression (24) for dw_1/ds in the integrand and performing the integration we have

$$C_1 = w_s\,\eta_1/\omega_1.$$

Thus the expression for dw_1/ds becomes

$$dw_1/ds = w_s\{\wp(s-s_0)+\eta_1/\omega_1\}. \tag{25}$$

Next, the constant w_s can be determined by comparing the expansion (23) for dw_1/ds with that for (25). From (25) we have

$$\frac{dw_1}{ds} = \frac{w_s}{(s-s_0)^2} + \text{positive integral powers of } (s-s_0). \tag{26}$$

and hence it is easily found that

$$w_s = 2aU(ds/df)_{s=s_0}. \tag{27}$$

However, we have from (8)

$$\begin{aligned}\frac{df}{ds} &= \frac{2\eta_1\nu}{\omega_1} - \zeta(s+\nu)+\zeta(s-\nu)\\ &= \frac{1}{2\omega_1}\left[\frac{\vartheta_1'\{\frac{1}{2}(s-\nu)/\omega_1\}}{\vartheta_1\{\frac{1}{2}(s-\nu)/\omega_1\}} - \frac{\vartheta_1'\{\frac{1}{2}(s+\nu)/\omega_1\}}{\vartheta_1\{\frac{1}{2}(s+\nu)/\omega_1\}}\right].\end{aligned}$$

Thus the expression for w_s becomes ultimately

$$w_s = 4aU\omega_1 \left[\frac{\vartheta_1'\{\frac{1}{2}(s_0-\nu)/\omega_1\}}{\vartheta_1\{\frac{1}{2}(s_0-\nu)/\omega_1\}} - \frac{\vartheta_1'\{\frac{1}{2}(s_0+\nu)/\omega_1\}}{\vartheta_1\{\frac{1}{2}(s_0+\nu)/\omega_1\}} \right]^{-1}. \tag{28}$$

The flow pattern in the s-plane is shown schematically in Fig. 8.

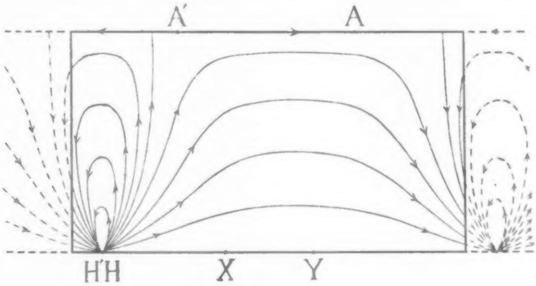

FIG. 8.

7. From the relation

$$\frac{dw_1}{dz} = \frac{dw_1}{ds}\frac{ds}{df}\frac{df}{dz},$$

and by taking into account the results that ds/df is infinite at $s = \mu$ and at $s = -\bar{\mu} = 2\omega_3 - \mu$, while dw_1/ds is in general finite there, and that df/dz is also finite at the corresponding points A and A', we find that for the flow with complex potential w_1 so far discussed, and for which there is no circulation round the arc-aerofoil AA', the fluid velocity becomes infinite at its two ends A and A'. In order to avoid the infinite fluid velocity at the trailing edge A of the aerofoil, we superpose on the above flow a rotational flow of circulation κ round the circular arc, choosing κ so that, as usual, the fluid velocity at the trailing edge becomes finite. The fluid will then leave the trailing edge smoothly.

We assume that the circulation κ round the arc-aerofoil in the z-plane takes place in the clockwise sense, as would be the case if the aerofoil is placed in the stream as shown in Fig. 1. It is evident that this circulating flow becomes, when transformed to the s-plane, a uniform flow parallel to the negative direction of the real axis. The complex velocity potential for this circulating flow, which satisfies the boundary conditions, is therefore given by

$$w_2 = -C_2 s. \tag{29}$$

The corresponding conjugate complex velocity becomes

$$dw_2/ds = -C_2, \tag{30}$$

where C_2 is a positive constant.

In the general case when there is circulation round the aerofoil, the

complex velocity potential for the continuous flow past the aerofoil is obtained by adding the complex velocity potential w_1 to w_2. Denoting this by w, we have

$$w = w_1 + w_2 = w_1 - C_2 s, \tag{31}$$

and so, from (25) and (30), we get

$$dw/ds = w_s\{\wp(s-s_0)+\eta_1/\omega_1\}-C_2. \tag{32}$$

The constant C_2 can be determined by the Kutta condition that the fluid leaves the trailing edge of the arc-aerofoil smoothly. Bearing in mind also that the trailing edge A corresponds to $s = \mu$ in the s-plane, the Kutta condition may be written as $(dw/ds)_{s=\mu} = 0$, and therefore we have

$$C_2 = w_s\{\wp(\mu-s_0)+\eta_1/\omega_1\}. \tag{33}$$

If we substitute this in (32), we have ultimately

$$dw/ds = w_s\{\wp(s-s_0)-\wp(\mu-s_0)\}. \tag{34}$$

In this case the circulation κ becomes, by (32),

$$\kappa = \int\limits_{-\omega_1+\omega_3}^{\omega_1+\omega_3} (dw/ds)\,ds = -2\omega_1 C_2 = -2\omega_1 w_s\{\wp(\mu-s_0)+\eta_1/\omega_1\},$$

and if use is made of theta functions, we have, after some reduction,

$$\kappa = \frac{w_s}{2\omega_1}\left\{\frac{\vartheta_4''\{\frac{1}{2}(m-s_0)/\omega_1\}}{\vartheta_4\{\frac{1}{2}(m-s_0)/\omega_1\}}-\left[\frac{\vartheta_4'\{\frac{1}{2}(m-s_0)/\omega_1\}}{\vartheta_4\{\frac{1}{2}(m-s_0)/\omega_1\}}\right]^2\right\}, \tag{35}$$

where m is the real quantity previously defined in (12) such that $\mu = m+\omega_3$.

Further, if we use the value of w_s given by (28) together with the first relation in (16), we have

$$\frac{\kappa}{lU} = \frac{\sin\theta}{\sin\gamma}\left\{\frac{\vartheta_4''\{\frac{1}{2}(m-s_0)/\omega_1\}}{\vartheta_4\{\frac{1}{2}(m-s_0)/\omega_1\}}-\left[\frac{\vartheta_4'\{\frac{1}{2}(m-s_0)/\omega_1\}}{\vartheta_4\{\frac{1}{2}(m-s_0)/\omega_1\}}\right]^2\right\}\times$$
$$\times\left\{\frac{\vartheta_1'\{\frac{1}{2}(s_0-\nu)/\omega_1\}}{\vartheta_1\{\frac{1}{2}(s_0-\nu)/\omega_1\}}-\frac{\vartheta_1'\{\frac{1}{2}(s_0+\nu)/\omega_1\}}{\vartheta_1\{\frac{1}{2}(s_0+\nu)/\omega_1\}}\right\}^{-1}. \tag{36}$$

8. The general expressions for the lift and moment forces acting on the circular-arc aerofoil

If, as is usual for a very thin aerofoil, we do not take into account the singularity at the trailing edge, the lift on the circular-arc aerofoil can be evaluated as usual by Blasius's first formula. Denoting the x- and y-components of the resultant force acting on the aerofoil by X and Y respectively, we have

$$X-iY = \tfrac{1}{2}i\rho\oint\limits_C \left(\frac{dw}{dz}\right)^2 dz, \tag{37}$$

where the integral is taken in the counterclockwise sense along any closed contour C surrounding the aerofoil and ρ is the density of the fluid.

The evaluation of the above integral can be conveniently carried out by transforming the integrand so that the integration takes place in the s-plane. Since, however, our calculations are similar to those in Green's paper (**1**), only the final results will be given here for brevity. Thus, putting

$$\frac{m}{2\omega_1}=\frac{\phi_1}{2\pi},\qquad \frac{s_0}{2\omega_1}=-\frac{\phi_2}{2\pi}, \tag{38}$$

we have

$$X=0,\qquad \frac{Y}{\frac{1}{2}\rho U^2 l}=-\frac{\sin\theta}{\sin\gamma}C^3E^2(Y_1+Y_2+Y_3+Y_4+Y_5), \tag{39}$$

where

$$\begin{aligned}Y_1=&-\left\{\frac{\vartheta_1'^2(0)\vartheta_3^2\{\frac{1}{2}(\phi_1+\phi_2)/\pi\}}{\vartheta_2^2(0)\vartheta_4^2\{\frac{1}{2}(\phi_1+\phi_2)/\pi\}}+\frac{\vartheta_2''(0)}{\vartheta_2(0)}\right\}\times\\&\times\left\{4E\left[\frac{\vartheta_1'^2(0)\vartheta_3^2\{\frac{1}{2}(\phi_1+\phi_2)/\pi\}}{\vartheta_2^2(0)\vartheta_4^2\{\frac{1}{2}(\phi_1+\phi_2)/\pi\}}+\frac{\vartheta_2''(0)}{\vartheta_2(0)}-\frac{\vartheta_1'''(0)}{3\vartheta_1'(0)}\right]+\right.\\&\left.+\vartheta_1'^3(0)\left[\frac{\vartheta_1\{(\phi_1-\phi_2)/\pi\}}{\vartheta_4^4\{\frac{1}{2}(\phi_1-\phi_2)/\pi\}}+\frac{\vartheta_1\{(\phi_1+\phi_2)/\pi\}}{\vartheta_4^4\{\frac{1}{2}(\phi_1+\phi_2)/\pi\}}\right]\right\},\end{aligned} \tag{40}$$

$$Y_2=\tfrac{2}{3}E\frac{\vartheta_1'^3(0)\vartheta_1\{(\phi_1+\phi_2)/\pi\}}{\vartheta_4^4\{\frac{1}{2}(\phi_1+\phi_2)/\pi\}}\left\{\frac{\vartheta_1'\{(\phi_1+\phi_2)/\pi\}}{\vartheta_1\{(\phi_1+\phi_2)/\pi\}}-2\frac{\vartheta_4'\{\frac{1}{2}(\phi_1+\phi_2)/\pi\}}{\vartheta_4\{\frac{1}{2}(\phi_1+\phi_2)/\pi\}}\right\}, \tag{41}$$

$$Y_3=-D\left\{\frac{\vartheta_1'(\phi_1/\pi)}{\vartheta_1(\phi_1/\pi)}-\frac{\vartheta_1'(\phi_2/\pi)}{\vartheta_1(\phi_2/\pi)}\right\}, \tag{42}$$

$$Y_4=-D\frac{2\pi\sin(\alpha-\gamma)}{\cos\theta+\cos(\alpha-\gamma)}, \tag{43}$$

$$\begin{aligned}Y_5=&\frac{\pi\cot\theta}{C}\left\{\frac{\vartheta_1'^2(0)}{\vartheta_2^2(0)}\left[\frac{\vartheta_3^2\{\frac{1}{2}(\phi_1+\theta)/\pi\}}{\vartheta_4^2\{\frac{1}{2}(\phi_1+\theta)/\pi\}}+\frac{\vartheta_3^2\{\frac{1}{2}(\phi_1-\theta)/\pi\}}{\vartheta_4^2\{\frac{1}{2}(\phi_1-\theta)/\pi\}}+\right.\right.\\&\left.+\frac{\vartheta_3^2\{\frac{1}{2}(\phi_1-\phi_2)/\pi\}}{\vartheta_4^2\{\frac{1}{2}(\phi_1-\phi_2)/\pi\}}-3\frac{\vartheta_3^2\{\frac{1}{2}(\phi_1+\phi_2)/\pi\}}{\vartheta_4^2\{\frac{1}{2}(\phi_1+\phi_2)/\pi\}}\right]-\\&\left.-\tfrac{2}{3}E\left[\frac{\vartheta_1'(\phi_1/\pi)}{\vartheta_1(\phi_1/\pi)}-2\frac{\vartheta_4'\{\frac{1}{2}(\phi_1+\theta)/\pi\}}{\vartheta_4\{\frac{1}{2}(\phi_1+\theta)/\pi\}}\right]\right\},\end{aligned} \tag{44}$$

$$C=\frac{\vartheta_4^2\{\frac{1}{2}(\phi_1+\theta)/\pi\}\vartheta_4^2\{\frac{1}{2}(\phi_1-\theta)/\pi\}}{\vartheta_1'^2(0)\vartheta_1(\phi_1/\pi)\vartheta_1(\theta/\pi)}, \tag{45}$$

$$D=\left[\frac{\vartheta_1'^2(0)\vartheta_1(\phi_1/\pi)\vartheta_1(\phi_2/\pi)}{\vartheta_4^2\{\frac{1}{2}(\phi_1+\phi_2)/\pi\}\vartheta_4^2\{\frac{1}{2}(\phi_1-\phi_2)/\pi\}}\right]^2, \tag{46}$$

and

$$E=\frac{\vartheta_1'(0)\vartheta_1(\phi_1/\pi)\vartheta_1\{\frac{1}{2}(\phi_2+\theta)/\pi\}\vartheta_1\{\frac{1}{2}(\phi_2-\theta)/\pi\}}{\vartheta_4\{\frac{1}{2}(\phi_1+\theta)/\pi\}\vartheta_4\{\frac{1}{2}(\phi_1-\theta)/\pi\}\vartheta_4\{\frac{1}{2}(\phi_1+\phi_2)/\pi\}\vartheta_4\{\frac{1}{2}(\phi_1-\phi_2)/\pi\}}. \tag{47}$$

9. By means of Blasius's second formula the moment Γ_1 of the forces acting on the aerofoil about the origin of the coordinate-axes, reckoned

positive in the clockwise sense, is given by

$$\Gamma_1 = \mathrm{re}\,\tfrac{1}{2}\rho \oint_C \left(\frac{dw}{dz}\right)^2 z\,dz, \tag{48}$$

where, as before, the integral is taken in the counterclockwise sense along the closed contour C surrounding the aerofoil. As in the case of the lift, the evaluation of the above integral can be conveniently carried out by transforming the integrand so that the integration takes place in the s-plane. Omitting intermediate analysis, the final result is

$$\frac{\Gamma_1}{\frac{1}{2}\rho U^2 l^2} = -\pi C^3 E^2 D \frac{\sin^3\theta}{\sin^2\gamma\{\cos\theta+\cos(\alpha-\gamma)\}}, \tag{49}$$

where C, D, and E are given by (45), (46), and (47) respectively.

Further, it is readily found that the moment Γ of the forces about the trailing edge of the circular-arc aerofoil is given by

$$\Gamma = \Gamma_1 + Yx_A, \tag{50}$$

where $$x_A = R\sin(\alpha+\gamma) = \tfrac{1}{2}l\sin(\alpha+\gamma)/\sin\gamma. \tag{51}$$

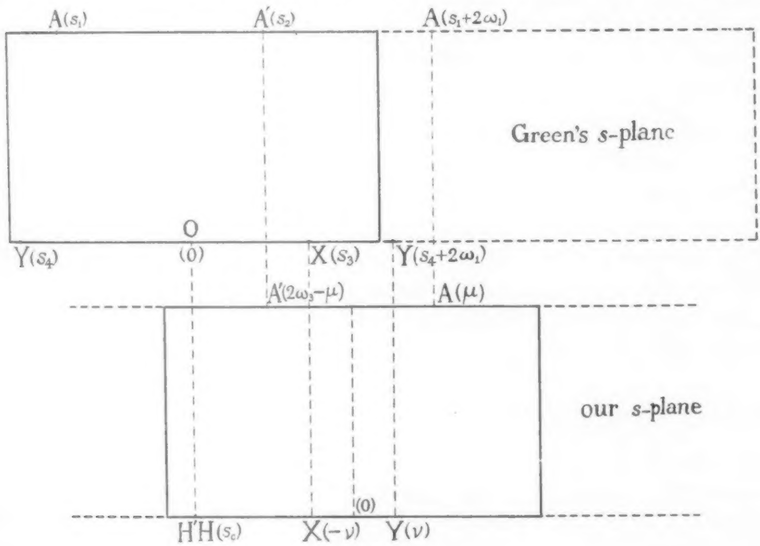

Fig. 9.

10. Comparison with Green's results

We shall now compare our expressions for the lift and moment acting on the aerofoil with the corresponding expressions obtained by Green (**1**).

The correspondence between various points in the s-plane in Green's analysis and in our s-plane is shown in Fig. 9 and in Table I. Thus it is

easily found that Green's θ_1, θ_2, θ_3, and θ_4 correspond to our $\phi_1+\phi_2-\pi$, $-\phi_1+\phi_2-\pi$, $\phi_2-\theta+\pi$, and $\phi_2+\theta-\pi$ respectively, where $\phi_1/\pi = m/\omega_1$, $\phi_2/\pi = -s_0/\pi$, $\theta/\pi = \nu/\omega_1$.

Further, we readily find that Green's δ is equal to our $\pi-\theta$ and that Green's α ($=\frac{1}{2}(\theta_1-\theta_2)$) and ϕ ($=\theta_3-\delta=\theta_4+\delta$) correspond to our ϕ_1 and ϕ_2 respectively. The correspondence between various angles is shown in Table II.

TABLE I

Green's analysis	*Present analysis*
s_1	$\mu-s_0-2\omega_1$
s_2	$2\omega_3-\mu-s_0$
s_3	$-\nu-s_0$
s_4	$\nu-s_0-2\omega_1$

TABLE II

Green's analysis	*Present analysis*
$\pi-\delta$	θ
α	ϕ_1
ϕ	ϕ_2

Taking these results into account, and bearing in mind that in Green's analysis $\theta_1 = \alpha+\phi-\pi$ and $\theta_2 = -\alpha+\phi-\pi$, we then compare our various expressions with those of Green. After some reductions, we found that, except for the difference in notation, our expressions for the lift and moment acting on the aerofoil are in perfect agreement with the corresponding ones of Green.†

11. Special cases

(*a*) *Centre of the circular arc on the bounding wall*

The general formulae for the lift and moment forces acting on the circular-arc aerofoil are very complicated, but they assume simple forms when the centre of the circular arc lies on the bounding wall and when the circle on which the arc lies touches the bounding wall.

We begin with the first case, i.e. when the centre of the circular arc lies on the wall. Then $\theta = \frac{1}{2}\pi$ and therefore we have

$$\nu = \tfrac{1}{2}\omega_1, \qquad \mu = \tfrac{1}{2}\omega_1+\omega_3, \qquad m = \tfrac{1}{2}\omega_1. \tag{52}$$

The first equation in (22) reduces to

$$\frac{\vartheta_3(0)}{\vartheta_4(0)} = \left\{\frac{\cos\alpha+\sin\gamma}{\cos\alpha-\sin\gamma}\right\}^{\frac{1}{2}}. \tag{53}$$

Also, remembering that we may write $\frac{1}{2}s_0/\omega_1+\frac{1}{4} = -\frac{1}{4}\epsilon/\pi$ $(\pi > \epsilon > 0)$, we have, from the second equation in (22),

$$\frac{\vartheta_1(\frac{1}{4}\epsilon/\pi)}{\vartheta_2(\frac{1}{4}\epsilon/\pi)} = \left\{\frac{\cos\gamma-\sin\alpha}{\cos\gamma+\sin\alpha}\right\}^{\frac{1}{2}}, \tag{54}$$

while the expression (19) for the ratio l/H reduces to

$$l/H = 2\tan\gamma/\cos\alpha. \tag{55}$$

† It may be remarked here that there is a misprint in Green's expression for Y_1: the last term should be read as: $\vartheta_1(\theta_2/\pi)/\vartheta_3^4(\frac{1}{2}\theta_2/\pi)$ instead of $\vartheta_2(\theta_2/\pi)/\vartheta_3^4(\frac{1}{2}\theta_2/\pi)$.

Finally, after a little reduction, the expression (39) for the lift coefficient becomes

$$\frac{Y}{\frac{1}{2}\rho U^2 l} = D_*(Y_1+Y_2+Y_3+Y_4), \tag{56}$$

where

$$D_* = -\frac{\vartheta_1^2(\frac{1}{4}\epsilon/\pi)\vartheta_2^2(\frac{1}{4}\epsilon/\pi)}{\pi^4\vartheta_2^8(0)\vartheta_3^2(\frac{1}{4}\epsilon/\pi)\vartheta_4^2(\frac{1}{4}\epsilon/\pi)\sin\gamma}, \tag{57}$$

$$E = \frac{\pi\vartheta_2^2(0)\vartheta_1(\frac{1}{4}\epsilon/\pi)\vartheta_2(\frac{1}{4}\epsilon/\pi)}{\vartheta_3(\frac{1}{4}\epsilon/\pi)\vartheta_4(\frac{1}{4}\epsilon/\pi)}, \tag{58}$$

$$\begin{aligned} Y_1 = &-\left\{\frac{\vartheta_1'^2(0)\vartheta_4^2(\frac{1}{4}\epsilon/\pi)}{\vartheta_2^2(0)\vartheta_3^2(\frac{1}{4}\epsilon/\pi)}+\frac{\vartheta_2''(0)}{\vartheta_2(0)}\right\}\times \\ &\times\left\{4E\left[\frac{\vartheta_1'^2(0)\vartheta_4^2(\frac{1}{4}\epsilon/\pi)}{\vartheta_2^2(0)\vartheta_3^2(\frac{1}{4}\epsilon/\pi)}+\frac{\vartheta_2''(0)}{\vartheta_2(0)}-\frac{\vartheta_1'''(0)}{3\vartheta_1'(0)}\right]-\right. \\ &\left.-\vartheta_1'^3(0)\vartheta_1(\tfrac{1}{2}\epsilon/\pi)\left[\frac{1}{\vartheta_3^4(\frac{1}{4}\epsilon/\pi)}+\frac{1}{\vartheta_4^4(\frac{1}{4}\epsilon/\pi)}\right]\right\}, \end{aligned} \tag{59}$$

$$Y_2 = -\tfrac{2}{3}E\frac{\vartheta_1'^3(0)\vartheta_1(\frac{1}{2}\epsilon/\pi)}{\vartheta_3^4(\frac{1}{4}\epsilon/\pi)}\left\{\frac{\vartheta_1'(\frac{1}{2}\epsilon/\pi)}{\vartheta_1(\frac{1}{2}\epsilon/\pi)}-2\frac{\vartheta_3'(\frac{1}{4}\epsilon/\pi)}{\vartheta_3(\frac{1}{4}\epsilon/\pi)}\right\}, \tag{60}$$

$$Y_3 = \frac{\vartheta_1'^4(0)\vartheta_2^2(0)\vartheta_2(\frac{1}{2}\epsilon/\pi)\vartheta_2'(\frac{1}{2}\epsilon/\pi)}{\vartheta_3^4(\frac{1}{4}\epsilon/\pi)\vartheta_4^4(\frac{1}{4}\epsilon/\pi)}, \tag{61}$$

$$Y_4 = -\frac{2\pi\vartheta_1'^4(0)\vartheta_2^2(0)\vartheta_2^2(\frac{1}{2}\epsilon/\pi)}{\vartheta_3^4(\frac{1}{4}\epsilon/\pi)\vartheta_4^4(\frac{1}{4}\epsilon/\pi)}\tan(\alpha-\gamma). \tag{62}$$

Also, the expression (49) for the moment Γ_1 about the origin of the coordinate-axes reduces to

$$\frac{\Gamma_1}{\frac{1}{2}\rho U^2 l^2} = -\frac{D_* Y_4}{2\sin\gamma\sin(\alpha-\gamma)}. \tag{63}$$

It is readily found that, except for the difference in notation, these expressions for the lift and moment are in agreement with the corresponding expressions given by Green.

(*b*) *The circle on which the arc lies touches the bounding wall*

In the second case in which the circle on which the arc lies touches the bounding wall, the quantities a and θ tend to zero in such a manner that $a/\theta \to R$, where R is the radius of the circular arc. Since $\theta = \pi\nu/\omega_1$, ν tends to zero also and equation (15) reduces to

$$\left[\frac{\vartheta_4'(\frac{1}{2}m/\omega_1)}{\vartheta_4(\frac{1}{2}m/\omega_1)}\right]^2 = \frac{\vartheta_4''(\frac{1}{2}m/\omega_1)}{\vartheta_4(\frac{1}{2}m/\omega_1)}. \tag{64}$$

If, as before, we put $m/\omega_1 = \phi_1/\pi$ and $s_0/\omega_1 = -\phi_2/\pi$, this equation becomes

$$\left[\frac{\vartheta_4'(\frac{1}{2}\phi_1/\pi)}{\vartheta_4(\frac{1}{2}\phi_1/\pi)}\right]^2 = \frac{\vartheta_4''(\frac{1}{2}\phi_1/\pi)}{\vartheta_4(\frac{1}{2}\phi_1/\pi)}, \tag{65}$$

while the limiting forms of the two equations in (22) become respectively

$$\frac{\vartheta_4'(\frac{1}{2}\phi_1/\pi)}{\vartheta_4(\frac{1}{2}\phi_1/\pi)} = \frac{\pi\sin\gamma}{\cos\alpha+\cos\gamma}, \tag{66}$$

and

$$\frac{\vartheta_1'(\frac{1}{2}\phi_2/\pi)}{\vartheta_1(\frac{1}{2}\phi_2/\pi)} = \frac{\pi\sin\alpha}{\cos\alpha+\cos\gamma}. \tag{67}$$

Also we have, from (19),

$$l/H = 2\sin\gamma/(1+\cos\alpha\cos\gamma). \tag{68}$$

By using the above limiting process the values of the lift and moment acting on the aerofoil can be deduced from the general values. We find

$$\frac{Y}{\frac{1}{2}\rho U^2 l} = -\frac{\pi}{3H_5^2\sin\gamma}\left[\frac{H_1 H_6^2}{H_4}(H_1^2+\pi^2)+H_3(H_3-2H_5)+ \right.$$
$$\left. +\frac{\pi^2}{3H_5}\{H_2+3H_5(H_6-2H_3)\}\right], \tag{69}$$

$$X = 0, \qquad \Gamma = \Gamma_1+\tfrac{1}{2}Yl\sin(\alpha+\gamma)/\sin\gamma, \tag{70}$$

$$\frac{\Gamma_1}{\frac{1}{2}\rho U^2 l^2} = -\frac{\pi^2 H_6^2}{2H_4 H_5^2\sin^2\gamma}(H_1^2+\pi^2), \tag{71}$$

where

$$H_1 = \frac{\vartheta_4'(\frac{1}{2}\phi_1/\pi)}{\vartheta_4(\frac{1}{2}\phi_1/\pi)} - \frac{\vartheta_1'(\frac{1}{2}\phi_2/\pi)}{\vartheta_1(\frac{1}{2}\phi_2/\pi)} = \frac{\pi(\sin\gamma-\sin\alpha)}{\cos\alpha+\cos\gamma}, \tag{72}$$

$$H_2 = 2H_4\left\{\frac{\vartheta_1'(\phi_1/\pi)}{\vartheta_1(\phi_1/\pi)} - 2\frac{\vartheta_4'(\frac{1}{2}\phi_1/\pi)}{\vartheta_4(\frac{1}{2}\phi_1/\pi)}\right\}, \tag{73}$$

$$H_3 = -\left\{\frac{\vartheta_1'^2(0)\vartheta_3^2\{\frac{1}{2}(\phi_1+\phi_2)/\pi\}}{\vartheta_2^2(0)\vartheta_4^2\{\frac{1}{2}(\phi_1+\phi_2)/\pi\}} + \frac{\vartheta_2''(0)}{\vartheta_2(0)}\right\}, \tag{74}$$

$$H_4 = \frac{\vartheta_1'^3(0)\vartheta_1(\phi_1/\pi)}{\vartheta_4^4(\frac{1}{2}\phi_1/\pi)}, \tag{75}$$

$$H_5 = \frac{\vartheta_1'^2(0)\vartheta_2^2(\frac{1}{2}\phi_2/\pi)}{\vartheta_2^2(0)\vartheta_1^2(\frac{1}{2}\phi_2/\pi)} - \frac{\vartheta_2''(0)}{\vartheta_2(0)}, \tag{76}$$

and

$$H_6 = -\frac{\vartheta_1'^2(0)\vartheta_1(\phi_1/\pi)\vartheta_1(\phi_2/\pi)}{\vartheta_4^2\{\frac{1}{2}(\phi_1+\phi_2)/\pi\}\vartheta_4^2\{\frac{1}{2}(\phi_1-\phi_2)/\pi\}}. \tag{77}$$

It can easily be shown that, except for the difference in notation, these expressions for the lift and moment are in accord with those of Green.

12. Numerical discussion

Green has carried out some numerical calculations for the case of a particular circular-arc aerofoil with camber approximately equal to 0·097 in the comparatively simple cases when the centre of the circular arc lies on the wall and when the circle on which the arc lies touches the wall. Two different values (i.e. 0° and 5°) have been taken for the angle of incidence of the aerofoil.

We have carried out detailed numerical calculations for three different circular-arc aerofoils, taking γ to be equal to 5°, 12°, and 22° respectively; these make the cambers of the aerofoils approximately equal to 0·022, 0·053, and 0·097 respectively. The value of the angle of incidence has been taken to be 5° in all cases. Our numerical calculations cover not only the simple cases considered by Green† but also the more general cases. The results are shown in Tables III, IV, and V, and they are also shown graphically in Figs. 10 and 11.

In these tables and figures the suffix 0 indicates the lift and moment coefficients for a circular-arc aerofoil in an unbounded stream. In Figs. 10

TABLE III

Camber $\sigma = 0{\cdot}022$ $(\gamma = 5°)$, $\alpha = 5°$

l/H	$Y/(\frac{1}{2}\rho U^2 l)$	Y/Y_0	$\Gamma/(\frac{1}{2}\rho U^2 l^2)$	Γ/Γ_0
0	0·8209	1	0·5445	1
0·0875	0·8166	0·9947	0·5416	0·9947
0·1756	0·8129	0·9902	0·5391	0·9901
0·8098	0·8046	0·9801	0·5320	0·9771
1·5925	0·8248	1·0048	0·5416	0·9946
2·6727	0·8743	1·0650	0·5677	1·0426
3·3069	0·9057	1·1033	0·5845	1·0735
22·95‡	1·3039	1·5884	0·7519	1·3809

TABLE IV

Camber $\sigma = 0{\cdot}053$ $(\gamma = 12°)$, $\alpha = 5°$

l/H	$Y/(\frac{1}{2}\rho U^2 l)$	Y/Y_0	$\Gamma/(\frac{1}{2}\rho U^2 l^2)$	Γ/Γ_0
0	1·2055	1	0·7341	1
0·2106	1·1840	0·9821	0·7209	0·9820
0·4267	1·1674	0·9684	0·7106	0·9680
1·0014	1·1456	0·9503	0·6961	0·9482
1·5555	1·1454	0·9501	0·6941	0·9456
3·0630	1·1840	0·9822	0·7116	0·9694
4·1663	1·2193	1·0115	0·7287	0·9926
22·95‡	1·3768	1·1421	0·7812	1·0642

TABLE V

Camber $\sigma = 0{\cdot}097$ $(\gamma = 22°)$, $\alpha = 5°$

l/H	$Y/(\frac{1}{2}\rho U^2 l)$	Y/Y_0	$\Gamma/(\frac{1}{2}\rho U^2 l^2)$	Γ/Γ_0
0	1·7643	1	1·0077	1
0·3895	1·6831	0·9540	0·9612	0·9539
0·8111	1·6246	0·9208	0·9274	0·9203
3·1003	1·5422	0·8741	0·8755	0·8688
22·95‡	1·4902	0·8446	0·8278	0·8215

† The values for the aerofoil with camber equal to 0·097 approximately in these simple cases have been recalculated, and we have obtained the same values as Green's.

‡ This is the value of l/H when the trailing edge of the arc touches the wall.

and 11 the results for the case of a flat plate shown by dotted lines are also drawn for comparison.

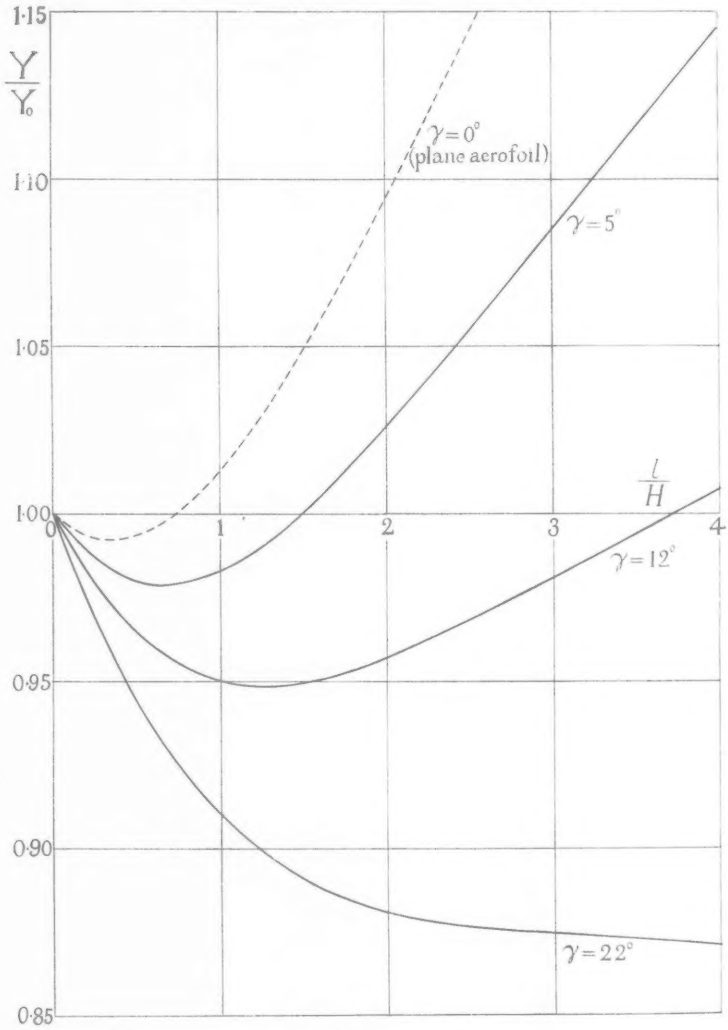

FIG. 10.

From these tables and figures it is seen that, for sufficiently small values of the camber, as well as for small values of the angle of incidence α (e.g. $\alpha = 5°$) usually adopted in practice, as the circular-arc aerofoil

approaches the bounding wall both the lift and moment coefficients first decrease and then increase to values greater than the values for a circular-arc aerofoil in an unbounded stream. These results are similar to those

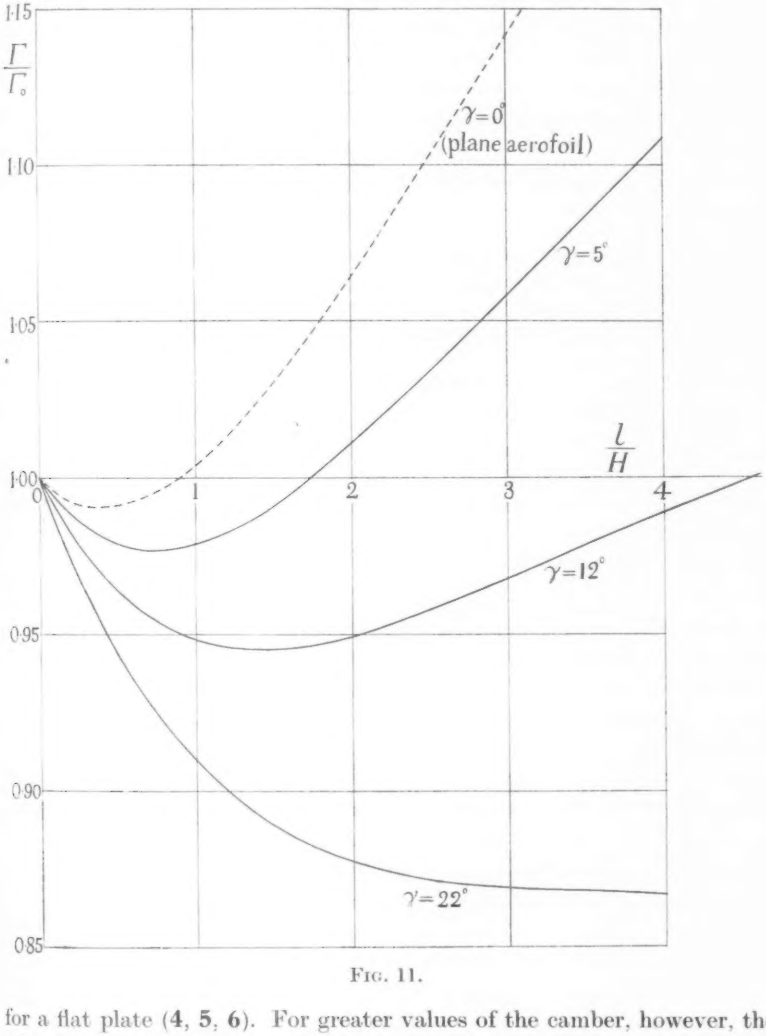

Fig. 11.

for a flat plate (**4**, **5**, **6**). For greater values of the camber, however, the lift and moment coefficients are decreased due to the presence of the wall for all values of l/H, even when the aerofoil is placed at small angles of incidence as in practice.

From Figs. 10 and 11 it is seen further that the effect of the wall upon the lift and moment of an aerofoil is greatly modified by its camber. Thus, for large distances of the aerofoil from the bounding wall the effect of the camber is to decrease both the lift and moment found for a flat plate as compared with the lift and moment in an unbounded stream. As the aerofoil gets nearer to the wall, both the lift and the moment eventually increase, as previously mentioned, above the values for an unbounded stream, for small angles of incidence occurring in practice, but the rates of increase in the lift and the moment are considerably decreased owing to the effect of the camber of the aerofoil.

REFERENCES

1. A. E. Green, 'The forces acting on a circular-arc aerofoil in a stream bounded by a plane wall', *Proc. London Math. Soc.* (2) **46** (1940), 19–54.
2. S. Tomotika and I. Imai, 'Note on the lift and moment of a circular-arc aerofoil which touches the ground with its trailing edge', *Proc. Phys.-Math. Soc. Japan*, **20** (1938), 15–31.
3. ——, K. Urano, and Z. Hasimoto, 'Further studies on the lift and moment of a circular-arc aerofoil which touches the ground with its trailing edge', ibid. **23** (1941), 713–24.
4. ——, T. Nagamiya, and Y. Takenouti, 'The lift on a flat plate placed near a plane wall, with special reference to the effect of the ground upon the lift of a monoplane aerofoil', *Report Aeron. Res. Inst. Tokyo Imp. Univ.*, No. 97 (1933).
5. ——, 'Further studies on the effect of the ground upon the lift of a monoplane aerofoil', ibid., No. 120 (1935).
6. —— and I. Imai, The moment of the fluid pressure acting on a flat plate in a semi-infinite stream bounded by a plane wall, I. case of lower boundary (the ground effect)', ibid., No. 152 (1937).
7. B. Hudimoto, 'The lift on an aerofoil with a circular-arc section placed near the ground', *Memoirs Coll. Eng. Kyoto Imp. Univ.* **8** (1934), 36–41.

THE RESISTANCE OF A RECTANGULAR METAL PLATE WITH AN INTERNAL ELECTRODE

By S. D. DAYMOND (*Mathematical Institute, The University, Liverpool*)

[Received 5 September 1950]

SUMMARY

A steady current enters a rectangular metal sheet through a small circular internal electrode and flows out through an electrode which coincides with the rectangular boundary. The problem of finding the effective resistance is essentially that of determining a harmonic function ϕ which is constant over each electrode. The appropriate complex potential function is expressible in Jacobean elliptic functions; the ϑ-functions, however, are found to be more suitable for the numerical work involved, and are used below. Altogether there are four parameters (two of these are coordinates of position of the inner electrode); numerical values of the resistance are found, therefore, only for certain special but representative values of these parameters. A brief discussion of the numerical results occurs at the end.

1. THE method of images is employed below to determine the effective resistance of a uniform rectangular metal plate, when the steady current enters through a small circular electrode within the plate, the other electrode coinciding with the whole perimeter of the rectangle. The solution of this problem is a preliminary step in an investigation of induction effects in such a plate when the current varies with time, and when the electrodes are disposed as they are for the steady-current case explained above. Near the stationary values of the variable current, where the effect of self-inductance is negligible, the conditions are practically those for a steady current. The resistance of the plate, which we set out to determine here, is then of some interest and importance. This type of problem is also of some interest to geophysicists who are concerned with the distribution of potential when an electrode is pushed into the ground.

In some actual experiments which were carried out on induction and discharge effects, the current entered by a small electrode at the centre of the plate and left by a very large number of conducting wires attached to the edge of the plate and distributed over the whole of its perimeter. For purposes of calculation this can be assumed to mean that the current flows out perpendicularly through the perimeter, i.e. that the whole of the perimeter is an electrode. This boundary condition is therefore assumed in the following determination of the resistance of the plate to the flow of steady current.

Notation

a, b ($b \geqslant a$) the dimensions of the rectangle.

$\tau = ib/a$ the modulus of the ϑ-functions.

$q = \exp(i\pi\tau) = \exp(-\pi b/a)$.

t, σ the constant thickness and constant specific conductivity (respectively) of the plate.

x, y Cartesian coordinates with origin at the centre of the plate and axes parallel to the edges (Fig. 1).

x_0, y_0 the coordinates of the centre of the inner small circular electrode.

$z = x+iy,\ z_0 = x_0+iy_0$.

$\nu = \xi+i\eta = z/2a,\ \nu_0 = \xi_0+i\eta_0 = z_0/2a$.

$w = \varphi+i\psi$ the complex potential function (the current density is proportional to the gradient of ϕ).

ϕ_0 the potential of the inner electrode.

c the radius of the inner electrode.

$\delta = c/2a$.

R the resistance of the plate.

In section 2 the function w, and subsequently ϕ_0 and the expression $2\pi\sigma tR$, are derived for such a system in which both the plate dimensions and the position of the inner electrode are arbitrary. The expression for ϕ_0 is a power series in δ, and terms of the order δ^3 and smaller are ultimately neglected.

[An expression for w can be obtained, by a conformal transformation, in terms of Jacobean elliptic functions: it is, in a usual notation,

$$w = -2\ln\{(t-t_0)/(t-\bar{t}_0)\},$$

where

$$t = \mathrm{sn}\{iK(2z+a)/b\},$$

and $K'/K = 2a/b$ determines the modulus k. For carrying out the numerical work, however, this form is less convenient than that derived below.]

2. The current density in the plate is $\mathbf{i} = -\sigma\,\mathrm{grad}\,\phi$, and, since in the space between the electrodes $\mathrm{div}\,\mathbf{i}$ is zero, therefore

$$\nabla^2\phi = 0. \tag{1}$$

The total current flowing out of the plate is

$$t\int (\mathbf{i}\cdot\mathbf{ds}),$$

where the integration is taken round the rectangle. The integral is equal to

$$-\sigma t\int \frac{\partial\phi}{\partial n}\,ds = -\sigma t[\psi].$$

by a property of conjugate functions. The square bracket indicates the increment which results from one complete description of the rectangular boundary. Taking the potential on the latter boundary to be zero, the value of the effective resistance is

$$(\sigma t)^{-1}|\phi_0/[\psi]|. \tag{2}$$

The function w, whose real part must satisfy (1) and the simple boundary conditions, is now determined by using the analogy between this problem and that of the two-dimensional conductor at zero potential under the influence of a unit positive line charge passing through the interior position (z_0) occupied by the electrode (see Fig. 1).

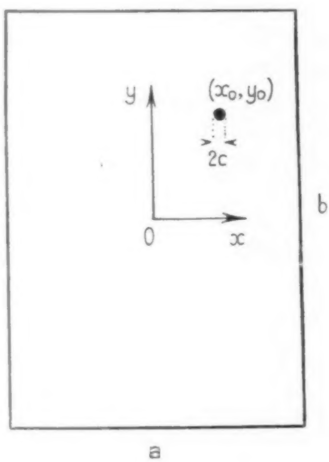

FIG. 1.

In this electrostatic problem the given charge and the image system consist of line charges

$$+1 \text{ through the points } \nu = \nu_0+m+n\tau$$

and

$$\nu = -\nu_0+\tfrac{1}{2}+\tfrac{1}{2}\tau+m+n\tau, \tag{3}$$

and

$$-1 \text{ through the points } \nu = \bar{\nu}_0+\tfrac{1}{2}\tau+m+n\tau$$

and

$$\nu = -\bar{\nu}_0+\tfrac{1}{2}+m+n\tau, \tag{4}$$

where $\bar{\nu}_0$ is the complex conjugate of ν_0, and $m, n = 0, \pm 1, \pm 2, \ldots$.

The required function w is $-2\ln\{f(\nu)\}$ where $f(\nu)$ has simple zeros at the

points (3) and simple poles at the points (4). Now $\vartheta_1(\nu/\tau)$ has simple zeros at the points $\nu = m+n\tau$ (see **1**, p. 255). Hence

$$\tfrac{1}{2}w = -\ln\frac{\vartheta_1(\nu-\nu_0)\vartheta_1(\nu+\nu_0-\frac{1}{2}-\frac{1}{2}\tau)}{\vartheta_1(\nu-\bar\nu_0-\frac{1}{2}\tau)\vartheta_1(\nu+\bar\nu_0-\frac{1}{2})}$$

$$= -\ln\frac{\vartheta_1(\nu-\nu_0)\vartheta_3(\nu+\nu_0)}{\vartheta_4(\nu-\bar\nu_0)\vartheta_2(\nu+\bar\nu_0)}$$

$$= -\ln\frac{\vartheta_1(\nu-\nu_0)\vartheta_3(2\nu_0+\nu-\nu_0)}{\vartheta_4(i2\eta_0+\nu-\nu_0)\vartheta_2(2\xi_0+\nu-\nu_0)}.$$

With the help of (**1**), p. 252, equations (1) to (4), and Taylor's theorem we now express the right-hand side as a certain function of $\nu-\nu_0$ and a series expansion in $\nu-\nu_0$. In the series the coefficients of $\nu-\nu_0$ and $(\nu-\nu_0)^2$ are simplified by the use of (**2**), p. 100, equations (4). Also, since the third and higher powers of $\delta = c/2a$ are being neglected, the potential ϕ_0 on the inner electrode is determined by substituting either $\eta = \eta_0$, $\xi = \xi_0\pm\delta$, or $\xi = \xi_0$, $\eta = \eta_0\pm\delta$, and retaining the real part of w. Thus

$$\tfrac{1}{2}\phi_0 = -\ln\left(\frac{1}{\pi}\frac{\vartheta_1'\vartheta_3}{\vartheta_4\vartheta_2}\right)+\ln\left(\frac{\cos 2\pi\xi_0}{\sin\pi\delta}\right)-$$
$$-2\sum_1^\infty Q_m[q^m(1-\cos 2m\pi\delta)+(-1)^m(1-\cos 4m\pi\xi_0\cosh 4m\pi\eta_0)+$$
$$+(\cosh 4m\pi\eta_0-1)+(-1)^m q^m(1-\cos 4m\pi\xi_0)]-$$
$$-4\pi\delta\left[\tfrac{1}{4}\tan 2\pi\xi_0+\sum_1^\infty(-1)^{m-1}mQ_m\sin 4m\pi\xi_0(q^m-\cosh 4m\pi\eta_0)\right]-$$
$$-4\pi^2\delta^2\left[\tfrac{1}{8}\sec 2\pi\xi_0-\right.$$
$$\left.-\sum_1^\infty m^2Q_m\{\cosh 4m\pi\eta_0+(-1)^m\cos 4m\pi\xi_0(q^m-\cosh 4m\pi\eta_0)\}\right]+O(\delta^3), \tag{5}$$

where ϑ represents $\vartheta(0/\tau)$ and $Q_m = q^m/m(1-q^{2m})$.

The function ψ for a line-charge of unit strength, through the point $z = z_0$, is $-2\arg(z-z_0)$. In this case $[\psi]$ is equal to -4π or zero according as the contour encloses z_0 or does not. When, therefore, the contour is the rectangle itself, only the complex potential arising from the given line-charge will be effective in the determination of $[\psi]$ as the images are all outside the rectangle. Thus $[\psi] = -4\pi$. From (2) the resistance of the plate is $(2\pi\sigma t)^{-1}\,\tfrac{1}{2}\phi_0$.

3. The largest value of q is $\exp(-\pi) = 0{\cdot}04321\ldots$ when b/a is unity, and q decreases from this value to zero as b/a increases from unity to

infinity. The function $\ln(\vartheta_1'\vartheta_3/\pi\vartheta_4\vartheta_2)$ also decreases steadily to zero as b/a increases in this way; some pairs of corresponding values are:

b/a	1·0	1·5	2·0	2·5	3
$\ln(\vartheta_1'\vartheta_3/\pi\vartheta_4\vartheta_2)$	0·165804	0·035614	0·007456	0·001552	0·000323

All of the series in (5) tend to zero as b/a tends to infinity. The rate of convergence of at least one of them is, however, slow, particularly in the case of a system where the plate is square and the inner electrode is fairly distant from the centre.

In the first table below are some values of $2\pi\sigma tR$, for the range

$$1 \leqslant b/a < \infty$$

and for the positions of the inner electrode represented by

$$\eta_0 = y_0/2a = 0; \qquad 40\xi_0 = 20x_0/a = 0,\ 1,\ 2,\ 3,\ 4, \text{ and } 5.$$

$y_0 = 0$ $\quad 20x_0/a =$	0	1	2	3	4	5
b/a						
1·0	4·7987	4·7893	4·7551	4·7124	4·6367	4·5255
	3·7001	3·6888	3·6599	3·6085	3·5300	3·4151
1·5	4·9289	4·9163	4·8799	4·8174	4·7243	4·5932
	3·8302	3·8153	3·7770	3·7119	3·6158	3·4810
2·0	4·9570	4·9437	4·9053	4·8397	4·7426	4·6072
	3·8583	3·8425	3·8021	3·7339	3·6338	3·4946
2·5	4·9629	4·9495	4·9106	4·8443	4·7465	4·6102
	3·8642	3·8483	3·8074	3·7384	3·6376	3·4974
3·0	4·9642	4·9507	4·9118	4·8453	4·7473	4·6108
	3·8654	3·8494	3·8085	3·7394	3·6383	3·4980
∞	4·9645	4·9521	4·9143	4·8491	4·7526	4·6179
	3·8660	3·8533	3·8158	3·7506	3·6540	3·5194

The two values of $2\pi\sigma tR$ occurring under each set of values of b/a, x_0, and y_0, are such that the upper and lower values correspond respectively to the values 1/450 and 1/150 of δ. The latter have been chosen partly because they are of the right order of magnitude and partly as a convenient pair of values (in the computational sense) to serve as a basis for the comparison of two different sets of numerical results.

When x_0 and y_0 have fixed values the convergence of each of the series in (5) is slowest when $b/a = 1$. In this case, because of the symmetry of the square plate about a diagonal, the convergence of each series must be slowest when $x_0 = y_0$. (This is also confirmed by some numerical results not included here.)

The short table below gives pairs of values of $2\pi\sigma tR$ for the case of a

square plate when the inner electrode has different positions represented by

$$\lambda = 20x_0/a = 20y_0/a = 1, 2, 3, 4, \text{ and } 5.$$

λ	1	2	3	4	5
$2\pi\sigma t R$	4·7808 3·6803	4·7284 3·6267	4·6412 3·5380	4·5177 3·4129	4·3539 3·2472

For any value of b/a the resistance decreases as the inner electrode is moved from the centre towards an edge. It decreases also in the case of the square plate when the inner electrode is moved from the centre towards a corner. The effect on the resistance is relatively greater, however, when the radius of the inner electrode is increased; it is true, for all values of b/a and for all the electrode positions considered here, that the resistance is reduced by about one-quarter when the small radius is trebled. On the other hand, a movement of the electrode from the centre of the plate to a point half-way between the centre and one of the longer edges (a movement of 30 diameters when $\delta = 1/450$) causes a fall in the resistance of less than one-twelfth.

REFERENCES

1. J. Tannery and J. Molk, *Fonctions Elliptiques*, vol. **2** (Paris, 1896).
2. ——, *Fonctions Elliptiques*, vol. **4** (Paris, 1902).

NOTE ON A CLASS OF SOLUTIONS OF THE NAVIER-STOKES EQUATIONS REPRESENTING STEADY ROTATIONALLY-SYMMETRIC FLOW

By G. K. BATCHELOR (*Trinity College, Cambridge*)

[Received 4 July 1950]

SUMMARY

This note describes one- and two-parameter families of solutions of steady rotationally-symmetric viscous flow. The solutions are such that the Navier–Stokes equations reduce to ordinary differential equations in a single position variable. The one-parameter family represents flow which is rigid-body rotation at infinity and over a plane through the origin; the solution given by von Kármán in 1921 is one member of this family. The two-parameter family represents flow which is rigid-body rotation over each of two planes at a finite distance apart. The case of large Reynolds number is particularly interesting, since the two bounding planes are then separated by a region of rigid-body rotation and translation in which viscous effects are negligible.

Introduction

T. v. Kármán (**1**) has pointed out a simple solution of the Navier–Stokes equations of motion which describes the steady flow of a viscous fluid in a semi-infinite region bounded by an infinite rotating disk. This 'solution' is not yet given analytically, since one is left with two ordinary non-linear differential equations in a single independent variable which must be solved numerically, but to have carried a solution of the Navier–Stokes equations even so far by exact analysis was (and still is) something of a novelty. Moreover, the solution has the very interesting property that it is also a solution of the appropriate boundary-layer equations, the terms neglected in boundary-layer theory being identically zero for this type of motion.

The purpose of this note is to show that there are one- and two-parameter families of solutions having the particular mathematical simplicity of Kármán's solution; Kármán's solution is one member of the one-parameter family. In Kármán's problem the flow far from the disk is assumed to be wholly normal to the disk and to be induced by the rotation of the disk. In general, if other conditions far from the disk are assumed, the particular simplicity of Kármán's solution is lost, but it will be shown below that the simple form of the solution is retained if the fluid at infinity has an arbitrary uniform angular velocity γ about the axis of rotation of the disk. If ω is the angular velocity of the disk, there is found to be a solution for each value of γ/ω between $-\infty$ and $+\infty$. Kármán's solution corresponds to

$\gamma/\omega = 0$, whereas $\gamma/\omega = \mp\infty$ describes a flow which is rotating uniformly at infinity and which is bounded by a stationary disk. In this latter case there is thus the opportunity of describing quantitatively the tendency for particles of sugar to migrate to the centre of a cup of tea which has been stirred. The qualitative explanation (**2**) of this phenomenon is well known, of course; the new point is that the flow away from the disk induced by the rotation is *uniform* over planes parallel to the disk, just as the flow towards the disk is uniform over these planes in Kármán's problem.

A two-parameter family of solutions of the same simple type describes the flow between two parallel infinite disks which are rotating about the same axis with different angular velocities; in addition to the ratio of the angular velocities of the disks, the Reynolds number based on the distance between the disks is now a relevant parameter. A numerical method of determining the flow field in the special case in which one disk is stationary and the Reynolds number of rotation of the other disk is small has recently been described by Casal (**3**).

A family of solutions of related type has been described by Miss Hannah (**4**). This family is obtained by combining the flow towards the disk produced by a source at infinity on the axis of rotation with the rotating flow induced by the disk. Kármán's solution is obtained when the source-flow is made zero, and, at the other limit, if the disk is stationary the viscous stagnation-point solution described by Homann (**5**) is recovered. This family of solutions will not be included in the following discussion.

The governing equations

If v_r, v_θ, v_z are velocity components in the directions of increase of cylindrical polar coordinates r, θ, z, and p is the pressure, the Navier–Stokes equations of steady motion of a fluid of density ρ which is symmetrical about the axis $r = 0$ are as follows:

$$v_r\frac{\partial v_r}{\partial r}+v_z\frac{\partial v_r}{\partial z}-\frac{v_\theta^2}{r} = -\frac{1}{\rho}\frac{\partial p}{\partial r}+\nu\left(\nabla^2 v_r-\frac{v_r}{r^2}\right), \tag{1}$$

$$v_r\frac{\partial v_\theta}{\partial r}+v_z\frac{\partial v_\theta}{\partial z}+\frac{v_r v_\theta}{r} = \nu\left(\nabla^2 v_\theta-\frac{v_\theta}{r^2}\right), \tag{2}$$

$$v_r\frac{\partial v_z}{\partial r}+v_z\frac{\partial v_z}{\partial z} = -\frac{1}{\rho}\frac{\partial p}{\partial z}+\nu\nabla^2 v_z, \tag{3}$$

where $$\nabla^2 \equiv \frac{\partial^2}{\partial r^2}+\frac{1}{r}\frac{\partial}{\partial r}+\frac{\partial^2}{\partial z^2}.$$

The continuity equation is

$$\frac{1}{r}\frac{\partial r v_r}{\partial r}+\frac{\partial v_z}{\partial z} = 0. \tag{4}$$

The plane $z = 0$ is identified with the plane of a uniformly rotating disk (angular velocity ω) so that one set of boundary conditions is

$$v_z = v_r = 0, \qquad v_\theta = \omega r, \quad \text{at} \quad z = 0. \tag{5}$$

The other set of boundary conditions will depend on the problem under discussion; if the fluid is unbounded in the z-direction the conditions to be assumed are

$$v_r \to 0, \quad v_\theta \to \gamma_1 r, \quad \text{as} \quad z \to \infty, \tag{6}$$

whereas if there is a second rotating disk at $z = d$ the conditions are

$$v_z = v_r = 0, \qquad v_\theta = \gamma_2 r, \quad \text{at} \quad z = d, \tag{7}$$

where γ_1, γ_2, and d are disposable constants. This excludes Miss Hannah's family of solutions, which give a radial velocity at $z = \infty$, but it includes the one- and the two-parameter families mentioned in the introduction.

The simple property of Kármán's solution and of the solutions sought herein is that the flow normal to the disk is uniform over planes parallel to the disk. That is,

$$v_z = v_z(z),$$

and as a consequence, from (4), and assuming that v_r is finite at $r = 0$,

$$v_r = -\frac{r}{2}\frac{dv_z}{dz}. \tag{8}$$

Equation (3) can then be integrated to give

$$p/\rho = \nu \frac{dv_z}{dz} - \tfrac{1}{2}v_z^2 + \Pi(r). \tag{9}$$

From equation (1) we find that the arbitrary function $\Pi(r)$ satisfies

$$\frac{1}{r}\frac{d\Pi(r)}{dr} - \frac{v_\theta^2}{r^2} = \text{function of } z \text{ only.}$$

The boundary condition (5) then requires

$$\Pi(r) = \tfrac{1}{2}r^2(\omega^2 + c), \tag{10}$$

where c is a constant, so that

$$v_\theta/r = \text{function of } z \text{ only.} \tag{11}$$

Equations (1) and (2) then become

$$\left(\frac{1}{2}\frac{dv_z}{dz}\right)^2 - \tfrac{1}{2}v_z\frac{d^2v_z}{dz^2} - \left(\frac{v_\theta}{r}\right)^2 = -(\omega^2+c) - \frac{\nu}{2}\frac{d^3v_z}{dz^3} \tag{12}$$

and

$$-\frac{dv_z}{dz}\frac{v_\theta}{r} + v_z\frac{d(v_\theta/r)}{dz} = \nu\frac{d^2(v_\theta/r)}{dz^2}. \tag{13}$$

In the case of the semi-infinite fluid with boundary conditions (5) and (6), the asymptotic form (as $z \to \infty$) of (12) is

$$c = \gamma_1^2 - \omega^2 \tag{14}$$

and only five boundary conditions are needed for the solution of (12) and (13). These are supplied by (5) and (6), the uniform axial velocity V at $z = \infty$ being determined as part of the solution. In the case of the two rotating disks all six of the boundary conditions (5) and (7) are needed to solve (12) and (13) and to determine the constant c.

The form of solution which has been assumed is still valid when there is a uniform suction through the surface of either or both of the disks, the boundary condition $v_z = 0$ being then replaced by $v_z =$ a prescribed constant. Suction through the surface of the disks will give rise to some interesting modifications of the flow patterns described below, but will not be considered further.

The variables may be made non-dimensional by using $(\nu\omega)^{\frac{1}{2}}$ as a reference velocity and $(\nu/\omega)^{\frac{1}{2}}$ as a reference length, the direction of positive rotation being so chosen that ω is always positive. Put

$$r = (\nu/\omega)^{\frac{1}{2}}\eta, \qquad z = (\nu/\omega)^{\frac{1}{2}}\zeta, \qquad v_\theta = (\nu\omega)^{\frac{1}{2}}\eta g(\zeta), \qquad v_z = (\nu\omega)^{\frac{1}{2}}h(\zeta),$$

in which case equations (12) and (13) become

$$\tfrac{1}{4}h'^2 - \tfrac{1}{2}hh'' - g^2 = -\left(\frac{\omega^2+c}{\omega^2}\right) - \tfrac{1}{2}h''', \tag{15}$$

$$-gh' + g'h = g'', \tag{16}$$

where dashes denote differentiation with respect to ζ. The boundary conditions are now

$$h = h' = 0, \qquad g = 1, \quad \text{at} \quad \zeta = 0, \tag{17}$$

and, for the semi-infinite fluid (in which case $c = \gamma_1^2 - \omega^2$),

$$h' \to 0, \quad g \to \gamma_1/\omega, \quad \text{as} \quad \zeta \to \infty, \tag{18}$$

or, for the fluid between two rotating disks,

$$h = h' = 0, \qquad g = \gamma_2/\omega, \quad \text{at} \quad \zeta = \left(\frac{d^2\omega}{\nu}\right)^{\frac{1}{2}}. \tag{19}$$

Numerical integration of equations (15) and (16) by the method used by Miss Hannah (**4**), and by Cochran (**6**) in the case of Kármán's problem, would probably be feasible, but tedious. Interest lies more in the general form of the solutions than in the numerical details so that only general observations about the streamlines in typical cases are presented here. The author has no evidence for the conclusions stated, other than that mentioned explicitly.

Streamlines of the flow bounded by a single disk

Consider first the family of solutions given by the boundary conditions (18). There is one member of this family for each value of γ_1/ω between $-\infty$ and $+\infty$, and for each member there is an appropriate value of V, the

axial velocity far from the disk. The members of the family may be divided into three classes within each of which the streamlines have much the same appearance.

Class (*a*). $+\infty > \gamma_1/\omega \geqslant 1$

The rotational velocity at the disk is, in this case, smaller than at any other point in the field so that the inward radial pressure gradient imposed

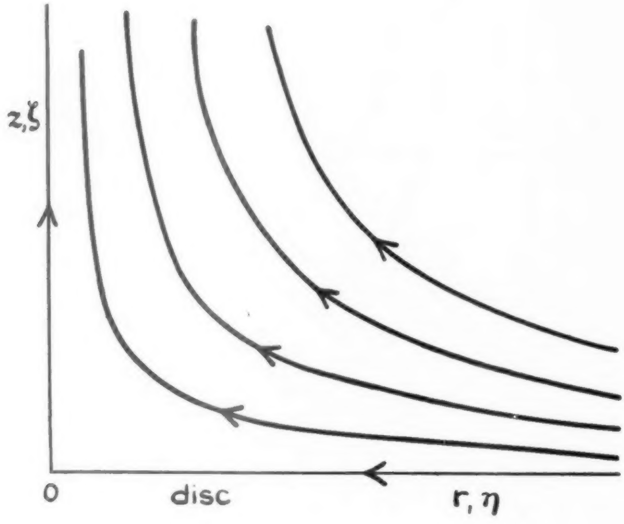

$\infty > \gamma_1/\omega > 1$

FIG. 1

by the fluid at infinity is more than sufficient to keep the fluid near the disk moving in circles. Hence there is a radial flow inwards at points near the disk and an axial flow away from the disk (see Fig. 1; in this and other figures the streamlines refer, of course, to components of the motion in an axial plane only). At one end of the range $\gamma_1/\omega = \infty$, corresponding to a stationary disk and giving an approximation to the tea-cup flow, and at the other extreme $\gamma_1/\omega = 1$, corresponding to uniform rotation of the whole fluid with no axial motion.

Class (*b*). $1 \geqslant \gamma_1/\omega \geqslant 0$

The angular velocity at the disk is here a maximum and the rotation is everywhere in the same direction, so that the axial velocity is towards the

disk (Fig. 2). The disk acts as a centrifugal fan, throwing fluid out radially and drawing it in axially. The extreme case $\gamma_1/\omega = 0$ is Kármán's problem. Note that the streamlines of members of this class are not obtained simply by reversing the streamlines of members of class (a).

Class (c). $0 > \gamma_1/\omega > -\infty$

The disk, and the fluid far from the disk, rotate in opposite directions, in this case so that at some value of ζ (i.e. of z), $g(\zeta) = 0$ and the fluid

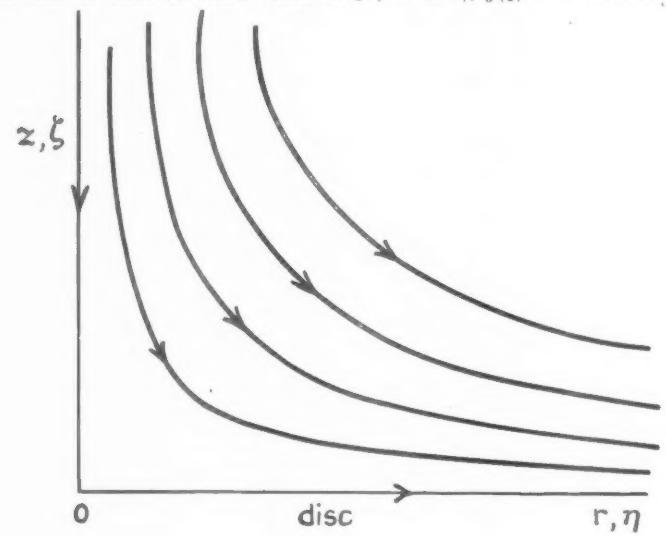

$1 > \gamma_1/\omega \geqslant 0$

FIG. 2

there has zero angular velocity about the axis $r = 0$. The angular velocity of the disk is thus greater in absolute magnitude than that of the fluid near it, and we anticipate that the radial velocity will be outward in the neighbourhood of the disk (i.e. the disk acts locally as a centrifugal fan) but inward elsewhere. This conclusion is supported by the following rough investigation of the form of the functions $g(\zeta)$ and $h(\zeta)$. At $\zeta = 0$ we have $g = 1$ and, it may be assumed, $g' < 0$. When ζ is large, g is asymptotic to the constant values γ_1/ω so that the function probably has the form shown in Fig. 3. Now equation (16) can be written in the form

$$h/g = -\int_0^\zeta \frac{g''}{g^2}\,d\zeta \quad \text{or} \quad = \frac{V}{(\nu\omega)^{\frac{1}{2}}}\Big/\frac{\gamma_1}{\omega} + \int_\zeta^\infty \frac{g''}{g^2}\,d\zeta, \tag{20}$$

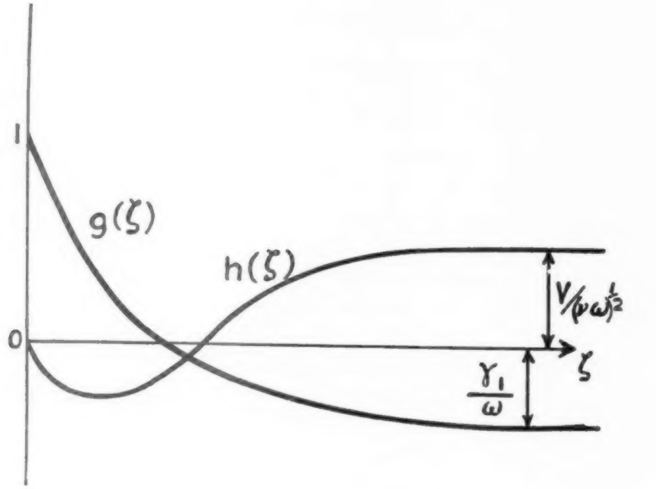

$0 > \gamma_1/\omega > -\infty$

FIG. 3

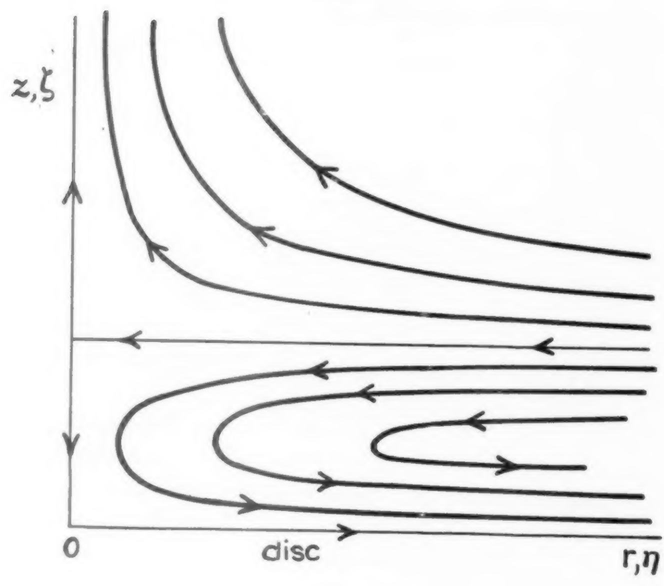

$0 > \gamma_1/\omega > -\infty$

FIG. 4

whichever range avoids the singularity at the point where $g = 0$. On the supposition that $g'' > 0$ for all ζ, as in the sketch in Fig. 3, the variation of h required by these equations is sketched in Fig. 3 and the streamlines are shown in Fig. 4. Equation (16) shows that the value of ζ for which $h = 0$ must be at least as great as that for which $g = 0$. Apparently the critical plane on which the axial velocity h vanishes, which may not coincide with the plane of zero angular velocity, divides the flow field into two self-contained regions. The dividing plane coincides with the disk when $\gamma_1/\omega = -\infty$ and moves away to infinity as γ_1/ω increases from $-\infty$ to 0.

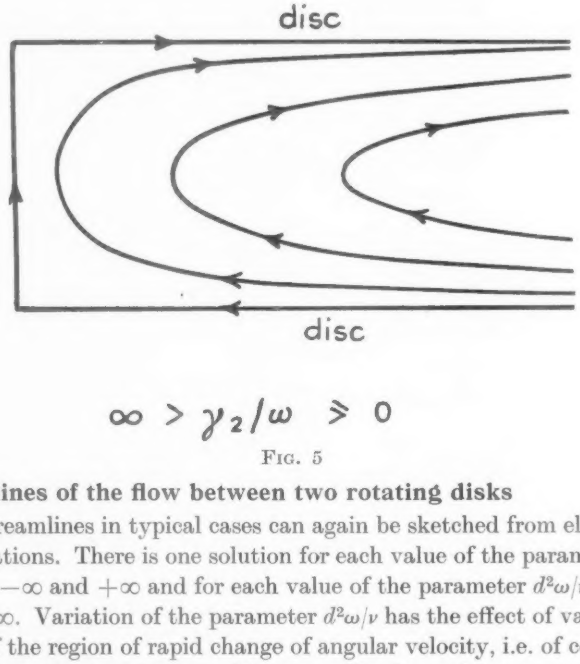

FIG. 5

Streamlines of the flow between two rotating disks

The streamlines in typical cases can again be sketched from elementary considerations. There is one solution for each value of the parameter γ_2/ω between $-\infty$ and $+\infty$ and for each value of the parameter $d^2\omega/\nu$ between 0 and $+\infty$. Variation of the parameter $d^2\omega/\nu$ has the effect of varying the extent of the region of rapid change of angular velocity, i.e. of controlling the boundary-layer character of the flow. The form of the streamlines does not vary radically with $d^2\omega/\nu$, so that the whole two-parameter family may be divided into two classes in which γ_2/ω takes opposite signs.

Class (*a*). $+\infty > \gamma_2/\omega \geqslant 0$

In this case the disks are rotating in the same direction and the magnitude of the angular velocity of the fluid varies monotonically with ζ. The radial velocity will be inwards near the slower rotating disk and outwards near the faster, which acts as a centrifugal fan, and the streamlines will be approximately as in Fig. 5. The extreme case $\gamma_2/\omega = 0$ has been

considered recently by Casal (**3**), who showed how the equations (15) and (16) can be integrated by expanding the velocities as power series in $d^2\omega/\nu$ which are convergent when $d^2\omega/\nu < 0{\cdot}17$.

An interesting situation arises when the Reynolds number $d^2\omega/\nu$ becomes very large. The effect of the no-slip condition is then confined to thin layers near each disk and the flow outside these layers is approximately as for a frictionless fluid, i.e. the angular velocity in this region is approximately independent of ζ. The streamlines are sketched in Fig. 6. The

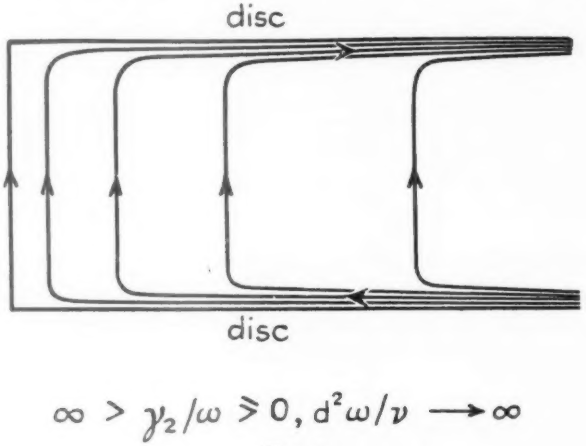

FIG. 6

uniform angular velocity in the interior of the fluid will presumably have a value such that the axial flow away from the slower rotating disk (considered as a disk rotating in a semi-infinite fluid which has constant angular velocity far from the disk) is just equal to the axial flow towards the faster rotating disk (considered in the same way). Thus if $V(\gamma_1/\omega)$ is the axial velocity far from a disk which has angular velocity ω in a semi-infinite fluid which has angular velocity γ_1 far from the disk, the angular velocity Ω in the region between the two disks at large Reynolds number is given by

$$V(\Omega/\omega) = -V(\Omega/\gamma_2). \tag{21}$$

The consideration of a single disk in a semi-infinite fluid showed that there will be a solution of this equation provided that, as already supposed, Ω is intermediate between ω and γ_2.

Class (*b*). $0 > \gamma_2/\omega > -\infty$

The disks now rotate in opposite directions and there is some plane between the disks on which the value of v_θ is zero. Thus the radial flow in the neighbourhood of each disk will be outward, with an inward radial

flow in the interior of the fluid, as sketched in Fig. 7. As in the case of the semi-infinite fluid there will be a division of the flow into two self-contained regions, the dividing plane on which $v_z = 0$ being not necessarily identical (so far as can be seen without detailed numerical work) with the plane on which $v_\theta = 0$. The dividing plane coincides with the upper disk (angular

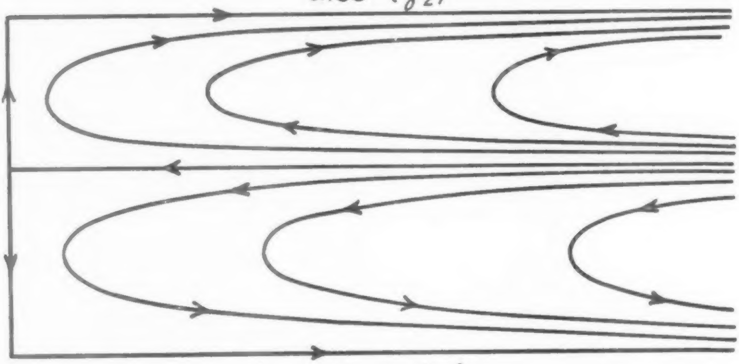

FIG. 7

velocity γ_2) when $\gamma_2/\omega = 0$ and moves down to the lower disk as γ_2/ω decreases from 0 to $-\infty$.

The case of very large Reynolds number is again very interesting. The effect of viscosity falls off rapidly with distance from each disk and outside thin layers near each disk the angular velocity is uniform and the streamlines in a plane through the axis are axial. The uniform axial motion outside the boundary layers will normally be from the slower to the faster rotating disk. However, the magnitude of the angular velocity decreases with distance from each disk and each disk must therefore act, locally at least, as a centrifugal fan. In the immediate neighbourhood of each disk the axial velocity must therefore be towards the disks, and the axial velocity must change sign somewhere between the disks. The means whereby this can happen have already been explored; the flow in the boundary layer near one disk (the slower) is presumably as sketched in Fig. 4, and near the other (the faster) as in Fig. 2. The streamlines thus have the

general shape shown in Fig. 8, which is drawn for the case $|\gamma_2| < |\omega|$. When $|\gamma_2|$ decreases to zero the outward radial flow near the upper disk vanishes and the flow reverts to that obtained by inverting Fig. 6. The angular velocity Ω in the region outside the two boundary layers is again determined by the equation

$$V(\Omega/\omega) = -V(\Omega/\gamma_2),$$

where V has the same meaning as in (21). Since Ω has the same sign

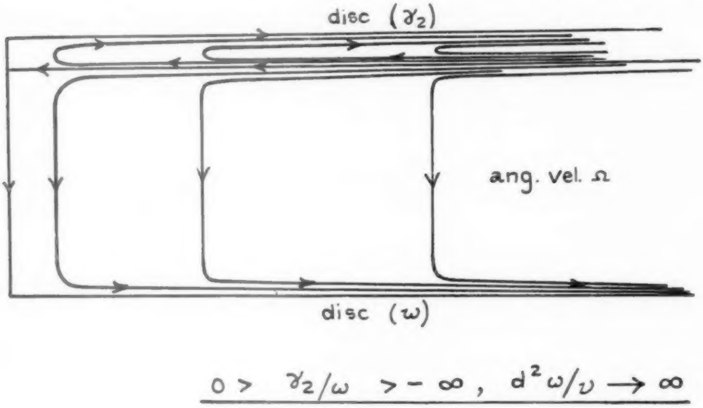

Fig. 8

as whichever of ω and γ_2 has the greater magnitude (so one believes intuitively), consistency of this equation for Ω with Figs. 1, 2, and 4 requires that

$$\text{if} \quad |\gamma_2/\omega| < 1, \quad \text{then} \quad 0 < \Omega/\omega < 1,$$

and reciprocally,

$$\text{if} \quad |\gamma_2/\omega| > 1, \quad \text{then} \quad 0 < \Omega/\gamma_2 < 1.$$

There does not appear to be any mathematical reason why there should not exist a solution for which the boundary layer on the faster rotating disk is the one in which the angular velocity changes direction. The axial velocity in the region outside the two boundary layers is in this case from the faster to the slower rotating disk. However, the solution would very probably be unstable, unlike that described above. The situation bears some resemblance to two-dimensional viscous flow through a diverging channel, and the analogy is closer if we imagine the two plane walls of the channel to be moving in their planes in the direction of flow at different speeds. There will be a region of reversed flow near one of the walls and two different solutions will be possible. But again it is probable that only the solution which gives reversed flow near the slower moving plane is stable.

The case $\gamma_2 = -\omega$ is singular, because there must then be a possible distribution of velocities symmetrical about the mid-plane (just as there is a singular symmetrical solution for flow in the diverging channel when the two planes have equal speeds—or in particular are stationary). Symmetry about the mid-plane implies that the boundary layers on each disk are mirror images of each other and that the axial velocity immediately

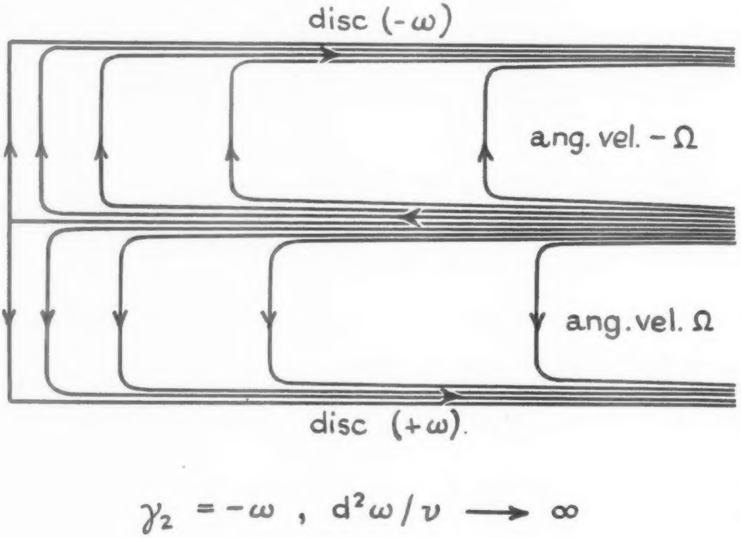

FIG. 9

outside each boundary layer is in each case towards the disk. Somewhere in the interior of the fluid the axial velocity must change appreciably and must reverse its direction. This cannot happen in the absence of a strong viscous effect, so that there is apparently a transition layer of rapid change as sketched in Fig. 9. The axial velocity and the angular velocity both change sign within this layer, while outside it (and outside the disk boundary layers) they are constant.

This singular solution may not be realizable experimentally, of course, but it has some intrinsic interest. For instance, it indicates that there is yet another solution of the type considered herein. The central transition layer is not directly connected with the two boundary layers (and in the limit of infinitely large Reynolds number, its position is arbitrary, provided it does not overlap with either of two of the boundary layers) and can be regarded as a transition region between two semi-infinite masses of fluid rotating with equal and opposite angular velocities $\mp\Omega$. Such a flow is

described by equations (15) and (16) (with $c = \Omega^2 - \omega^2$; note also that the reference angular velocity ω ought now to be replaced by Ω) with the new boundary conditions

$$h = h'' = 0, \qquad g = 0, \quad \text{at} \quad \zeta = 0,$$

and

$$h' \to 0, \quad g \to \mp\Omega/\omega, \quad \text{as} \quad \zeta \to \mp\infty.$$

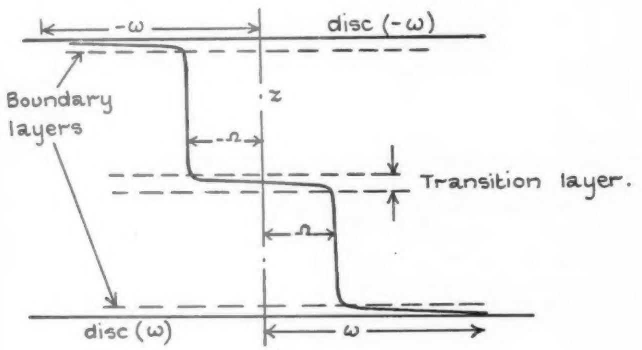

Distribution of angular velocity between the discs.
$(\gamma_2 = -\omega,\ d^2\omega/\nu \to \infty)$.

FIG. 10

If this solution gives an asymptotic axial flow $U(\Omega/\omega)$ away from the transition layer, the condition which determines the angular velocities $\mp\Omega$ in the non-viscous regions of the flow in Fig. 9 is

$$U(\Omega/\omega) = -V(\Omega/\omega),$$

which will have a solution provided $|\Omega| < |\omega|$. The angular velocity of the fluid between two disks evidently varies with z in the manner shown in Fig. 10.

REFERENCES

1. T. v. KÁRMÁN, *Zeits. f. angew. Math. u. Mech.* **1** (1921), 244.
2. S. GOLDSTEIN (ed.), *Modern Developments in Fluid Dynamics* (Oxford, 1938), Section 28.
3. P. CASAL, *C.R. Acad. Sci.* **230** (1950), 178.
4. D. M. HANNAH, *Brit. A.R.C.* Paper No. 10,482 (1947).
5. F. HOMANN, *Zeits. f. angew. Math. u. Mech.* **16** (1936), 153.
6. W. G. COCHRAN, *Proc. Camb. Phil. Soc.* **30** (1934), 365.

THE VELOCITY DISTRIBUTION IN THE LAMINAR BOUNDARY LAYER BETWEEN PARALLEL STREAMS

By R. C. LOCK (*Gonville and Caius College, Cambridge*)

[Received 13 June 1950]

SUMMARY

A method is given for obtaining the solution of the laminar boundary layer equations for the steady flow of a stream of viscous incompressible fluid over a parallel stream of different density and viscosity. An approximate solution is also obtained by means of the momentum equation. It is shown that the solutions depend only on the ratio U_2/U_1 of the velocities of the two streams and on the product $\rho\mu$ of the corresponding density and viscosity ratios. Numerical results are given, in the case where the lower fluid is at rest, for four values of $\rho\mu$, and also when $\rho\mu = 1$, for one non-zero value of the velocity ratio.

1. Introduction

In a paper on the stability of the flow of a stream of fluid over a layer of the same fluid at rest, Lessen (**1**) has obtained the velocity distribution of steady motion in the free laminar boundary layer separating the two streams, using a method equivalent to that of Blasius for the boundary layer on a flat plate. In the present paper the more general problem, when the two fluids are of different densities and viscosities, is considered. Sir Geoffrey Taylor, in an unpublished note, has already given a simple approximate solution by von Kármán's momentum integral method, but it was thought worth while to investigate the accurate solutions of the boundary layer equations for this case, since it is hoped later to consider the problem of the stability of the same motion.

2. The boundary layer equations

We consider the two-dimensional motion of a stream of fluid with velocity U_1, density ρ_1, and viscosity μ_1, over a parallel stream with velocity U_2, density ρ_2, and viscosity μ_2. Both fluids are assumed to be incompressible.

We take the axis of x to be horizontal, in the direction of motion of the free streams, and the axis of y to be vertically upwards. The origin is taken as the point at which the two fluids are supposed first to come into contact (see Fig. 1). The corresponding components of velocity are u and v.

On the usual assumptions that the change of velocity from U_2 to U_1 takes place in a layer of small thickness, and that v is everywhere small compared

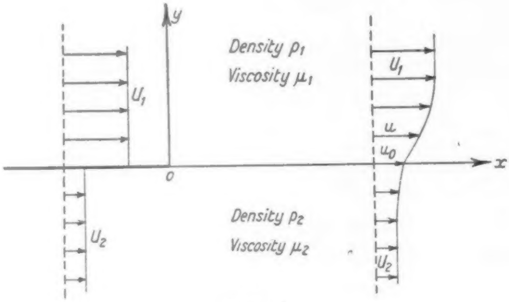

FIG. 1

with u, the boundary layer equations are

$$u\frac{\partial u}{\partial x}+v\frac{\partial u}{\partial y}=\nu_1\frac{\partial^2 u}{\partial y^2} \tag{1}$$

for the upper fluid, and

$$u\frac{\partial u}{\partial x}+v\frac{\partial u}{\partial y}=\nu_2\frac{\partial^2 u}{\partial y^2} \tag{2}$$

for the lower fluid, where ν_1 and ν_2 are the kinematic viscosities of the two fluids.

The equation of continuity is

$$\frac{\partial u}{\partial x}+\frac{\partial v}{\partial y}=0, \tag{3}$$

so that there exists a stream function ψ such that

$$u=\frac{\partial\psi}{\partial y},\qquad v=-\frac{\partial\psi}{\partial x}.$$

In order to solve equation (1) we use the non-dimensional variable

$$\eta_1=\left(\frac{U_1}{\nu_1 x}\right)^{\frac{1}{2}}y \tag{4}$$

and look for a solution in which

$$\psi=(\nu_1 U_1 x)^{\frac{1}{2}}f_1(\eta_1). \tag{5}$$

Then

$$u=U_1 f_1'(\eta_1), \tag{6}$$

$$v=\frac{1}{2}\left(\frac{U_1\nu_1}{x}\right)^{\frac{1}{2}}\{\eta_1 f_1'(\eta_1)-f_1(\eta_1)\} \tag{7}$$

and

$$\frac{\partial u}{\partial y}=U_1\left(\frac{U_1}{\nu_1 x}\right)^{\frac{1}{2}}f_1''(\eta_1). \tag{8}$$

Equation (1) then reduces to

$$2\frac{d^3f_1}{d\eta_1^3}+f_1\frac{d^2f_1}{d\eta_1^2}=0. \tag{9}$$

In the lower fluid it is convenient to use a different variable η_2 defined by

$$\eta_2=\left(\frac{U_1}{\nu_2 x}\right)^{\frac{1}{2}}y, \tag{10}$$

so that

$$\eta_2=\left(\frac{\nu_1}{\nu_2}\right)^{\frac{1}{2}}\eta_1,$$

and to put

$$\psi=(\nu_2 U_1 x)^{\frac{1}{2}}f_2(\eta_2). \tag{11}$$

Then

$$u=U_1 f_2'(\eta_2), \tag{12}$$

$$v=\frac{1}{2}\left(\frac{U_1\nu_2}{x}\right)^{\frac{1}{2}}\{\eta_2 f_2'(\eta_2)-f_2(\eta_2)\} \tag{13}$$

and

$$\frac{\partial u}{\partial y}=U_1\left(\frac{U_1}{\nu_2 x}\right)^{\frac{1}{2}}f_2''(\eta_2). \tag{14}$$

Equation (2) then reduces to

$$2\frac{d^3f_2}{d\eta_2^3}+f_2\frac{d^2f_2}{d\eta_2^2}=0. \tag{15}$$

Boundary conditions

The boundary conditions at infinity are

$$u\to U_1 \quad \text{as} \quad \eta_1\to+\infty$$

and

$$u\to U_2 \quad \text{as} \quad \eta_2\to-\infty,$$

so that

$$f_1'\to 1 \quad \text{as} \quad \eta_1\to+\infty \tag{16}$$

and

$$f_2'\to\frac{U_2}{U_1} \quad \text{as} \quad \eta_2\to-\infty. \tag{17}$$

Since the motion is steady, the interface between the fluids is the streamline $\psi=0$ which passes through the origin, and is therefore given by

$$f_1=f_2=0.$$

If η_2^0 is the value of η_2 such that $f_2(\eta_2^0)=0$, then we must have also

$$f_1(\eta_1^0)=0,$$

where

$$\eta_1^0=\left(\frac{\nu_2}{\nu_1}\right)^{\frac{1}{2}}\eta_2^0.$$

(It will appear later that $\eta_1^0=\eta_2^0=0$ unless $\rho_1=\rho_2$.)

The other conditions to be satisfied at the interface are that the velocity and the normal and transverse components of stress should be continuous. We must therefore have

$$f_1'(\eta_1^0) = f_2'(\eta_2^0), \tag{18}$$

which ensures that both u and v shall be continuous, even if $\eta_1^0 \neq 0$.

The *tangential stress* is $\mu(\partial u/\partial y)$ approximately; using equations (8) and (14) we see that this will be continuous provided that

$$\rho_1 \nu_1^{\frac{1}{2}} f_1''(\eta_1^0) = \rho_2 \nu_2^{\frac{1}{2}} f_2''(\eta_2^0). \tag{19}$$

This result may also be obtained from considerations of momentum. For, if the boundary between the two fluids is given by $y = y_0(x)$, then, since there are no solid boundaries and therefore no frictional resistance to the motion as a whole,

$$\int_{y_0}^{\infty} \rho_1 u(U_1-u)\, dy + \int_{-\infty}^{y_0} \rho_2 u(U_2-u)\, dy = 0.$$

In terms of the variables η_1 and η_2 this becomes

$$\rho_1 \nu_1^{\frac{1}{2}} \int_{\eta_1^0}^{\infty} \rho_1 f_1'(1-f_1')\, d\eta_1 + \int_{-\infty}^{\eta_2^0} \rho_2 f_2'\left(\frac{U_2}{U_1}-f_2'\right) d\eta_2 = 0.$$

Using the fact that

$$\int f'^2\, d\eta = ff' - \int ff''\, d\eta$$
$$= ff' + 2f'',$$

from (9) or (15), we get

$$\rho_1 \nu_1^{\frac{1}{2}}\left[f_1 - f_1 f_1' - 2f_1''\right]_{\eta_1^0}^{\infty} + \rho_2 \nu_2^{\frac{1}{2}}\left[\frac{U_2}{U_1} f_2 - f_2 f_2' - 2f_2''\right]_{-\infty}^{\eta_2^0} = 0.$$

Now $f_1'(\infty) = 1$, $f_1''(\infty) = 0$, and it can be shown that

$$\lim_{\eta_1 \to \infty} f_1(1-f_1') = 0;$$

similarly $f_2'(-\infty) = \dfrac{U_2}{U_1}$, $f_2''(-\infty) = 0$, and $\lim\limits_{\eta_2 \to -\infty} f_2\left(\dfrac{U_2}{U_1}-f_2'\right) = 0$, and also $f_1(\eta_1^0) = f_2(\eta_2^0) = 0$.

Therefore, $\rho_1 \nu_1^{\frac{1}{2}} f_1''(\eta_1^0) = \rho_2 \nu_2^{\frac{1}{2}} f_2''(\eta_2^0)$ as before.

The *normal stress* is

$$p_{yy} = -p + 2\mu \frac{\partial v}{\partial y}.$$

It is easy to see that if $\mu(\partial u/\partial y)$ is continuous, then $\mu(\partial v/\partial y)$ will also be continuous. The pressure p must, therefore, also be continuous at the interface.

Now the variation in $p/(\rho_1 U_1^2)$ across the boundary layer is known to be of order $(\delta/x)^2$, where δ is the boundary layer thickness. On the other hand, the difference between the hydrostatic pressures at the two sides of the interface is given by

$$\frac{p_1-p_2}{\rho_1 U_1^2} = \left(1-\frac{\rho_2}{\rho_1}\right)\frac{gy_0}{U_1^2}$$

$$= \left(1-\frac{\rho_2}{\rho_1}\right) g \left(\frac{\nu_1 x}{U_1}\right)^{\frac{1}{2}} \frac{\eta_1^0}{U_1^2},$$

and, if $\rho_1 \neq \rho_2$ and η_1^0 is of order unity, this is of order δ/x. Thus when $\rho_1 < \rho_2$ it is evident that η_1^0 must be small, of order δ/x, and may be taken as a sufficient approximation to be zero, so that the effect of gravity will be to maintain the interface horizontal.

In this case, therefore, the solution of equations (9) and (15) is completely determined by the boundary conditions

$$f_1'(\infty) = 1, \tag{20}$$

$$f_2'(-\infty) = \frac{U_2}{U_1}, \tag{21}$$

$$f_1(0) = f_2(0) = 0, \tag{22}$$

$$f_1'(0) = f_2'(0), \tag{23}$$

and

$$\rho_1 \nu_1^{\frac{1}{2}} f_1''(0) = \rho_2 \nu_2^{\frac{1}{2}} f_2''(0). \tag{24}$$

When $\rho_1 = \rho_2$, however, gravity has no effect and η_1^0 is left apparently arbitrary (see **1**). This does not in fact materially affect the solution; there are certainly an infinity of solutions of the equation

$$ff''+2f''' = 0$$

which satisfy the boundary conditions

$$f'(\infty) = 1, \qquad f'(-\infty) = \frac{U_2}{U_1},$$

but if f and g are any two such solutions it is easy to see that they must be connected by a relation of the form

$$f(\eta) = g(\eta+b),$$

where b is a constant, so that also $f'(\eta) = g'(\eta+b)$.
The difference between the two solutions is, therefore, simply equivalent to a shift of the velocity distribution as a whole in the y-direction.

In a given physical case, however, there must be a unique solution and a definite value of η_1^0. In order to fix this it will be necessary to specify a

further condition at infinity. Now it can be shown that the displacements of the streamlines at great distances from the interface are

$$\delta_1^* = \left(\frac{\nu_1 x}{U_1}\right)^{\frac{1}{2}} \lim_{\eta_1\to\infty} (\eta_1 - f_1)$$

for the upper stream and

$$\delta_2^* = \left(\frac{\nu_2 x}{U_1}\right)^{\frac{1}{2}} \lim_{\eta_2\to\infty} (\eta_2 - f_2)$$

for the lower stream. These displacements will depend on the value of η_1^0, so that one of them may be chosen arbitrarily without interfering with the flow in the boundary layer, and the physical conditions will then be fixed completely. (If $U_2 = 0$ only δ_1^* has any meaning and this may be chosen arbitrarily.) It should be noted that the situation is quite different from the case of boundary layer flow along a flat plate, when the presence of a constraint at infinity, such as a wind-tunnel wall, will cause definite interference.

3. Approximate solutions by the momentum equation method

Before discussing the accurate numerical solutions of equations (9) and (15) it seems of interest to obtain some idea of the general nature of the velocity distributions by means of von Kármán's momentum equation (**2**, p. 131).

The momentum equations in this case reduce to

$$\frac{\tau_0}{\rho_1} = \nu_1\left(\frac{\partial u}{\partial y}\right)_{y\to 0+} = \frac{\partial}{\partial x}\int_0^{\delta_1} (U_1 - u)u\,dy, \tag{25}$$

for the upper fluid, and

$$\frac{\tau_0}{\rho_2} = \nu_2\left(\frac{\partial u}{\partial y}\right)_{y\to 0-} = \frac{\partial}{\partial x}\int_0^{-\delta_2} (U_2 - u)u\,dy, \tag{26}$$

for the lower fluid, where τ_0 is the skin friction and δ_1 and δ_2 are the boundary-layer thicknesses on either side of the interface.

In the upper fluid, we suppose that

$$\frac{u}{U_1} = \phi_1(\eta_1^*),$$

where

$$\eta_1^* = \frac{y}{\delta_1}.$$

Then equation (25) becomes

$$\frac{\nu_1}{U_1}\phi_1'(0) = \delta_1 \frac{d\delta_1}{dx}\int_0^1 (\phi_1 - \phi_1^2)\,d\eta_1^*,$$

whence

$$\frac{2\nu_1 x}{U_1}\phi_1'(0) = \delta_1^2 \int_0^1 (\phi_1 - \phi_1^2)\,d\eta_1^*. \tag{27}$$

In the lower fluid, we suppose similarly that

$$\frac{u}{U_1} = \phi_2(\eta_2^*),$$

where
$$\eta_2^* = -\frac{y}{\delta_2},$$

and then equation (26) becomes

$$\frac{2\nu_2 x}{U_1}\phi_2'(0) = \delta_2^2\int\limits_0^1 (\lambda\phi_2-\phi_2^2)\,d\eta_2^*, \tag{28}$$

where
$$\lambda = \frac{U_2}{U_1}.$$

If we write
$$I_1 = \int\limits_0^1 (\phi_1-\phi_1^2)\,d\eta_1^*,$$

$$I_2 = \int\limits_0^1 (\lambda\phi_2-\phi_2^2)\,d\eta_2^*,$$

and eliminate x from equations (27) and (28), making use of the relations

$$\tau_0 = \frac{\mu_1}{\delta_1}\phi_1'(0) = -\frac{\mu_2}{\delta_2}\phi_2'(0),$$

we get
$$\rho\delta I_2+I_1 = 0, \tag{29}$$

where $\delta = \dfrac{\delta_2}{\delta_1}$ and $\rho = \dfrac{\rho_2}{\rho_1}$.

The functions ϕ_1 and ϕ_2 may be chosen so that they satisfy as many of the conditions

$$\phi_1(1) = 1,\ \phi_1'(1) = \phi_1''(1) = ... = 0,$$
$$\phi_1''(0) = \phi_1'''(0) = ... = 0,$$
$$\phi_1(0) = \phi_2(0),$$
$$\frac{\mu_1}{\delta_1}\phi_1'(0) = -\frac{\mu_2}{\delta_2}\phi_2'(0),$$
$$\phi_2''(0) = \phi_2'''(0) = ... = 0,$$
$$\phi_2(1) = \lambda,\ \phi_2'(1) = \phi_2''(1) = ... = 0$$

as is convenient. The integrals I_1 and I_2 can then be evaluated, and δ found from equation (29).

3.1 In suggesting this problem, Sir Geoffrey Taylor pointed out the possibility of using the simple expressions

$$\phi_1 = 1+(c-1)e^{-\eta_1^*} \tag{30}$$

and
$$\phi_2 = \lambda+(c-\lambda)e^{-\eta_2^*} \quad (\text{with } \lambda = 0). \tag{31}$$

The boundary conditions at $\eta_1^* = 1$, $\eta_2^* = 1$ are now replaced by similar conditions at infinity, all of which are satisfied. The conditions

$$\phi_1(0) = \phi_2(0) = c,$$

and $\delta\phi_1'(0) = -\mu\phi_2'(0)$, where $\mu = \mu_2/\mu_1$, are also satisfied, provided that

$$c = \frac{\delta+\mu\lambda}{\delta+\mu}. \tag{32}$$

Then
$$I_1 = \int\limits_0^\infty (\phi_1-\phi_1^2)\,d\eta_1^* = \tfrac{1}{2}(1-c^2),$$

and
$$I_2 = \int\limits_0^\infty (\lambda\phi_2-\phi_2^2)\,d\eta_2^* = \tfrac{1}{2}(\lambda^2-c^2).$$

Substituting these expressions in (29) and using the value of c given by (32), we obtain eventually the equation

$$\mu[2\delta+\mu(1+\lambda)] = \rho\delta^2[\delta(1+\lambda)+2\mu\lambda]. \tag{33}$$

This may be written in the form

$$\left(\frac{\delta}{\mu}\right)^2 = \frac{1}{\rho\mu}\frac{\{2(\delta/\mu)+1+\lambda\}}{[(\delta/\mu)(1+\lambda)+2\lambda]} \tag{34}$$

which is suitable for solution by successive approximations, the first approximation when $\rho\mu$ is large being

$$\frac{\delta}{\mu} = \left(\frac{1+\lambda}{2\lambda\rho\mu}\right)^{\frac{1}{2}} \quad \text{if} \quad \lambda > 0$$

or
$$\frac{\delta}{\mu} = (\rho\mu)^{-\frac{1}{3}} \quad \text{if} \quad \lambda = 0.$$

The velocity u_0 at the interface is given by (32);

thus
$$\frac{u_0}{U_1} = c = \frac{\lambda+(\delta/\mu)}{1+(\delta/\mu)},$$

so that $u_0 = \dfrac{U_2+U_1(\delta/\mu)}{1+(\delta/\mu)} \doteqdot U_2+U_1(\delta/\mu)$ if $\rho\mu$ is large.

The skin friction τ_0 at the interface is given by

$$\tau_0 = \frac{\mu_1}{\delta_1}U_1\phi_1'(0),$$

so that the skin friction coefficient is

$$c_{\tau_0} = \frac{\tau_0}{\rho_1 U_1^2}\left(\frac{U_1 x}{\nu_1}\right)^{\frac{1}{2}} = \left(\frac{I_1\phi_1'(0)}{2}\right)^{\frac{1}{2}}. \tag{35}$$

In this case
$$c_{\tau_0} = \tfrac{1}{2}(1-c)(1+c)^{\frac{1}{2}}.$$

The first approximation when $\rho\mu$ is large is

$$c_{\tau_0} = \tfrac{1}{2}(1-\lambda)(1+\lambda)^{\frac{1}{2}}, \tag{36}$$

being in fact the limit as $\rho\mu$ tends to infinity, which is the value for a solid lower boundary moving with velocity U_2.

3.2. A better approximation should be obtained by taking the functions ϕ_1 and ϕ_2 to be quartic polynomials in η_1^* and η_2^*.

Thus
$$\phi_1 = c+(1-c)(2\eta_1^*-2\eta_1^{*3}+\eta_1^{*4}) \tag{37}$$
and
$$\phi_2 = c+(\lambda-c)(2\eta_2^*-2\eta_2^{*3}+\eta_2^{*4}) \tag{38}$$
satisfy the conditions

$$\phi_1(1) = 1, \quad \phi_1'(1) = 0, \quad \phi_1''(1) = 0,$$
$$\phi_2(1) = \lambda, \quad \phi_2'(1) = 0, \quad \phi_2''(1) = 0,$$
$$\phi_1(0) = \phi_2(0) = c,$$
$$\phi_1''(0) = \phi_2''(0) = 0,$$
and
$$\delta\phi_1'(0) = -\mu\phi_2'(0),$$

provided that $c = \dfrac{\delta+\mu\lambda}{\delta+\mu}$ as before (equation (32)).

Then
$$I_1 = \tfrac{37}{315}+\tfrac{41}{630}c-\tfrac{23}{126}c^2$$
and
$$I_2 = \tfrac{37}{315}\lambda^2+\tfrac{41}{630}c\lambda-\tfrac{23}{126}c^2,$$
and the equation corresponding to (34) is

$$\left(\frac{\delta}{\mu}\right)^2 = \frac{1}{\rho\mu}\frac{[189(\delta/\mu)+74+115\lambda]}{[(\delta/\mu)(74\lambda+115)+189\lambda]}. \tag{39}$$

When $\rho\mu$ is large, the first approximation to δ/μ is

$$\frac{\delta}{\mu} = \left(\frac{74+115\lambda}{189\lambda\rho\mu}\right)^{\frac{1}{2}} \quad \text{if} \quad \lambda > 0,$$
or
$$\frac{\delta}{\mu} = 0{\cdot}857(\mu\rho)^{-\frac{1}{3}} \quad \text{if} \quad \lambda = 0.$$

The velocity at the interface is given as before by equation (32), and the skin friction coefficient is given by equation (35), the first approximation when $\rho\mu$ is large being

$$c_{\tau_0} = 0{\cdot}343(1-\lambda)(1+1{\cdot}556\lambda)^{\frac{1}{2}}.$$

3.3. Good results have also been obtained in the case of flow along a flat plate by taking the velocity profile to be part of a sine curve. This suggests trying
$$\phi_1 = c+(1-c)\sin\tfrac{1}{2}\pi\eta_1^* \tag{40}$$
and
$$\phi_2 = c+(\lambda-c)\sin\tfrac{1}{2}\pi\eta_2^*, \tag{41}$$

which satisfy the conditions

$$\phi_1(1) = 1, \qquad \phi_1'(1) = 0,$$
$$\phi_2(1) = \lambda, \qquad \phi_2'(1) = 0,$$
$$\phi_1(0) = \phi_2(0) = c,$$
$$\phi_1''(0) = \phi_2''(0) = 0$$

and

$$\delta\phi_1'(0) = -\mu\phi_2'(0),$$

provided that c is given as before by equation (32).

Then

$$I_1 = \left(\frac{2}{\pi}-\frac{1}{2}\right)+2c\left(1-\frac{3}{\pi}\right)+c^2\left(\frac{4}{\pi}-\frac{3}{2}\right),$$
$$I_2 = \left(\frac{2}{\pi}-\frac{1}{2}\right)\lambda^2+2c\lambda\left(1-\frac{3}{\pi}\right)+c^2\left(\frac{4}{\pi}-\frac{3}{2}\right),$$

and the equation for δ/μ is

$$\left(\frac{\delta}{\mu}\right)^2 = \frac{1}{\rho\mu}\frac{[(2\pi-4)(\delta/\mu)+(3\pi-8)\lambda+(4-\pi)]}{[(\delta/\mu)\{(3\pi-8)+(4-\pi)\lambda\}+(2\pi-4)\lambda]}. \tag{42}$$

The first approximation to δ/μ is

$$\frac{\delta}{\mu} = \left(\frac{1\cdot425\lambda+0\cdot858}{2\cdot283\lambda\rho\mu}\right)^{\frac{1}{2}} \quad \text{if} \quad \lambda > 0,$$

or

$$\frac{\delta}{\mu} = 0\cdot844(\mu\rho)^{-\frac{1}{3}} \quad \text{if} \quad \lambda = 0.$$

The velocity at the interface and the skin friction coefficient are given as before by equations (32) and (35), the first approximation to the latter when $\rho\mu$ is large being

$$c_{\tau_0} = 0\cdot328(1-\lambda)(1+1\cdot657\lambda)^{\frac{1}{2}}.$$

The velocity and skin friction coefficients at the interface have been calculated, using equations (39) and (42), for the values $5\cdot965\times10^4$, 100, 10, and 1 for $\rho\mu$, with $\lambda = 0$, and also for $\rho\mu = 1$, with $\lambda = 0\cdot25$, $0\cdot501$, and $0\cdot75$. They are compared in Table I of section 5 with the values obtained by accurate numerical integration of the differential equation. The agreement is quite good in all cases; the method of section 3.3 gives the best results for the velocity at the interface, and the method of section 3.2 for the skin friction.

4. The integration of the exact boundary layer equations

4.1. *Asymptotic expansions*

Before it is possible to start the numerical integration of the boundary-layer equations it is first necessary to investigate the asymptotic forms which the solutions of the equation

$$2f'''(\eta)+f(\eta)f''(\eta) = 0 \tag{43}$$

take when η is large.

This equation has the property (see e.g. **1**) that, if $f(\eta)$ is any solution, then $g(\xi)$ is also a solution, provided that

$$\xi = a\eta + b$$

and
$$f(\eta) = ag(\xi),$$

where a and b are any constants. Then

$$f'(\eta) = a^2 g'(\xi),$$
$$f''(\eta) = a^3 g''(\xi),$$

and so on, where dashes denote derivatives.

We will first suppose that $f'(\eta) \to \lambda$ as $\eta \to -\infty$. There are two cases to be considered, $\lambda = 0$ and $\lambda > 0$. In the first case, when $\lambda = 0$, we can suppose that $f(\eta) \to -a$ as $\eta \to -\infty$, where a is a constant. If we substitute $-a$ for f in equation (43) and integrate three times, we get

$$f(\eta) \sim -a + Ae^{\frac{1}{2}a\eta},$$

where A is a constant. This suggests that we try the expansion

$$f(\eta) = A_0 + A_1 e^{\frac{1}{2}a\eta} + A_2 e^{a\eta} + A_3 e^{\frac{3}{2}a\eta} + \dots.$$

Substituting in (43), and equating to zero the coefficients of successive powers of $e^{\frac{1}{2}a\eta}$, we obtain the recurrence relations

$$aA_1 + A_0 A_1 = 0,$$
$$8aA_2 + 4A_0 A_2 + A_1^2 = 0,$$
$$27aA_3 + 9A_0 A_3 + 5A_1 A_2 = 0,$$
$$\dots\dots\dots\dots$$

Hence $A_0 = -a$ and A_1 may be chosen arbitrarily. A standard solution $g(\xi)$ may be obtained by putting $a = 1$, $A_1 = 1$; then

$$g(\xi) = -1 + e^{\frac{1}{2}\xi} - \tfrac{1}{4}e^{\xi} + \tfrac{5}{72}e^{\frac{3}{2}\xi} - \tfrac{17}{864}e^{2\xi} + \dots. \tag{44}$$

Any other solution with the same boundary condition can be obtained from this by making use of the property mentioned above. The expansion (44) is in fact convergent for $\xi \leqslant 0$.

In the second case, if $\lambda > 0$, we can assume that

$$\lim_{n \to -\infty} (f - \lambda\eta) = B,$$

where B is a constant. Equation (43) then becomes approximately

$$2f''' + (\lambda\eta + B)f'' = 0,$$

the solution of which may be written

$$f'' \sim A\lambda \exp\left\{-\tfrac{1}{4}\lambda\left(\eta + \frac{B}{\lambda}\right)^2\right\},$$

where A is a constant, so that

$$f' \sim \lambda+2A\lambda^{\frac{1}{2}}\operatorname{erf}\left\{-\tfrac{1}{2}\lambda^{\frac{1}{2}}\left(\eta+\frac{B}{\lambda}\right)\right\},$$

where $$\operatorname{erf} z = \int\limits_{z}^{\infty} e^{-t^2}\,dt,$$

and $$f \sim \lambda\eta+B+2A\lambda^{\frac{1}{2}} \int\limits_{-\infty}^{\eta} \operatorname{erf}\left\{-\tfrac{1}{2}\lambda^{\frac{1}{2}}\left(\eta+\frac{B}{\lambda}\right)\right\}d\eta.$$

Now it is known that an asymptotic expansion for $\operatorname{erf} z$ is

$$\operatorname{erf} z \sim \frac{1}{2}\frac{e^{-z^2}}{z}\left(1-\frac{1}{2z^2}+\frac{1}{2}\cdot\frac{3}{2}\cdot\frac{1}{z^4}-\frac{1}{2}\cdot\frac{3}{2}\cdot\frac{5}{2}\cdot\frac{1}{z^6}+\dots\right).$$

Integration of this expansion leads to

$$f \sim \lambda\eta+B+\frac{Ae^{-z^2}}{z^2}\left(1-\frac{3}{2z^2}+\frac{15}{4z^4}-\dots\right),$$

where $$z = -\tfrac{1}{2}\lambda^{\frac{1}{2}}\left(\eta+\frac{B}{\lambda}\right). \tag{45}$$

A second approximation can be obtained by substituting the expression $\left(\lambda\eta+B+\dfrac{Ae^{-z^2}}{z^2}\right)$ for f in equation (43). We get eventually, when η is large and negative,

$$f \sim \lambda\eta+B+\frac{Ae^{-z^2}}{z^2}\left(1-\frac{3}{2z^2}+\frac{15}{4z^4}-\dots\right)-\frac{1}{8}\frac{A^2e^{-2z^2}}{\lambda^{\frac{1}{2}}z^5}+\dots \tag{46}$$

$$f' \sim \lambda+2A\lambda^{\frac{1}{2}}\operatorname{erf} z-\frac{1}{4}\frac{A^2e^{-2z^2}}{z^4}+\dots \tag{47}$$

and $$f'' \sim A\lambda e^{-z^2}-\tfrac{1}{2}A^2\lambda^{\frac{1}{2}}\frac{e^{-2z^2}}{z^3}+\dots, \tag{48}$$

where z is given by (45).

The corresponding asymptotic expansions for $f(\eta)$ when η is large and positive, and when $\lim\limits_{\eta\to\infty} f'(\eta) = 1$, $\lim\limits_{\eta\to\infty}(f-\eta) = D$, can be obtained in a similar way, or from (46), (47), and (48) by using the fact that $-f(-\eta)$ is also a solution of (43), putting $\lambda = 1$ and writing $-C$ for A, $-D$ for B. They are

$$f \sim \eta+D+\frac{Ce^{-w^2}}{w^2}\left(1-\frac{3}{2w^2}+\frac{15}{4w^4}-\dots\right)+\frac{1}{8}\frac{C^2e^{-2w^2}}{w^5}+\dots \tag{49}$$

$$f' \sim 1-2C\operatorname{erf} w-\frac{1}{4}\frac{C^2e^{-2w^2}}{w^4}+\dots \tag{50}$$

and $$f'' \sim Ce^{-w^2}+\frac{1}{2}\frac{C^2e^{-2w^2}}{w^3}+\dots \tag{51}$$

where $$w = \tfrac{1}{2}(\eta+D)$$

and C is a further arbitrary constant.

4.2. *Methods of numerical integration*

For the case when the lower fluid is at rest, i.e. when $\lambda = 0$, the property mentioned at the beginning of section 4.1 makes it extremely simple to obtain a numerical solution for given values of the density ratio ρ and the viscosity ratio μ. The standard solution $g(\xi)$, defined by equation (44), is first integrated numerically from the differential equation, using (44) as a starting-point, until the zero ξ_0 of $g(\xi)$ is reached. This function $g(\xi)$ can be used in all cases to give the solution for the lower fluid, by choosing appropriate values for the constants a and b. The solution $g_1(\xi)$, for $\xi > \xi_0$, is then defined by the conditions

$$\begin{aligned} g_1(\xi_0) &= 0, \\ g_1'(\xi_0) &= g'(\xi_0), \\ g_1''(\xi_0) &= (\mu\rho)^{\frac{1}{2}} g''(\xi_0). \end{aligned}$$

This function is integrated numerically, starting with a series solution to give a few initial values, until a constant value of $g_1'(\xi)$ is reached. The constants a and b are then given by

$$a = \frac{1}{\sqrt{\{g_1'(\infty)\}}}, \quad b = \xi_0,$$

and it is easy to see that the functions $f_1(\eta_1)$, $f_2(\eta_2)$ defined by

$$\begin{aligned} f_2(\eta_2) &= ag(\xi), \\ f_1(\eta_1) &= ag_1(\xi), \end{aligned}$$

where $$\xi = a\eta_2 + b \quad (\xi < \xi_0)$$

and $$\xi = a\eta_1 + b \quad (\xi > \xi_0),$$

satisfy all the conditions of the problem. It is evident that in this case there is a single infinity of solutions, depending only on the parameter $\rho\mu$.

When λ is not zero, there is a double infinity of solutions, depending on the parameters $\rho\mu$ and λ; and for given values of these parameters it is not easy to find the appropriate solution. If, however, $\rho\mu$ is given, a set of solutions with different (initially unknown) values of λ could be obtained by starting at large positive values of η, with the functions defined by the asymptotic expressions (49) to (51), using a set of values for the arbitrary constant C, and integrating numerically to large negative values of η_2 to find the corresponding values of λ, at the same time satisfying the correct boundary conditions at the interface. Alternatively, the methods of sections 3.2 and 3.3 could be used to obtain approximate values of the velocity and velocity gradient on either side of the interface for given values of $\rho\mu$ and λ. These would define solutions of the differential equation for positive η_1 and negative η_2 which could be integrated numerically,

starting at the origin, until the velocity became constant in both directions. By choosing the scaling factor a in the same way as before an accurate solution would thus be obtained with a value of λ nearly equal to the given value. This seems in fact the best method and has been used in the only example worked out.

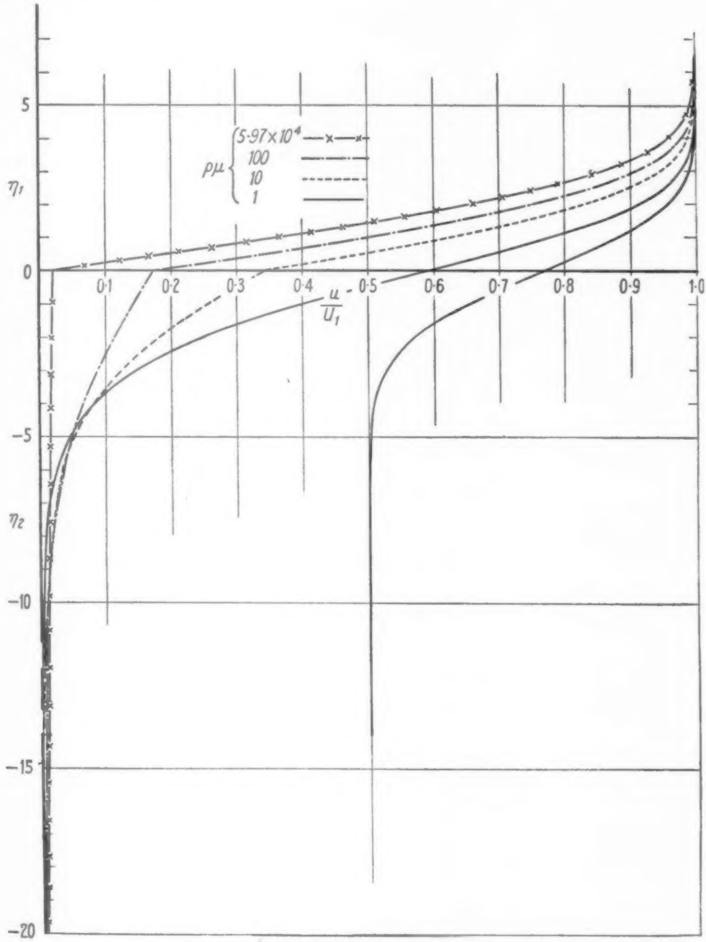

FIG. 2. Velocity distributions.

5. Results

The standard solution $g(\xi)$, defined by equation (44), from which, when $\lambda = 0$, all the solutions for negative η_2 are obtained, is given in Table II. The integration was carried out by means of a step-by-step method,

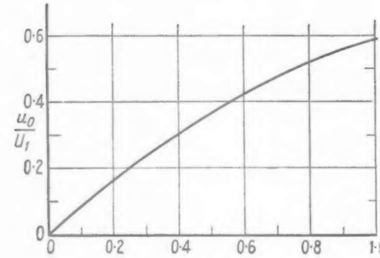

FIG. 3. Velocities at the interface. ($U_2 = 0$.)

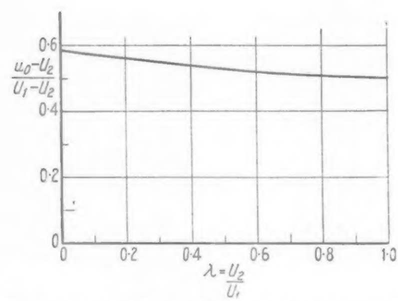

FIG. 4. Velocities at the interface. ($\rho\mu = 1$.)

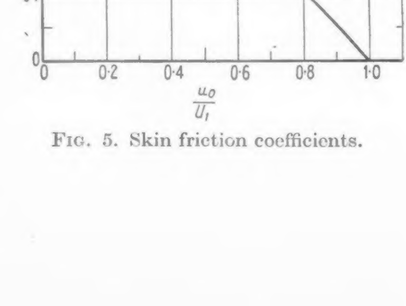

FIG. 5. Skin friction coefficients.

starting at $\xi = -3$, and using five places of decimals, of which four are retained in the table. The values for $\xi < -3$ were calculated from the series (44).

Complete solutions have been obtained, in the case when the lower fluid is at rest ($\lambda = 0$), for $\rho\mu = 5{\cdot}965 \times 10^4$, corresponding to air flowing over water at a temperature of 10° C., and for $\rho\mu = 100$, 10, and 1. (The last solution has evidently been obtained before in the course of the work described in (1), but numerical details were not given.) For the case $\rho\mu = 1$, the solution has also been calculated when the lower fluid is in motion, with $\lambda = 0{\cdot}5$. The numerical results are given in Tables III–VII, and the velocity distributions are shown graphically in Fig. 2.

The principal features of these results are summarized in Table I below, which gives the values of the velocity ratio u_0/U_1 and the skin friction coefficient c_{τ_0} at the interface for the five cases. u_0/U_1 is plotted against $(\rho\mu)^{-\frac{1}{3}}$ for $\lambda = 0$, in Fig. 3, and $(u_0-U_2)/(U_1-U_2)$ is plotted against λ, for $\rho\mu = 1$, in Fig. 4. It is evident that the value of c_{τ_0} depends only on u_0/U_1, whatever the value of λ; c_{τ_0} is therefore plotted against u_0/U_1 in Fig. 5. Values obtained by the approximate methods of 3.2 and 3.3 are also included in the table for comparison.

REFERENCES

1. Martin Lessen, *On the Stability of the Free Laminar Boundary Layer between Parallel Streams*, N.A.C.A. Tech. Note 1929, August 1949 (unpublished).
2. S. Goldstein, *Modern Developments in Fluid Dynamics*, vol. i (Oxford, 1938).

TABLE I

	$\frac{u_0}{U_1}$			$c_{\tau_0} = \frac{\tau_0}{\rho_1 U_1^2}\left(\frac{U_1 x}{\nu_1}\right)^{\frac{1}{2}}$		
	Accurate method	*Method of 3.2*	*Method of 3.3*	*Accurate method*	*Method of 3.2*	*Method of 3.3*
$\lambda = 0,\ \rho\mu = 5{\cdot}965\times 10^4$	0·0211	0·0220	0·0215	0·3318	0·3309	0·3262
$\lambda = 0,\ \rho\mu = 100$	0·1727	0·1770	0·1742	0·3183	0·3186	0·3071
$\lambda = 0,\ \rho\mu = 10$	0·3428	0·3480	0·3440	0·2815	0·2774	0·2693
$\lambda = 0,\ \rho\mu = 1$	0·5873	0·5907	0·5871	0·1996	0·1943	0·1901
$\lambda = 0{\cdot}501,\ \rho\mu = 1$	0·7657	0·7668	0·7661	0·1219	0·1184	0·1155
$\lambda = 0{\cdot}25,\ \rho\mu = 1$	..	0·6678	0·6661	..	0·1603	0·1587
$\lambda = 0{\cdot}75,\ \rho\mu = 1$	..	0·8785	0·8784	..	0·0641	0·0624

TABLE II

The standard solution $g(\xi)$

ξ	$g(\xi)$	$g'(\xi)$	$g''(\xi)$
$-\infty$	-1	0	0
-16	$-0{\cdot}9997$	0·0002	0·0001
-14	$-0{\cdot}9991$	0·0005	0·0002
-12	$-0{\cdot}9975$	0·0012	0·0006
-10	$-0{\cdot}9933$	0·0034	0·0017
-9	$-0{\cdot}9889$	0·0055	0·0028
-8	$-0{\cdot}9818$	0·0091	0·0045
-7	$-0{\cdot}9700$	0·0149	0·0073
-6	$-0{\cdot}9508$	0·0243	0·0119
$-5{\cdot}0$	$-0{\cdot}9196$	0·0394	0·0189
$-4{\cdot}6$	$-0{\cdot}9022$	0·0477	0·0227
$-4{\cdot}2$	$-0{\cdot}8812$	0·0577	0·0271
$-3{\cdot}8$	$-0{\cdot}8558$	0·0695	0·0323
$-3{\cdot}4$	$-0{\cdot}8253$	0·0836	0·0382
$-3{\cdot}0$	$-0{\cdot}7886$	0·1002	0·0449
$-2{\cdot}6$	$-0{\cdot}7447$	0·1196	0·0523
$-2{\cdot}2$	$-0{\cdot}6925$	0·1421	0·0604
$-1{\cdot}8$	$-0{\cdot}6306$	0·1680	0·0690
$-1{\cdot}4$	$-0{\cdot}5576$	0·1974	0·0777
$-1{\cdot}0$	$-0{\cdot}4722$	0·2302	0·0862
$-0{\cdot}6$	$-0{\cdot}3731$	0·2662	0·0938
$-0{\cdot}2$	$-0{\cdot}2589$	0·3050	0·0999
$+0{\cdot}2$	$-0{\cdot}1288$	0·3458	0·1039
0·5537	0	0·3828	0·1051

TABLE III

Solution for the case $\rho\mu = 5{\cdot}965\times10^4$, $\lambda = 0$

η_2	$f_2(\eta_2)$	$\frac{u}{U_1} = f_2'(\eta_2)$	$f_2''(\eta_2)$
$-\infty$	−0·2347	0	0
−60	−0·2344	0·0000	0·00000
−50	−0·2338	0·0001	0·00001
−40	−0·2319	0·0003	0·00004
−30	−0·2256	0·0011	0·00012
−25	−0·2185	0·0019	0·00021
−20	−0·2060	0·0033	0·00036
−18	−0·1987	0·0041	0·00044
−16	−0·1896	0·0050	0·00054
−14	−0·1784	0·0062	0·00064
−12	−0·1646	0·0076	0·00076
−10	−0·1477	0·0093	0·00089
−8	−0·1273	0·0112	0·00103
−6	−0·1027	0·0134	0·00115
−4	−0·0736	0·0158	0·00126
−2	−0·0395	0·0184	0·00133
0	0	0·0211	0·00136

η_1	$f_1(\eta_1)$	$\frac{u}{U_1} = f_1'(\eta_1)$	$f_1''(\eta_1)$
0	0	0·0211	0·3318
0·4	0·0350	0·1537	0·3310
0·8	0·1229	0·2853	0·3261
1·2	0·2628	0·4136	0·3140
1·6	0·4528	0·5353	0·2925
2·0	0·6896	0·6463	0·2612
2·4	0·9680	0·7431	0·2214
2·8	1·2817	0·8228	0·1769
3·2	1·6238	0·8846	0·1324
3·6	1·9871	0·9293	0·0923
4·0	2·3653	0·9594	0·0597
4·4	2·7531	0·9782	0·0358
4·8	3·1468	0·9891	0·0199
5·2	3·5437	0·9949	0·0102
5·6	3·9423	0·9978	0·0048
6·0	4·3417	0·9991	0·0021
6·4	4·7415	0·9997	0·0008
6·8	5·1414	0·9999	0·0003
∞	$\eta_1 - 1{\cdot}6586$	1	0

Table IV

Solution for the case $\rho\mu = 100$, $\lambda = 0$

η_2	$f_2(\eta_2)$	$\frac{u}{U_1} = f_2'(\eta_2)$	$f_2''(\eta_2)$
$-\infty$	−0·6716	0	0
−24·647	−0·6714	0·0001	0·0000
−21·670	−0·6710	0·0002	0·0001
−18·692	−0·6700	0·0006	0·0002
−15·714	−0·6671	0·0015	0·0005
−14·225	−0·6642	0·0025	0·0008
−12·736	−0·6594	0·0041	0·0014
−11·247	−0·6515	0·0067	0·0022
−9·758	−0·6386	0·0110	0·0036
−8·269	−0·6176	0·0178	0·0057
−7·674	−0·6059	0·0215	0·0069
−7·078	−0·5918	0·0260	0·0082
−6·482	−0·5748	0·0314	0·0098
−5·887	−0·5543	0·0377	0·0116
−5·291	−0·5296	0·0452	0·0136
−4·696	−0·5002	0·0539	0·0159
−4·100	−0·4651	0·0641	0·0183
−3·504	−0·4235	0·0758	0·0209
−2·909	−0·3745	0·0890	0·0235
−2·313	−0·3172	0·1038	0·0261
−1·718	−0·2506	0·1201	0·0284
−1·122	−0·1739	0·1376	0·0303
−0·527	−0·0865	0·1560	0·0315
0	0	0·1727	0·0318

η_1	$f_1(\eta_1)$	$\frac{u}{U_1} = f_1'(\eta_1)$	$f_1''(\eta_1)$
0	0	0·1727	0·3183
0·395	0·0929	0·2979	0·3157
0·789	0·2348	0·4208	0·3059
1·184	0·4242	0·5381	0·2870
1·578	0·6581	0·6459	0·2580
1·973	0·9321	0·7405	0·2207
2·367	1·2403	0·8193	0·1782
2·762	1·5763	0·8811	0·1350
3·156	1·9333	0·9264	0·0956
3·551	2·3054	0·9574	0·0629
3·945	2·6873	0·9771	0·0385
4·340	3·0752	0·9887	0·0218
4·734	3·4667	0·9951	0·0114
5·129	3·8600	0·9974	0·0055
5·523	4·2538	0·9989	0·0025
5·918	4·6480	0·9996	0·0010
6·312	5·0424	0·9998	0·0004
6·707	5·4369	0·9999	0·0001
7·101	5·8314	1·0000	0·0001
∞	$\eta_1 - 1·2699$	1	0

TABLE V

Solution for the case $\rho\mu = 10$, $\lambda = 0$

η_2	$f_2(\eta_2)$	$\frac{u}{U_1} = f_2'(\eta_2)$	$f_2''(\eta_2)$
$-\infty$	−0·9462	0	0
−19·608	−0·9461	0·0001	0·0000
−17·495	−0·9459	0·0002	0·0001
−15·381	−0·9454	0·0004	0·0002
−13·267	−0·9439	0·0011	0·0005
−11·154	−0·9399	0·0030	0·0014
−10·097	−0·9357	0·0050	0·0023
−9·040	−0·9290	0·0081	0·0038
−7·983	−0·9179	0·0133	0·0062
−6·926	−0·8997	0·0217	0·0100
−5·869	−0·8701	0·0353	0·0160
−5·447	−0·8537	0·0427	0·0192
−5·024	−0·8338	0·0516	0·0230
−4·601	−0·8098	0·0623	0·0273
−4·178	−0·7809	0·0748	0·0324
−3·756	−0·7462	0·0897	0·0380
−3·333	−0·7047	0·1071	0·0443
−2·910	−0·6552	0·1273	0·0512
−2·488	−0·5967	0·1504	0·0584
−2·065	−0·5276	0·1767	0·0658
−1·642	−0·4468	0·2061	0·0730
−1·219	−0·3530	0·2383	0·0794
−0·797	−0·2450	0·2730	0·0846
−0·374	−0·1219	0·3096	0·0880
0	0	0·3428	0·0890

η_1	$f_1(\eta_1)$	$\frac{u}{U_1} = f_1'(\eta_1)$	$f_1''(\eta_1)$
0	0	0·3428	0·2815
0·423	0·1700	0·4611	0·2767
0·846	0·3893	0·5752	0·2611
1·268	0·6550	0·6802	0·2340
1·691	0·9625	0·7717	0·1974
2·114	1·3051	0·8463	0·1554
2·536	1·6755	0·9031	0·1135
2·959	2·0662	0·9430	0·0764
3·382	2·4708	0·9688	0·0473
3·805	2·8839	0·9842	0·0269
4·227	3·3019	0·9926	0·0140
4·650	3·7225	0·9968	0·0067
5·073	4·1444	0·9987	0·0029
5·496	4·5668	0·9995	0·0012
5·918	4·9894	0·9999	0·0004
6·341	5·4121	1·0000	0·0001
6·764	5·8348	1·0000	0·0000
∞	$\eta_1 - 0·9289$	1	0

Table VI

Solution for the case $\rho\mu = 1$, $\lambda = 0$

η_2	$f_2(\eta_2)$	$\frac{u}{U_1} = f'_2(\eta_2)$	$f''_2(\eta_2)$
$-\infty$	−1·2386	0	0
−14·980	−1·2384	0·0001	0·0001
−13·365	−1·2381	0·0003	0·0002
−11·751	−1·2374	0·0007	0·0004
−10·136	−1·2355	0·0019	0·0012
−8·521	−1·2302	0·0052	0·0032
−7·714	−1·2248	0·0085	0·0052
−6·906	−1·2160	0·0139	0·0085
−6·099	−1·2014	0·0228	0·0139
−5·291	−1·1776	0·0372	0·0225
−4·484	−1·1389	0·0605	0·0359
−4·161	−1·1174	0·0732	0·0431
−3·838	−1·0914	0·0885	0·0516
−3·515	−1·0600	0·1067	0·0613
−3·192	−1·0221	0·1282	0·0726
−2·869	−0·9767	0·1537	0·0853
−2·546	−0·9224	0·1835	0·0994
−2·223	−0·8577	0·2180	0·1148
−1·900	−0·7810	0·2577	0·1311
−1·577	−0·6906	0·3028	0·1476
−1·254	−0·5849	0·3531	0·1637
−0·932	−0·4621	0·4083	0·1782
−0·609	−0·3207	0·4678	0·1898
−0·286	−0·1596	0·5305	0·1974
0	0	0·5873	0·1996

η_1	$f_1(\eta_1)$	$\frac{u}{U_1} = f'_1(\eta_1)$	$f''_1(\eta_1)$
0	0	0·5873	0·1996
0·360	0·2246	0·6588	0·1958
0·683	0·4474	0·7205	0·1855
1·006	0·6895	0·7779	0·1693
1·329	0·9492	0·8293	0·1483
1·652	1·2244	0·8734	0·1245
1·975	1·5125	0·9096	0·0998
2·298	1·8111	0·9380	0·0763
2·621	2·1176	0·9592	0·0556
2·944	2·4300	0·9743	0·0385
3·267	2·7464	0·9845	0·0253
3·590	3·0655	0·9911	0·0159
3·913	3·3863	0·9951	0·0094
4·236	3·7081	0·9974	0·0053
4·559	4·0304	0·9987	0·0028
4·882	4·3531	0·9994	0·0014
5·205	4·6759	0·9997	0·0007
5·528	4·9988	0·9999	0·0003
5·851	5·3217	0·9999	0·0001
6·174	5·6447	1·0000	0·0001
6·497	5·9676	1·0000	0·0000
∞	$\eta_1 -$ 0·5289	1	0

Table VII

Solution for the case $\rho\mu = 1$, $\lambda = 0\cdot501$

η_2	$f_2(\eta_2)$	$\frac{u}{U_1} = f'_2(\eta_2)$	$f''_2(\eta_2)$
$-\infty$	. .	0·5014	0
−7·602	−4·1839	0·5014	0·0000
−7·202	−3·9833	0·5014	0·0001
−6·801	−3·7827	0·5014	0·0001
−6·401	−3·5821	0·5015	0·0003
−6·001	−3·3814	0·5017	0·0005
−5·601	−3·1806	0·5020	0·0011
−5·201	−2·9797	0·5026	0·0019
−4·801	−2·7784	0·5036	0·0034
−4·401	−2·5766	0·5054	0·0058
−4·001	−2·3738	0·5085	0·0096
−3·601	−2·1695	0·5133	0·151
−3·201	−1·9627	0·5208	0·0228
−2·801	−1·7522	0·5319	0·0331
−2·401	−1·5365	0·5477	0·0460
−2·000	−1·3133	0·5690	0·0612
−1·600	−1·0803	0·5968	0·0777
−1·200	−0·8349	0·6312	0·0942
−0·800	−0·5744	0·6718	0·1084
−0·400	−0·2966	0·7174	0·1183
0	0	0·7657	0·1219

η_1	$f_1(\eta_1)$	$\frac{u}{U_1} = f'_1(\eta_1)$	$f''_1(\eta_1)$
0	0	0·7657	0·1219
0·400	0·3160	0·8140	0·1182
0·800	0·6509	0·8593	0·1073
1·200	1·0029	0·8991	0·0910
1·600	1·3694	0·9317	0·718
2·000	1·7473	0·9565	0·5260
2·401	2·1338	0·9741	0·0356
2·801	2·5259	0·9855	0·0224
3·201	2·9217	0·9925	0·0130
3·601	3·3197	0·9963	0·0069
4·001	3·7187	0·9983	0·0034
4·401	4·1184	0·9993	0·0016
4·801	4·5183	0·9997	0·0007
5·201	4·9183	0·9999	0·0003
5·601	5·3183	1·0000	0·0001
6·001	5·7184	1·0000	0·0000
∞	$\eta_1-0\cdot2829$	1	0

THE EFFECT OF THE NON-UNIFORMITY OF THE STREAM ON THE AERODYNAMIC CHARACTERISTICS OF A MOVING AEROFOIL

By E. E. JONES (*The University, Nottingham*)

[Received 5 September 1950]

SUMMARY

The problem of the motion of a cylinder of aerofoil section in an incompressible inviscid fluid, the velocity of which is non-uniform, involves the application of the two-dimensional complex potential function theory to a class of boundary-value problem which has not yet been considered to any great extent. A functional solution of the potential equation is determined, regular in the space external to a simple closed curve, which takes certain values on the boundary of the curve and certain values at infinite distance from this curve. A general solution in the form of a complex potential function is found in terms of these given values and the coefficients determining the profile of the cylinder section.

The forces and couple on the cylinder, which moves in a general manner, are determined by use of the Blasius formulae for a moving cylinder. The effect of a general type of vortex wake extending behind the cylinder is also discussed.

The results are applied to determine the effect of the non-uniformity of the stream on the aerodynamic characteristics of a moving aerofoil having small thickness and camber.

1. Introduction

THE air streams usually encountered in actual flight are such that the stream velocity varies from point to point in space. Another example of such a non-uniform stream is that existing in a wind-tunnel, due to the pressure gradient along its axis producing the effect of a convergent stream. In practice this necessitates a correction to the lift and drag acting on the aerofoil placed in the tunnel, and methods of evaluating this have been given by Taylor (**1**) and Goldstein (**2**). Taylor, making use of general hydrodynamical concepts but without reference to any particular type of stream, deduced expressions for the lift and drag on a stationary body in terms of certain pressure derivatives. Goldstein, by use of a two-dimensional transformation, deduced the forces and couple acting on a cylinder of aerofoil section at rest in a stream possessing curvature, the results of which reduce to those deduced by Taylor in a particular case.

The complex potential theory developed in this paper has been successfully applied by Morris (**3**) to the case of a cylinder moving in a general manner in a stream at rest at infinity, and in a uniform stream, and expressions for the lift, drag, and couple acting on the cylinder were

deduced. The non-uniformity of the stream is also likely to have considerable effect on these characteristics, and in this paper general expressions are deduced as the cylinder moves relative to the non-uniform stream.

2. General results

The cylinder moves in an inviscid incompressible fluid with velocity components u, v along axes Ox, Oy fixed in a right section of the cylinder, and has angular velocity ω about an axis perpendicular to this section. If z $(= x+iy)$ defines the position of any point on the contour of the cylinder section referred to these axes, then the component forces X, Y are given by the Blasius formulae

$$Y+iX = \tfrac{1}{2}\rho \int\limits_c (w+i\omega z)(\bar{w}-i\omega\bar{z})\,d\bar{z}-\tfrac{1}{2}\rho \int\limits_c \left(\bar{w}-i\omega\bar{z}-\frac{\partial\Omega}{\partial z}\right)^2 dz - -\tfrac{1}{2}\rho \int\limits_c \left(\frac{\partial\Omega}{\partial t}+\frac{\partial\bar{\Omega}}{\partial t}\right) d\bar{z}, \tag{1}$$

and the couple Γ is the real part of

$$\tfrac{1}{2}\rho \int\limits_c (w+i\omega z)(\bar{w}-i\omega\bar{z})z\,d\bar{z}-\tfrac{1}{2}\rho \int\limits_c \left(\bar{w}-i\omega\bar{z}-\frac{\partial\Omega}{\partial z}\right)^2 z\,dz - -\tfrac{1}{2}\rho \int\limits_c \left(\frac{\partial\Omega}{\partial t}+\frac{\partial\bar{\Omega}}{\partial t}\right) z\,d\bar{z}. \tag{2}$$

The integrals are taken in a positive anti-clockwise sense round c, the contour of the cylinder section in the z-plane. As usual $w = u+iv$, and Ω is the complex potential function for the fluid motion round the cylinder, its gradient defining the complex velocity of the fluid.

The cylinder profile is defined as the curve $\eta = 0$ in the conformal transformation

$$z = \sum_{n=0}^{\infty} a_n e^{(n-1)i\zeta}, \qquad \zeta = \xi+i\eta, \tag{3}$$

which transforms the space outside the cylinder in the z-plane to the inside of a rectangle in the ζ-plane, where $\eta = +\infty$ is chosen to correspond to $z = +\infty$.

If the cylinder has a sharp trailing edge, the above transformation ceases to be conformal at this point, and in general this leads to an infinite fluid velocity there. This difficulty is avoided by assuming the Joukowski condition for finite fluid velocity at the trailing edge, which determines the value of the circulation. However, when a trailing vortex wake forms behind the cylinder the condition that the motion is irrotational does not apply in the region of the wake, and thus Bernoulli's equation for the pressure cannot be used at points on the cylinder in the neighbourhood

of the trailing edge. To avoid this difficulty it must be assumed that the trailing wake is confined to a narrow band from the trailing edge, and the contour integrals can then be taken from the trailing edge, round the contour, and back to the trailing edge. Thus in transforming the contour integrals in the z-plane to integrals in the ζ-plane, the limits for ζ are from ζ_t to $\zeta_t - 2\pi$, where ζ_t is the value of ζ at the trailing edge, and ζ_t and ζ are real on the contour of the cylinder section.

3. The general method of determining the complex potential function for a cylinder moving in a given stream has been discussed by Morris (**4**). The function Ω can be divided into two parts Ω_1 and Ω_2, which are defined in the following manner: Ω_1 is the complex potential for the motion of the cylinder in a fluid at rest at infinity, and Ω_2 is the complex potential for the cylinder at rest in a given stream. These two motions can be superposed by the addition of Ω_1 and Ω_2 to give the required motion relative to the cylinder in the stream.

If a circulation κ exists round the cylinder, then Morris (**4**) has shown that

$$\Omega_1 = \sum_{n=1}^{\infty} \Omega'_n e^{ni\zeta} - \frac{\kappa\zeta}{2\pi} - \int_{s(z_t)}^{s(z_1)} \frac{ik_s}{2\pi} \log\left\{\frac{1-e^{-i(\zeta-\zeta_s)}}{1-e^{i(\zeta-\bar{\zeta}_s)}}\right\} ds, \tag{4}$$

where

$$\Omega'_1 = a_2\bar{w} - \bar{a}_0 w - i\omega b_1,$$

$$\Omega'_n = a_{n+1}\bar{w} - i\omega b_n \quad (n > 1),$$

and

$$b_n = \sum_{r=0}^{\infty} a_{n+r}\bar{a}_r.$$

In this result the effect of a trailing vortex wake, extending behind the cylinder, has been included. The trail, forming a surface of discontinuity, extends from z_t to z_1 in the z-plane, where z_t is the position of the trailing edge, and k_s is the strength per unit length of the vortex trail at a distance s along the trail from the trailing edge.

To determine Ω_2 we proceed in the following way. If Ω_0 is the complex potential of the undisturbed stream in the absence of the cylinder, then Ω_2 must be such that it reduces to Ω_0 at infinity and its imaginary part at the boundary of the cylinder must be zero. Divide Ω_0 into two parts, $F_1(\zeta)$ and $F_2(\zeta)$, where $F_1(\zeta)$ tends to zero at infinity, and $\bar{F}_1(\zeta)$ diverges there; $F_2(\zeta)$ diverges at infinity, and $\bar{F}_2(\zeta)$ tends to zero there. To form a function which is to be purely real on the boundary $\eta = 0$, we may either add the conjugate of the terms in Ω_0 treating ζ as real, or subtract these terms altogether. The first part $F_1(\zeta)$ has a conjugate $\bar{F}_1(\zeta)$ which by definition diverges at infinity, while $\bar{F}_2(\zeta)$ tends to zero there. Consequently the required function is

$$\Omega_2 = F_2(\zeta) + \bar{F}_2(\zeta). \tag{5}$$

The forces and couple on the cylinder, moving in a general manner in a stream at rest at infinity, with a vortex wake extending behind the cylinder, have been determined by Morris (**5**), and these results will be quoted wherever they occur. These were deduced by the application of the Blasius formulae to the complex potential Ω_1, and the following investigation deals with the change in the characteristics of the cylinder, due to the inclusion of the term Ω_2 in the complete complex potential.

4. The motion of a cylinder in the stream defined by the undisturbed complex potential: $\Omega_0 = \sum_{n=1}^{n=4} A_n z^n$.

Although the method is applicable to the stream defined by Ω_0 as a polynomial in z of any finite degree, the rest of this investigation will be confined to a polynomial of the fourth degree. Let Ω_0 be referred to axes $O_1 x_1$, $O_1 y_1$ fixed in space, hereafter called the stream axes, so that

$$\Omega_0 = \sum_{n=1}^{n=4} A_n z_1^n,$$

where the A_n's are in general complex constants. This stream has a complex velocity A_1 at the origin of coordinates, and the terms containing A_2, A_3, A_4 contribute to form the curvature of the stream. Since the velocity at a great distance is large, the results, if they are to have any practical application, can only be expected to give the approximate effect of local curvature of the stream at the cylinder.

The potential Ω_0 can be referred to the axes Ox, Oy fixed in the cylinder section, hereafter called the cylinder axes. If these axes are inclined at angle θ to the stream axes, and the origin O is at a position z_2 referred to the fixed origin O_1, then

$$z_1 = z_2 + z e^{i\theta},$$

where z is referred to the cylinder axes. The complex potential then takes the form

$$\Omega_0 = \sum_{n=1}^{n=4} \delta_n z^n,$$

where

$$\left.\begin{aligned} \delta_0 &= A_1 z_2 + A_2 z_2^2 + A_3 z_2^3 + A_4 z_2^4, \\ \delta_1 &= (A_1 + 2A_2 z_2 + 3A_3 z_2^2 + 4A_4 z_2^3)e^{i\theta}, \\ \delta_2 &= (A_2 + 3A_3 z_2 + 6A_4 z_2^2)e^{2i\theta}, \\ \delta_3 &= (A_3 + 4A_4 z_2)e^{3i\theta}, \\ \delta_4 &= A_4 e^{4i\theta}. \end{aligned}\right\} \qquad (6)$$

The z-plane is mapped on to the ζ-plane by equation (3), hence by evaluating z^2, z^3, and z^4, and substituting in Ω_0, we have

$$\Omega_0 = \sum_{n=1}^{n=4} m_n e^{-ni\zeta} + f(e^{i\zeta}),$$

where

$$\left.\begin{aligned} m_1 &= \delta_1 a_0 + 2\delta_2 a_0 a_1 + 3\delta_3 a_0 a_1(a_0+a_1) + 4\delta_4 a_0(a_0^2 a_3 + 3a_0 a_1 a_2 + a_1^3), \\ m_2 &= \delta_2 a_0^2 + 3\delta_3 a_0^2 a_1 + 2\delta_4 a_0^2(2a_0 a_2 + 3a_1), \\ m_3 &= \delta_3 a_0^2 + 4\delta_4 a_0^3 a_1, \\ m_4 &= \delta_4 a_0^4, \end{aligned}\right\} \tag{7}$$

and $f(e^{i\zeta})$ is a function of positive exponential functions. Hence in this case

$$F_2(\zeta) = \sum_{n=1}^{n=4} m_n e^{-ni\zeta},$$

and thus from equation (5),

$$\Omega_2 = \sum_{n=1}^{n=4} m_n e^{-ni\zeta} + \sum_{n=1}^{n=4} \bar{m}_n e^{ni\zeta}.$$

The complete complex potential function defining the motion of the cylinder in the given non-uniform stream is thus given by

$$\Omega = \sum_{n=1}^{\infty} \Omega_n' e^{ni\zeta} - \frac{\kappa\zeta}{2\pi} - \int_{s(z_t)}^{s(z_1)} \frac{ik_s}{2\pi} \log\left\{\frac{1-e^{-i(\zeta-\zeta_s)}}{1-e^{i(\zeta-\bar{\zeta}_s)}}\right\} ds + \\ + \sum_{n=1}^{n=4} m_n e^{-ni\zeta} + \sum_{n=1}^{n=4} \bar{m}_n e^{ni\zeta}. \tag{8}$$

5. The force on the cylinder

In order to evaluate the force on the cylinder, it is sufficient to determine the contribution due to Ω_2. The additional terms arising in the Blasius formula of equation (1) are

$$-\rho \int_c \left(i\omega\bar{z}\frac{\partial\Omega_2}{\partial z} - \bar{w}\frac{\partial\Omega_2}{\partial z}\right) dz - \tfrac{1}{2}\rho \int_c \left(\frac{\partial\Omega_2}{\partial t} + \frac{\partial\bar{\Omega}_2}{\partial t}\right) d\bar{z} + \\ + \text{terms involved in the integral } -\tfrac{1}{2}\rho \int_c \left(\frac{\partial\Omega}{\partial z}\right)^2 dz.$$

The following integrals have to be evaluated:

(i) $$\bar{w}\rho \int_c \frac{\partial\Omega_2}{\partial z} dz = -\bar{w}\rho \int_{\zeta_t-2\pi}^{\zeta_t} \frac{\partial\Omega_2}{\partial\zeta} d\zeta = 0.$$

(ii) $$-i\omega\rho \int_c \bar{z}\frac{\partial\Omega_2}{\partial z} dz = i\omega\rho \int_{\zeta_t-2\pi}^{\zeta_t} \bar{z}(\zeta)\frac{\partial\Omega_2}{\partial\zeta} d\zeta$$

$$= \omega\rho \int_{\zeta_t-2\pi}^{\zeta_t} \left\{\sum_{n=1}^{n=4} nm_n e^{-ni\zeta} - \sum_{n=1}^{n=4} n\bar{m}_n e^{ni\zeta}\right\} \sum_{n=0}^{\infty} \bar{a}_n e^{-(n-1)i\zeta} d\zeta$$

$$= 2\pi\rho\omega\left\{\bar{a}_0 m_1 - \sum_{n=1}^{n=4} n\bar{a}_{n+1}\bar{m}_n\right\}.$$

(iii) $$-\tfrac{1}{2}\rho\int_{c}\left(\frac{\partial\Omega_2}{\partial t}+\frac{\partial\bar{\Omega}_2}{\partial t}\right)d\bar{z}$$

$$=\rho\int_{\zeta_t-2\pi}^{\zeta_t}\left\{\sum_{n=1}^{n=4}\dot{m}_n\,e^{-ni\zeta}+\sum_{n=1}^{n=4}\dot{\bar{m}}_n\,e^{ni\zeta}\right\}\sum_{n=1}^{\infty}(n-1)\bar{a}_n\,e^{-(n-1)i\zeta}\,d\zeta$$

$$=2i\pi\rho\left\{\bar{a}_0\,\dot{m}_1-\sum_{n=1}^{n=4}n\bar{a}_{n+1}\dot{\bar{m}}_n\right\}.$$

(iv) In order to evaluate the integral

$$-\tfrac{1}{2}\rho\int_{c}\left(\frac{\partial\Omega}{\partial z}\right)^2 dz=\tfrac{1}{2}\rho\int_{\zeta_t-2\pi}^{\zeta_t}\left(\frac{\partial\Omega}{\partial\zeta}\right)^2\frac{d\zeta}{dz/d\zeta},$$

we note that the space outside the cylinder and wake in the z-plane transforms on to the inside of the contour in the ζ-plane, given by

(*a*) the real axis from $\zeta_t-2\pi$ to ζ_t,
(*b*) the curve from ζ_t to ζ_1, corresponding to one side of the wake,
(*c*) the line parallel to the imaginary axis $\xi=\xi_1$,
(*d*) the line $\eta=+\infty$,
(*e*) the line parallel to the imaginary axis $\xi=\xi_1-2\pi$,
(*f*) the other side of the wake curve from $\zeta_1-2\pi$ to $\zeta_t-2\pi$.

The contour is indented at ζ_t, $\zeta_t-2\pi$, and at these points we choose $\partial\Omega/\partial\zeta=0$, so that the fluid velocity at $z=z_t$ is finite. Also the curve corresponding to the wake must be indented at every point on it, since poles exist all along the wake.

The above integral taken round this complete contour is zero, since no poles occur within the contour. Since the discontinuity due to the vortex wake does not extend beyond ζ_1 the integrals along the paths (*c*) and (*e*) of the contour cancel each other. It has also been shown by Morris (**4**) that the integrals along the paths (*b*) and (*f*) reduce to

$$-\rho\int_{s(z_t)}^{s(z_1)}k_s(\dot{\bar{z}}_s-i\omega\bar{z}_s+\bar{w})\,ds.$$

It thus remains to calculate the integral along a line parallel to the ξ-axis at $\eta=+\infty$. At $\eta=+\infty$, we have

$$\frac{\partial\Omega}{\partial\zeta}=\sum_{n=1}^{\infty}in\Omega'_n\,e^{ni\zeta}-\frac{\kappa}{2\pi}+\int_{s(z_t)}^{s(z_1)}\frac{k_s}{2\pi}\left\{\sum_{n=1}^{\infty}e^{ni(\zeta-\bar{\zeta}_s)}-\sum_{n=0}^{\infty}e^{ni(\zeta-\zeta_s)}\right\}ds+$$
$$+\sum_{n=1}^{n=4}in\bar{m}_n\,e^{ni\zeta}-\sum_{n=1}^{n=4}inm_n\,e^{-ni\zeta}.$$

We now write $$\left\{\sum_{n=1}^{\infty}in\Omega'_n\,e^{ni\zeta}-\frac{\kappa}{2\pi}-\sum_{n=1}^{n=4}inm_n\,e^{-ni\zeta}\right\}^2,$$

in the form
$$\sum_{n=0}^{n=8} d_n e^{-ni\zeta} + f(e^{i\zeta}),$$
where

$$\left.\begin{aligned}
d_0 &= \kappa^2/4\pi^2 + 32m_4(a_5\bar{w} + \bar{m}_4 - i\omega b_4) + 18m_3(a_2\bar{w} + \bar{m}_3 - ib_3\omega) + \\
&\qquad + 8m_2(a_3\bar{w} + \bar{m}_2 - ib_2\omega) + 2m_1(a_2\bar{w} - \bar{a}_0 w + \bar{m}_1 - ib_1\omega), \\
d_1 &= 24m_4(a_4\bar{w} + \bar{m}_3 - ib_3\omega) + 12m_3(a_3\bar{w} + \bar{m}_2 - ib_2\omega) + \\
&\qquad + 4m_2(a_2\bar{w} - \bar{a}_0 w + \bar{m}_1 - ib_1\omega) + i\kappa m_1/\pi, \\
d_2 &= 16m_4(a_3\bar{w} + \bar{m}_2 - ib_2\omega) + 6m_3(a_2\bar{w} - \bar{a}_0 w + \bar{m}_1 - ib_1\omega) - \\
&\qquad - m_1^2 + 2i\kappa m_2/\pi, \\
d_3 &= 8m_4(a_2\bar{w} - \bar{a}_0 w + \bar{m}_1 - ib_1\omega) - 4m_1 m_2 + 3i\kappa m_3/\pi, \\
d_4 &= -4m_2^2 - 6m_1 m_3 + 4i\kappa m_4/\pi, \\
d_5 &= -8m_1 m_4 - 12m_2 m_3, \qquad d_6 = -9m_3^2 - 16m_2 m_4, \\
d_7 &= -24m_3 m_4, \qquad d_8 = -16m_4^2,
\end{aligned}\right\} \quad (9)$$

and $f(e^{i\zeta})$ is a function of positive exponential functions. Also at $\eta = +\infty$ we write
$$(dz/d\zeta)^{-1} = i\sum_{n=1}^{\infty} c_n e^{ni\zeta},$$
where

$$\left.\begin{aligned}
c_1 &= 1/a_0, \qquad c_2 = 0, \qquad c_3 = a_2/a_0^2, \qquad c_4 = 2a_3/a_0^2, \\
c_5 &= (3a_0 a_4 + a_2^2)/a_0^3, \qquad c_6 = 4(a_0 a_5 + a_2 a_3)/a_0^3, \\
c_7 &= (5a_0^2 a_6 + 4a_0 a_3^2 + 6a_0 a_2 a_4 + a_2^3)/a_0^4, \\
c_8 &= (6a_0^2 a_7 + 8a_0 a_2 a_5 + 12a_0 a_3 a_4 + 6a_3 a_2^2)/a_0^4, \\
c_9 &= (7u_0^3 a_8 + 10a_0^2 a_2 a_6 + 9a_0^2 a_4^2 + 16a_0^2 a_3 a_5 + 9a_0^3 a_4 + 12a_0 a_2 a_3^2 + a_2^4)/a_0^5.
\end{aligned}\right\} \quad (9\,\text{a})$$

Since the constant terms in the integrand are the only contributions to the value of the integral at $\eta = +\infty$, then these occur in the expressions

$$\tfrac{1}{2}i\rho \int_{\zeta_1}^{\zeta_1-2\pi} \left\{\sum_{n=0}^{\infty} d_n e^{-ni\zeta}\right\}\left\{\sum_{n=1}^{\infty} c_n e^{ni\zeta}\right\} d\zeta +$$
$$+\rho \int_{s(z_t)}^{s(z_1)} \frac{k_s}{2\pi}\, ds \int_{\zeta_1}^{\zeta_1-2\pi} \left\{\sum_{n=1}^{\infty} e^{ni(\zeta-\bar{\zeta}_s)} - \sum_{n=0}^{\infty} e^{ni(\zeta-\zeta_s)}\right\}\left\{\sum_{n=1}^{n=4} nm_n e^{-ni\zeta}\right\}\left\{\sum_{n=1}^{\infty} c_n e^{ni\zeta}\right\} d\zeta.$$

The first integral reduces to
$$-i\pi\rho\sum_{n=1}^{n=8} c_n d_n,$$
and if we put
$$\left\{\sum_{n=1}^{n=4} nm_n e^{-ni\zeta}\right\}\left\{\sum_{n=1}^{\infty} c_n e^{ni\zeta}\right\} = \sum_{n=0}^{n=3} p_{n+1} e^{-ni\zeta} + f(e^{i\zeta}),$$
where
$$p_n = \sum_{r=n}^{r=4} rm_r c_{r-n+1},$$

then the second integral reduces to

$$-\rho \int_{s(z_t)}^{s(z_1)} k_s \left\{ \sum_{n=1}^{n=3} p_{n+1} e^{-ni\bar{\zeta}_s} - \sum_{n=0}^{n=3} p_{n+1} e^{-ni\zeta_s} \right\} ds.$$

In order to deduce the force acting on the cylinder, the above results are added to those already deduced by Morris (**5**) for the motion of the cylinder in a stream otherwise at rest.

When a vortex trail exists behind the cylinder, following Helmholtz, we have

$$\kappa + \int_{s(z_t)}^{s(z_1)} k_s \, ds = 0,$$

and then the force is given by the expression

$$\begin{aligned} Y+iX = {} & \pi\rho(2\bar{B}\dot{w} - A\dot{\bar{w}} + i\bar{D}\dot{\omega}) + \pi\rho\omega(2\bar{B}w - A\bar{w} + i\bar{D}\omega) + \\ & + i\pi\rho \sum_{n=1}^{n=8} c_n d_n + 2\pi\rho\omega \left\{ \bar{a}_0 m_1 - \sum_{n=1}^{n=4} n\bar{a}_{n+1} \bar{m}_n \right\} + \\ & + 2i\pi\rho \left\{ \bar{a}_0 \dot{m}_1 - \sum_{n=1}^{n=4} n\bar{a}_{n+1} \dot{\bar{m}}_n \right\} + i\omega\bar{a}_0 \rho \int_{s(z_t)}^{s(z_1)} k_s (e^{i\zeta_s} - e^{i\bar{\zeta}_s}) \, ds - \\ & - \rho \int_{s(z_t)}^{s(z_1)} \dot{k}_s (\bar{z}_s - \bar{a}_1 - \bar{a}_0 e^{i\bar{\zeta}_s} + \bar{a}_0 e^{i\zeta_s}) \, ds - i\rho\bar{a}_0 \int_{s(z_t)}^{s(z_1)} k_s (\dot{\zeta}_s e^{i\zeta_s} - \dot{\bar{\zeta}}_s e^{i\bar{\zeta}_s}) \, ds + \\ & + \rho \int_{s(z_t)}^{s(z_1)} k_s \left\{ \sum_{n=1}^{n=3} p_{n+1} e^{-ni\bar{\zeta}_s} - \sum_{n=0}^{n=3} p_{n+1} e^{-ni\zeta_s} \right\} ds, \end{aligned}$$

where

$$A = a_0 \bar{a}_0 + \sum_{n=1}^{\infty} n a_{n+1} \bar{a}_{n+1},$$

$$B = a_0 a_2,$$

$$C = \sum_{n=1}^{\infty} n b_n \bar{b}_n,$$

$$D = b_1 a_0 + \sum_{n=1}^{\infty} n\bar{b}_n a_{n+1}.$$

The expression for the force now has four extra terms, all of which involve the effect of the non-uniformity of the stream.

It is also of interest to consider the value of the force when the vortex trail effect is not considered. It is then determined by the expression

$$\begin{aligned} Y+iX = {} & i\pi\rho(2\bar{B}\dot{w} - A\dot{\bar{w}} + i\bar{D}\dot{\omega}) + \pi\rho\omega(2\bar{B}w - A\bar{w} + i\bar{D}\omega) + \\ & + \rho\kappa(\bar{w} - i\omega\bar{a}_1) + \rho\dot{\kappa} \left\{ \bar{a}_1 - \sum_{n=0}^{\infty} \bar{a}_n e^{-(n-1)i\zeta_t} \right\} + i\pi\rho \sum_{n=1}^{n=8} c_n d_n + \\ & + 2\pi\rho\omega \left\{ \bar{a}_0 m_1 - \sum_{n=1}^{n=4} n\bar{a}_{n+1} \bar{m}_n \right\} + 2i\pi\rho \left\{ \bar{a}_0 \dot{m}_1 - \sum_{n=1}^{n=4} n\bar{a}_{n+1} \dot{\bar{m}}_n \right\}, \end{aligned} \qquad (10)$$

where the term in $\dot\kappa$ has been modified from that deduced by Morris (**5**) to allow for the fact that the trailing edge corresponds to $\zeta = \zeta_t$.

Using the relations $\omega = \dot\theta$, and $w = \dot z_2 e^{-i\theta}$ the functions $\dot m_n$ can be determined as functions of δ_n, and therefore of A_n, from equations (6) and (7).

6. The couple on the cylinder

The couple on the cylinder is similarly deduced from the Blasius formula for the moving cylinder, and the extra terms due to Ω_2 occurring in equation (2) are the real part of

$$\rho\int\limits_c \left(\bar w\frac{\partial\Omega_2}{\partial z} - i\omega\bar z\frac{\partial\Omega_2}{\partial z}\right) z\,dz - \tfrac{1}{2}\rho\int\limits_c\left(\frac{\partial\Omega_2}{\partial t}+\frac{\partial\bar\Omega_2}{\partial t}\right)z\,d\bar z +$$

$$+\text{extra terms in the integral } -\tfrac{1}{2}\rho\int\limits_c\left(\frac{\partial\Omega}{\partial z}\right)^2 z\,dz.$$

These integrals are evaluated as follows:

(i) $$\rho\bar w\int\limits_c \frac{\partial\Omega_2}{\partial z}z\,dz = -\rho\bar w\int\limits_{\zeta_t-2\pi}^{\zeta_t}\frac{\partial\Omega_2}{\partial\zeta}z\,d\zeta,$$

$$= i\rho\bar w\int\limits_{\zeta_t-2\pi}^{\zeta_t}\left\{\sum_{n=1}^{n=4} nm_n e^{-ni\zeta} - \sum_{n=1}^{n=4} n\bar m_n e^{ni\zeta}\right\}\sum_{n=0}^{\infty}a_n e^{(n-1)i\zeta}\,d\zeta$$

$$= -2i\pi\rho\bar w\left\{a_0\bar m_1 - \sum_{n=1}^{n=4} nm_n a_{n+1}\right\}. \tag{11}$$

(ii) $$-i\rho\omega\int\limits_c\frac{\partial\Omega_2}{\partial z}z\bar z\,dz = i\rho\omega\int\limits_{\zeta_t-2\pi}^{\zeta_t}\frac{\partial\Omega_2}{\partial\zeta}z\bar z\,d\zeta,$$

the real part of which is zero, since $\partial\Omega_2/\partial\zeta = \partial\bar\Omega_2/\partial\zeta$ on the contour.

The real part of the integral involving the acceleration terms is

$$-\tfrac{1}{4}\rho\int\limits_c\left(\frac{\partial\Omega_2}{\partial t}+\frac{\partial\bar\Omega_2}{\partial t}\right)d(z\bar z),$$

where $$z\bar z = \sum_{n=0}^{\infty} b_n e^{ni\zeta} + \sum_{n=1}^{\infty}\bar b_n e^{-ni\zeta}.$$

The integral may be written as

$$\tfrac{1}{2}i\rho\int\limits_{\zeta_t-2\pi}^{\zeta_t}\left\{\sum_{n=1}^{n=4}\dot m_n e^{-ni\zeta}+\sum_{n=1}^{n=4}\dot{\bar m}_n e^{ni\zeta}\right\}\left\{\sum_{n=0}^{\infty}nb_n e^{ni\zeta} - \sum_{n=1}^{\infty}n\bar b_n e^{-ni\zeta}\right\}d\zeta,$$

$$= i\pi\rho\left\{\sum_{n=1}^{n=4}nb_n\dot m_n - \sum_{n=1}^{n=4}n\bar b_n\dot{\bar m}_n\right\}. \tag{12}$$

It now remains to calculate the extra terms occurring in the integral

$$-\tfrac{1}{2}\rho\int\limits_c\left(\frac{\partial\Omega}{\partial z}\right)^2 z\,dz = \tfrac{1}{2}\rho\int\limits_{\zeta_t-2\pi}^{\zeta_t}\left(\frac{\partial\Omega}{\partial\zeta}\right)^2 z\left(\frac{\partial z}{d\zeta}\right)^{-1}d\zeta.$$

Considering this integral taken round the same contour as for the force, since no poles occur within the contour, the integral round the complete contour is zero. As before, the integrals along the lines parallel to the η-axis at ξ_1 and $\xi_1-2\pi$ cancel each other, and along the sides of the vortex wake curves the integral has the value

$$-\rho \int_{s(z_t)}^{s(z_1)} k_s(\dot{\bar{z}}_s - i\omega\bar{z}_s + \bar{w})z_s\, ds.$$

At $\eta = +\infty$ we have

$$z\left(\frac{dz}{d\zeta}\right)^{-1} = i\left\{\sum_{n=0}^{\infty} a_n\, e^{(n-1)i\zeta}\right\}\left\{\sum_{n=1}^{\infty} c_n\, e^{ni\zeta}\right\},$$

$$= i\sum_{n=0}^{\infty} g_n\, e^{ni\zeta},$$

where $$g_n = \sum_{r=0}^{\infty} a_r\, c_{n+1-r}.$$

The terms which contribute to the integral are the constant terms in the integrand, and these are given by

$$-i\pi\rho\sum_{n=0}^{n=8} d_n\, g_n - \rho\int_{s(z_t)}^{s(z_1)} k_s\left\{\sum_{n=1}^{n=4} q_n\, e^{-ni\bar{\zeta}_s} - \sum_{n=0}^{n=4} q_n\, e^{-ni\zeta_s}\right\} ds, \tag{13}$$

where $$q_n = \sum_{r=n}^{r=4} r m_r\, g_{r-n}.$$

The real part of equation (11), and equations (12) and (13), when added to those deduced by Morris (**5**), give the couple on the cylinder moving in the given non-uniform stream with an accompanying vortex wake, as

$$\begin{aligned}
\Gamma &= i\pi\rho(w^2\bar{B}-\bar{w}^2B)-\tfrac{1}{2}\pi\rho\omega(w\bar{D}+\bar{w}D)+\tfrac{1}{2}i\pi\rho(\bar{D}\dot{w}-D\dot{\bar{w}})-\pi\rho C\dot{\omega}+\\
&\quad+\tfrac{1}{2}\rho a_0\bar{w}\int_{s(z_t)}^{s(z_1)} k_s(e^{-i\zeta_s}-e^{-i\bar{\zeta}_s})\, ds-\tfrac{1}{2}\rho\int_{s(z_t)}^{s(z_1)} \dot{k}_s\sum_{n=1}^{\infty}(b_n\, e^{ni\zeta_s}+\bar{b}_n\, e^{-ni\bar{\zeta}_s})\, ds+\\
&\quad+\tfrac{1}{2}\rho\bar{a}_0 w\int_{s(z_t)}^{s(z_1)} k_s(e^{i\bar{\zeta}_s}-e^{i\zeta_s})\, ds-\tfrac{1}{2}\rho\int_{s(z_t)}^{s(z_1)} k_s\left\{\dot{\zeta}_s\sum_{n=1}^{\infty} nb_n\, e^{ni\zeta_s}-\dot{\bar{\zeta}}_s\sum_{n=1}^{\infty} n\bar{b}_n\, e^{-ni\bar{\zeta}_s}\right\} ds+\\
&\quad+\tfrac{1}{2}\rho\int_{s(z_t)}^{s(z_1)} k_s\frac{d}{dt}(z_s\bar{z}_s)\, ds+\tfrac{1}{2}i\pi\rho\sum_{n=0}^{n=8} g_n\, d_n-\tfrac{1}{2}i\pi\rho\sum_{n=0}^{n=8}\bar{g}_n\,\bar{d}_n-\\
&\quad-i\pi\rho\bar{w}\left\{a_0\,\bar{m}_1-\sum_{n=1}^{n=4} nm_n\, a_{n+1}\right\}+i\pi\rho w\left\{\bar{a}_0\, m_1-\sum_{n=1}^{n=4} n\bar{m}_n\,\bar{a}_{n+1}\right\}+\\
&\quad+\tfrac{1}{2}\rho\int_{s(z_t)}^{s(z_1)} k_s\sum_{n=1}^{n=4} q_n(e^{-ni\bar{\zeta}_s}-e^{-ni\zeta_s})\, ds+\tfrac{1}{2}\rho\int_{s(z_t)}^{s(z_1)} k_s\sum_{n=1}^{n=4}\bar{q}_n(e^{ni\zeta_s}-e^{ni\bar{\zeta}_s})\, ds+\\
&\quad+i\pi\rho\left\{\sum_{n=1}^{n=4} nb_n\,\dot{m}_n-\sum_{n=1}^{n=4} n\bar{b}_n\,\dot{\bar{m}}_n\right\}.
\end{aligned} \tag{14}$$

In the expression for the couple extra terms occur, giving the effect of the non-uniformity of the stream.

The couple on the cylinder, when the effect of the vortex trail is not considered, is

$$\begin{aligned}\Gamma = {} & i\pi\rho(w^2\bar{B}-\bar{w}^2B)-\tfrac{1}{2}\pi\rho(w\bar{D}+\bar{w}D)+\tfrac{1}{2}i\pi\rho(\bar{D}\dot{w}-D\dot{\bar{w}})-\pi\rho C\dot{\omega}+ \\ & +\tfrac{1}{2}\rho\kappa(\bar{w}a_1+w\bar{a}_1)-\tfrac{1}{2}\rho\dot{\kappa}\sum_{n=1}^{\infty}(b_n e^{ni\zeta_t}+\bar{b}_n e^{-ni\zeta_t})+ \\ & +\tfrac{1}{2}i\pi\rho\sum_{n=0}^{n=8}g_n d_n-i\pi\rho\bar{w}\Big\{a_0\bar{m}_1-\sum_{n=1}^{n=4}nm_n a_{n+1}\Big\}- \\ & -\tfrac{1}{2}i\pi\rho\sum_{n=0}^{n=8}\bar{g}_n \bar{d}_n+i\pi\rho w\Big\{\bar{a}_0 m_1-\sum_{n=1}^{n=4}n\bar{m}_n \bar{a}_{n+1}\Big\}+ \\ & +i\pi\rho\Big\{\sum_{n=1}^{n=4}nb_n \dot{m}_n-\sum_{n=1}^{n=4}n\bar{b}_n \dot{\bar{m}}_n\Big\}. \qquad (15)\end{aligned}$$

7. (i) These general results can be shown to agree with those deduced by Goldstein (**2**) when the cylinder is at rest, with no vortex trail behind the cylinder. In this case $\omega = w = z_2 = 0$, then equation (10) reduces to

$$Y+iX = i\pi\rho\sum_{n=1}^{n=8}c_n d_n, \qquad (16)$$

and the couple given by equation (15) reduces to

$$\Gamma = \tfrac{1}{2}i\pi\rho\sum_{n=0}^{n=8}g_n d_n-\tfrac{1}{2}i\pi\rho\sum_{n=0}^{n=8}\bar{g}_n \bar{d}_n. \qquad (17)$$

If squares and products of A_3 and A_4 are neglected, and A_1 assumed real, these results reduce to those given by Goldstein, noting that the transformation used is the inverse of that defined by equation (3).

(ii) When the cylinder is at incidence α to the real stream axis O_1x_1, and is at rest with its centre at the origin, and if there is no circulation round the cylinder, equation (16) reduces to

$$Y+iX = 4i\pi\rho a_0 A_1 A_2(a_0 e^{-i\alpha}-a_2 e^{3i\alpha}),$$

where $A_3 = A_4 = 0$, and assuming A_1 to be real and negative and A_2 to be small. In this case the lift and drag on the cylinder, given by

$$L+iD = (Y+iX)e^{-i\alpha},$$

can be put in the form

$$L = -(A+S)\frac{\partial p}{\partial y}+H\frac{\partial p}{\partial x},$$

$$D = -(A+S)\frac{\partial p}{\partial x}-H\frac{\partial p}{\partial y},$$

where

$$A+S = \pi a_0(2a_0-\bar{a}_2 e^{-2i\alpha}-a_2 e^{2i\alpha}),$$

$$H = i\pi a_0(a_2 e^{2i\alpha}-\bar{a}_2 e^{-2i\alpha}).$$

Here A and H are the energy coefficients for motion in a stream at rest at infinity, S is the cross-sectional area of the cylinder, and $\partial p/\partial x$ and $\partial p/\partial y$ are the pressure gradients along the stream axes at the origin when the cylinder is removed from the stream. These pressure gradients have the values

$$\frac{\partial p}{\partial x} = -\rho A_1(A_2+\bar{A}_2), \qquad \frac{\partial p}{\partial y} = -i\rho A_1(A_2-\bar{A}_2).$$

These results for the lift and drag agree with those deduced by Taylor (**1**).

8 The condition that $\partial\Omega/\partial\zeta = 0$ at $\zeta = \zeta_t$, where $z'(\zeta_t) = 0$, is equivalent to the Joukowski condition for finite fluid velocity at the trailing edge. However, it is known that this condition gives the correct pressure distribution over the cylinder only when the incidence to the main stream is small, and when this is so it is possible to determine κ and $\dot{\kappa}$ uniquely.

For the stream under discussion the Joukowski condition gives

$$\frac{\kappa}{2\pi} = i\sum_{n=1}^{\infty} n\Omega'_n e^{ni\zeta_t} - i\sum_{n=1}^{n=4} nm_n e^{-ni\zeta_t} + i\sum_{n=1}^{n=4} n\bar{m}_n e^{ni\zeta_t} + \\ + \int\limits_{s(z_t)}^{s(z_1)} \frac{k_s}{2\pi}\left\{\frac{e^{-i(\zeta_t-\zeta_s)}}{1-e^{-i(\zeta_t-\zeta_s)}} + \frac{e^{i(\zeta_t-\bar{\zeta}_s)}}{1-e^{i(\zeta_t-\bar{\zeta}_s)}}\right\} ds, \tag{18}$$

where also
$$\kappa + \int\limits_{s(z_t)}^{s(z_1)} k_s\, ds = 0.$$

When the effect of the trail is excluded, then we have simply

$$\frac{\kappa}{2\pi} = i\sum_{n=1}^{\infty} n\Omega'_n e^{ni\zeta_t} - i\sum_{n=1}^{n=4} nm_n e^{-ni\zeta_t} + i\sum_{n=1}^{n=4} n\bar{m}_n e^{ni\zeta_t}. \tag{19}$$

9. Aerofoils with small thickness and camber

The forces and couple acting on a cylinder in the presence or absence of a vortex trail have been expressed as functions of the velocities and accelerations of the cylinder, the coefficients determining the profile of the cylinder section, the coefficients determining the non-uniformity of the stream, and the position coordinates of the cylinder relative to the stream. Hence if the path of the cylinder is known as it moves relative to the stream, the change in the aerodynamic characteristics of the cylinder can be calculated at all points of its path.

Although the effect of the trailing vortex wake has been included in these expressions, the integrals involved are extremely complicated. This is due to the fact that in a non-uniform stream the vortex wake does not extend in a straight line behind the cylinder but assumes a curved path. Thus in the further investigation of the effect of the non-uniformity of the stream on the characteristics of particular types of cylinders the effect of

the trailing vortex wake is not included, as further research is necessary before this problem can be pursued.

In order to include the effect of the thickness and camber of the cylinder of aerofoil section, the following Joukowski transformation is used:

$$z = ae^{-i\zeta}+\frac{b^2}{z_0+ae^{-i\zeta}}, \quad |z_0| < a.$$

The magnitude of the thickness and camber of any given aerofoil is determined by the value of z_0 in the transformation, and for a thin aerofoil with small camber it is possible to neglect squares of z_0. The trailing edge occurs at ζ_t, where

$$z_0+ae^{-i\zeta_t} = -b,$$

or approximately

$$b = a-x_0.$$

As shown by Morris (**6**), the transformation can be expanded in powers of $z_0 e^{i\zeta}/a$, and the values of the constants occurring in the equations for the force and couple deduced.

If we consider the motion of the cylinder in the particular type of stream given by

$$A_1 = -U, \qquad A_2 = -\mu U, \qquad A_3 = A_4 = 0,$$

the undisturbed complex potential of the stream is given by

$$\Omega_0 = -Uz_1-\mu U z_1^2,$$

and further μ, U are assumed to be real, with μ small.

The cylinder is given a small anticlockwise angular velocity ω about an axis perpendicular to the section, and has a velocity V ($> U$) along the positive x_1-axis. The cylinder is at small incidence α ($= \theta$) to this axis, and at any instant has a position coordinate $z_1 = z_2 = x$, say, referred to the origin O_1.

In this example, since α is small, the circulation round the cylinder can be determined uniquely from equation (18), and has a value

$$\frac{\kappa}{2\pi} = 2(U+V)(a\sin\alpha+y_0\cos\alpha)-4a^2\mu U\sin 2\alpha+4a\mu Ux\sin\alpha.$$

Substituting the known values of the variables and constants in equation (10), the lift L and the drag D opposing the motion, are given by

$$\begin{aligned}\frac{L}{\pi\rho} = {} & 4a\dot{V}\{3(a-x_0)\sin 2\alpha+y_0(1+3\cos 2\alpha)\}+8a^3\dot{\omega}\cos\alpha+ \\ & +4a^2\omega(V+4U)\cos^2\alpha+4(U+V)^2(a\sin\alpha+y_0\cos\alpha)+ \\ & +4a^2\mu U(2V-U)\sin 2\alpha+16aU(U+V)\mu x\sin\alpha,\end{aligned}$$

$$\begin{aligned}\frac{D}{\pi\rho} = {} & 12a\dot{V}\{y_0\cos\alpha+(a-x_0)\sin\alpha\}\sin\alpha+8a^3\dot{\omega}\sin\alpha+ \\ & +2a^2\omega(V+4U)\sin 2\alpha+8a^2\mu U(2V-U)\sin^2\alpha,\end{aligned}$$

and from equation (15), the couple is given by

$$\frac{\Gamma}{\pi\rho} = -4a^2(a+x_0)\dot{V}\sin\alpha - 6a^2y_0\dot{V}\cos\alpha - 6a^4\dot{\omega} + 4a^3\omega U\cos\alpha +$$
$$+2a(a-2x_0)(U+V)^2\sin 2\alpha + 8a^3\mu U^2(\sin 3\alpha - \sin\alpha) +$$
$$+8a^3\mu UV(2\cos 2\alpha - 1) + 8a^2U(U+V)\mu x\sin 2\alpha.$$

When μ is positive, the cylinder moves as if towards a source with velocity V, and angular velocity ω at small incidence α. The effect of the curvature and divergence of the stream is to increase the lift, drag, and the couple on the cylinder as compared with that for motion in a uniform stream of velocity U. The lift and couple increase uniformly as the cylinder moves towards the region of divergence, the drag remaining constant to the same order of approximation.

When μ is negative, the cylinder moves as if away from a sink, the lift, drag, and couple decrease below their values occurring in a uniform stream, and as the cylinder moves away from the region of convergence the lift and the couple increase uniformly, the drag remaining constant.

The stream defined by

$$\Omega_0 = -Uz_1 - i\mu Uz_1^2,$$

can be similarly investigated to deduce the effect of asymmetric local stream curvature on the characteristics of the cylinder.

In conclusion, the author wishes to thank Dr. R. M. Morris for her interest in this paper, which forms part of a thesis for the Ph.D. degree of the University of Wales.

REFERENCES

1. G. I. Taylor, 'The forces on a body placed in a curved or converging stream of fluid', *Proc. Roy. Soc.* A, **120** (1928), 260.
2. S. Goldstein, *Steady Flight Two-dimensional Flow past a solid Cylinder in a Non-uniform Stream, and Two-dimensional Wind-tunnel Interference*, A.R.C. R. and M. No. 1092 (1942).
3. R. M. Morris, 'The two-dimensional hydrodynamical theory of moving aerofoils, I', *Proc. Roy. Soc.* A, **161** (1937), 406.
4. —— 'The two-dimensional hydrodynamical theory of moving aerofoils, II', ibid. **164** (1938), 346.
5. —— 'The two-dimensional hydrodynamical theory of moving aerofoils, IV', ibid. **188** (1947), 439.
6. —— 'The two-dimensional hydrodynamical theory of moving aerofoils, III', ibid. **172** (1939), 213.

THE BEHAVIOUR OF FRAMED STRUCTURES UNDER REPEATED LOADING

By B. G. NEAL (*Engineering Laboratory, University of Cambridge*)

[Received 7 February 1950; revised 4 July 1950]

SUMMARY

When a structure is subjected to several loads, each of which may vary independently of the other loads between certain limits, it becomes necessary to consider the possibility that failure may occur by the establishment of a cycle of plastic deformation, even though no possible combination of the loads could cause collapse. If, for example, a flexural member was bent repeatedly first in one sense and then in the other sense, so that yield occurred at each reversal of stress, fracture would be expected to occur after a comparatively short time. Alternatively, the permanent deformations might continue to increase each time a particular sequence of loads was repeated, so that large deformations would be developed after a few repetitions of the loads. In such cases the structure must be designed so that after a few applications of the various possible peak load combinations, a state of residual stress is reached which enables all further variations of the loads to be supported elastically. When this happens the structure is said to have shaken down.

In this paper the behaviour of framed structures under variable loads is discussed, and a theorem is established which enables framed structures to be examined with a view to determining whether shake-down will occur under a given set of loads which may alternate between prescribed limits.

Introduction

In recent years methods of plastic design have been developed for structures of ductile material, such as mild steel, which are based on the calculation of the load at which a structure collapses owing to excessive plastic deformation. Such methods of design may lead to substantial economies of material, such as have been discussed by Baker (**1**). In most investigations into the problem of plastic design it has been assumed that each load increases steadily from zero to its maximum value, and that the loads bear a constant ratio to one another. It often happens, however, that a structure is subjected to several loads, each of which may vary a large number of times between prescribed maximum and minimum values independently of the values of the other loads at the same time. Such conditions of loading might arise, for example, in the steel frame of a factory building, which might be stressed by a wind load which varied independently of other loads on the frame, such as those due to overhead travelling cranes. The possibility then arises that although no possible load combination could cause collapse, a cycle of plastic deformations might be established in the structure, no matter how often and in what order the loads were applied. For

instance, a member might be bent back and forth repeatedly, so that yield occurred alternately in tension and compression in its outer fibres. This would soon lead to fracture of the member. Alternatively, the permanent deformations might increase by definite amounts each time a cycle of loads was repeated, leading to failure of the structure owing to the building up of large deflexions. It is therefore necessary that in such cases the structure should be proportioned in such a way that plastic flow eventually ceases, a state of residual stress being reached which enables all further variations of the loads to be supported in a purely elastic manner. When this happens, the structure is said to have shaken down (**2**).

The present paper deals with framed structures with rigid joints which carry load by virtue of the resistance of the members to flexure, and its object is to establish the following theorem governing their behaviour under variable loads:

THEOREM. *If any particular system of residual moments exists which would enable all further variations of the applied loads between their prescribed limits to be supported in a purely elastic manner, then the structure will shake down, although the actual system of residual moments existing in the structure when it has shaken down will not necessarily be the particular system which has been found.*

The shake-down theorem was first stated in a general form by H. Bleich (**3**). However, Bleich only proved this theorem for the particular case of structures possessing not more than two redundancies. A general proof for the case of trusses with any number of redundant members was given by Melan (**4**) and the proof given in this paper for the case of framed structures follows along somewhat similar lines.

The analysis is based on assumptions which do not represent the behaviour of actual materials of construction very closely. However, this enables the presentation to be greatly simplified, and it is felt that the main features of the problem are demonstrated.

Assumptions

It will be assumed that the relation between bending moment and curvature is of the type shown in Fig. 1. Thus the behaviour is assumed to be elastic unless the magnitude of the bending moment is M_p, in which case the curvature can increase indefinitely while the bending moment remains constant. In practice this assumption is not borne out, for elastic behaviour ceases when the most highly stressed fibres reach the yield point, whereas the curvature does not increase indefinitely under constant bending moment until the entire cross-section has yielded at a somewhat higher

bending moment. For instance, a typical mild steel beam of I-section, when loaded from a stress-free condition, may be expected to yield at a bending moment which is only about $0{\cdot}8M_p$. Nevertheless, it is felt that the analysis which follows illustrates the essential features of the problem.

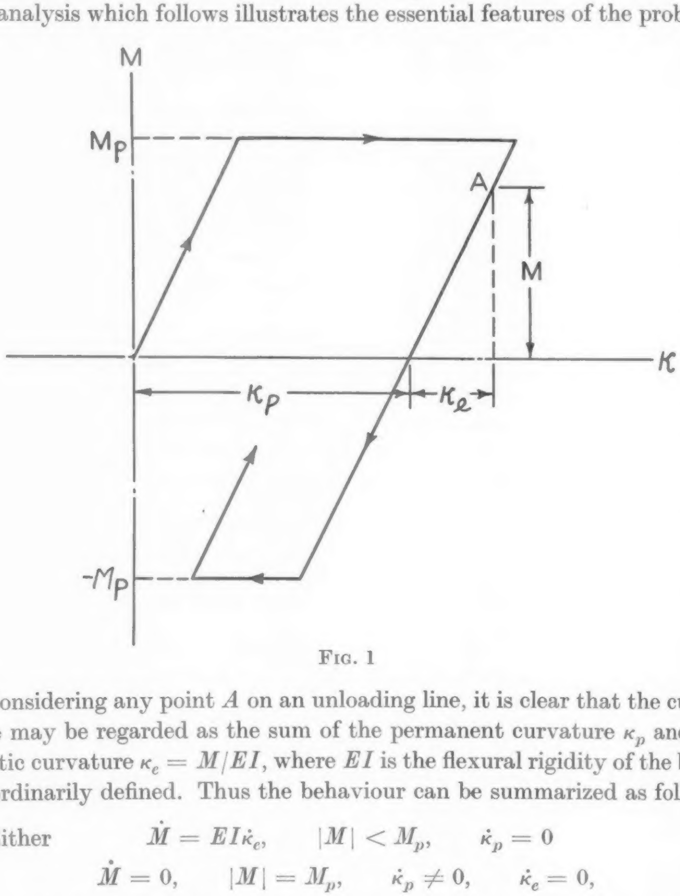

FIG. 1

Considering any point A on an unloading line, it is clear that the curvature may be regarded as the sum of the permanent curvature κ_p and the elastic curvature $\kappa_e = M/EI$, where EI is the flexural rigidity of the beam as ordinarily defined. Thus the behaviour can be summarized as follows:

Either $\qquad \dot{M} = EI\dot{\kappa}_e, \qquad |M| < M_p, \qquad \dot{\kappa}_p = 0$

or $\qquad \dot{M} = 0, \qquad |M| = M_p, \qquad \dot{\kappa}_p \neq 0, \qquad \dot{\kappa}_e = 0,$

where the dots denote increments of the bending moments and curvatures. This notation for increments will be retained throughout the paper.

It is also assumed that the members are so proportioned that conditions of instability do not occur. The conditions under which this assumption would be justified have recently been discussed by Baker (**1**), who also showed that in most cases the effects of shear and direct thrust are negligible. A further assumption is that the structure is only subjected to concentrated loads, applied at a finite number of points. In this case the

bending-moment diagram consists of a series of straight-line segments between sections which are termed the joints of the structure. Joints therefore occur at any section where a load is applied, or where a member is supported or joins other members. It is then assumed that yield can only occur at the joints in a structure. This is clearly true in the special case in which the cross-sections of the members are uniform between the joints, and is also justified in many other cases (**5**).

If yield occurs at a joint, the curvature can increase indefinitely, and this implies that the slope of the member could undergo a discrete change at the joint. If this happens, a plastic hinge is said to have formed. In practice, of course, such an abrupt change of slope cannot occur, since the strains must remain finite, but large changes of slope do take place over short lengths of members at joints, and the idealization involved in the concept of a plastic hinge has been justified by numerous experiments (**1**).

The shake-down theorem

Let $\mathscr{M}_i$ denote the bending moment at a joint i of a member, calculated on the assumption that the frame behaves elastically everywhere, and suppose that when all possible combinations of the external loads between their prescribed limits are considered, it is found that the maximum and minimum values of $\mathscr{M}_i$ are $\mathscr{M}_i^{\max}$ and $\mathscr{M}_i^{\min}$. Further, let m_i denote a set of residual moments at the joints, satisfying only the conditions of equilibrium when the external loads are zero. The actual bending moment M_i at a joint is defined to be $m_i+\mathscr{M}_i$. Then the shake-down theorem states that if any particular set of residual moments $\bar{m}_i$ can be found which satisfies at every joint the conditions

$$\left.\begin{aligned} \mathscr{M}_i^{\max}+\bar{m}_i &\leqslant (M_p)_i \\ \mathscr{M}_i^{\min}+\bar{m}_i &\geqslant -(M_p)_i \end{aligned}\right\}, \tag{1}$$

the frame will shake down, although the residual moments existing in the frame after shake-down will not necessarily be the $\bar{m}_i$.

Before presenting the proof of this theorem it is necessary to state the principle of virtual work in the following simplified form suitable for the present discussion:

$$\int M'\kappa'\,ds+\sum M'\psi_p' = 0. \tag{2}$$

In this equation M' denotes any system of bending moments in equilibrium with zero external load, and κ' denotes any system of curvatures which is compatible with rotations ψ_p' of the plastic hinges at the joints. The integration extends over all lengths of the members between joints, and the summation includes all the joints in the structure.

To establish the shake-down theorem, consider the positive definite quantity E, defined by

$$E = \int \frac{(m-\bar{m})^2}{2EI} ds. \tag{3}$$

In this expression m represents the actual system of residual moments in the frame at any particular stage during the loading process, and $\bar{m}$ is a particular system of residual moments which has been found to satisfy the inequalities (1) at every joint. The integration extends over all the members of the structure.

The change in E due to small increments in the applied load is

$$\dot{E} = \int \frac{(m-\bar{m})\dot{m}}{EI} ds. \tag{4}$$

Consider now the application of the principle of virtual work. The system of bending moments will be chosen as $(m-\bar{m})$, this system being in equilibrium with zero applied load. For the system of compatible displacements the changes of curvature and plastic hinge rotation associated with the increments $\dot{m}$ of the residual moments in the unloaded frame are chosen. Then from equation (2)

$$\int \frac{(m-\bar{m})\dot{m}}{EI} ds + \sum (m-\bar{m})\dot{\psi}_p = 0. \tag{5}$$

Combining equations (4) and (5), it is seen that

$$\dot{E} = -\sum (m-\bar{m})\dot{\psi}_p. \tag{6}$$

Suppose now that at any section of a beam adjacent to a joint,

$$m_i - \bar{m}_i < 0.$$

From (1), $\bar{m}_i \leqslant (M_p)_i - \mathscr{M}_i^{\max}$. Hence $m_i + \mathscr{M}_i^{\max} < (M_p)_i$.

Now $m_i + \mathscr{M}_i^{\max} = M_i^{\max}$, where $M_i^{\max}$ is the maximum possible bending moment which could arise at the cross-section i when the residual bending moment is m_i. Thus $M_i^{\max} < (M_p)_i$. It follows that if yield is occurring at this cross-section, $\dot{\psi}_p < 0$.

By a similar argument, it can be shown that if $m_i - \bar{m}_i > 0$, then $\dot{\psi}_p \geqslant 0$, so that

$$(m_i - \bar{m}_i)\dot{\psi}_p \geqslant 0. \tag{7}$$

Comparing this result with equation (6) it is seen that $\dot{E} \leqslant 0$. This shows that E decreases if yielding takes place, but remains constant while the structure behaves elastically. Since E is a positive definite quantity, it follows that it must eventually become zero or settle down at some positive value and thereafter remain constant, so that shake-down will occur. In the latter case the system of residual moments existing in the structure in the shaken down condition will differ from the $\bar{m}_i$.

It should perhaps be noted that the residual moments m_i, referred to in the foregoing proof as the actual system of residual moments at any particular stage of the loading process, may not represent the residual moments that would arise in the structure upon removal of all the loads at this stage, for it is possible that some yielding might take place as the loads were removed. At any joint i, where the loads would produce a bending moment $\mathscr{M}_i$ if the structure were entirely elastic, and the actual bending moment is M_i, m_i is defined to be $M_i-\mathscr{M}_i$. This would only correspond to the residual moment at the joint i which would arise if all the loads were removed provided that such a removal did not involve further plastic flow.

In conclusion, it should be mentioned that if, by some means of analysis based on the theorem just proved, it is found that a structure will shake down, it is not necessary to carry out a separate investigation to ensure that there is no permissible combination of loads which will cause collapse. A structure that fulfils the conditions (1) cannot collapse, as has been shown by Greenberg (**6**).

Discussion

The assumptions made as to the relation between bending moment and curvature, as indicated in Fig. 1, do not represent the behaviour of actual materials of construction very closely, owing to the range of bending moment which always exists between first yield and the development of full plasticity over the entire cross-section of a beam. However, it is believed that the principal features of the behaviour of framed structures are described by the analysis based on those simplifying assumptions, and it should be remarked that a shake-down theorem has been established which takes into account the range of bending moment which exists between first yield and full plasticity in a beam (**7**).

It has been shown that shake-down will occur if any set of residual bending moments $\bar{m}_i$ can be found which satisfies the inequalities (1) at every joint in the frame, together with the conditions of equilibrium under zero applied load. General methods are available for examining systems of linear inequalities of this type (**8**), and the application of these methods to the shake-down problem has been investigated (**9**).

In conclusion, it should perhaps be remarked that in many problems where alternating loads have to be considered, the design may be governed by the fatigue limit of the material if the peak loads may be repeated a very large number of times. The criterion of shake-down is intended to be applicable in cases where relatively few applications of the peak loads are expected to occur.

Acknowledgement

The results presented in this paper were obtained in the course of research sponsored jointly by the U.S. Office of Naval Research and Bureau of Ships, when the author was a staff member at Brown University, Providence, R.I., U.S.A.

REFERENCES

1. J. F. Baker, 'A review of recent investigations into the behaviour of steel frames in the plastic range', *J. Inst. Civ. Eng.* **31** (1949), 188.
2. W. Prager, 'Problem types in the theory of perfectly plastic materials', *J. Aero. Sci.* **15** (1948), 337.
3. H. Bleich, 'Über die Bemessung statisch unbestimmter Stahltragwerke unter Berücksichtigung des elastisch-plastischen Verhaltens des Baustoffes', *Der Bauingenieur*, **19/20** (1932), 261.
4. E. Melan, 'Theorie statisch unbestimmter Systeme', *Preliminary Publication, 2nd Congr. Int. Ass. Bridge and Structural Engineering* (Berlin, 1936), p. 45.
5. B. G. Neal, 'The behaviour of continuous beams and plane frames under repeated loading', *Technical Report No.* A11–32, *Brown Univ., to Office of Naval Research*, April, 1949.
6. H. Greenberg, 'The principle of limiting stress for structures', paper presented at the 2nd Symposium on Plasticity, Brown University, April 1949.
7. B. G. Neal, 'Plastic collapse and shake-down theorems for structures of strain-hardening material', *J. Aero. Sci.* **17** (1950), 297.
8. L. L. Dines, 'Systems of linear inequalities', *Annals of Mathematics*, **20** (1918–19), 191.
9. P. S. Symonds and B. G. Neal, 'The calculation of failure loads on plane frames under arbitrary loading programmes', *J. Inst. Civ. Eng.* **35** (1950).

THE COMPATIBILITY CONDITIONS FOR LARGE STRAINS

By A. S. LODGE

(*British Rayon Research Association, 58 Whitworth Street, Manchester, 1*)

[Received 15 June 1950]

SUMMARY

The compatibility conditions for large strains are shown to be sufficient. A theorem is proved which states that a given initial configuration and a given strain field determine the corresponding final configuration to within an arbitrary rigid movement of the whole medium.

1. Introduction

MOST of the early work on the theory of elasticity has been restricted for reasons of mathematical simplicity to the case of infinitesimally small strains;† and most of the recent work has been devoted to removing this restriction.

A field of strain in a continuous medium can be described relative to a given coordinate system by six functions of position, known as strain components; not every set of six functions of position can be so used, however, because the strain components necessarily satisfy a certain set of six partial differential equations, known as compatibility conditions. These conditions restrict the way in which the values of the strain components can vary from one particle to another; the strain components at any one particle are independent and can be given values at will. The conditions are purely kinematic in origin, and their existence can be traced to the fact that the medium is assumed to be continuous and to deform in a continuous manner. When the strain is infinitesimally small and the coordinate system is rectangular Cartesian, the form of the conditions is well known; in fact one method of calculating the distribution of stress in an elastic solid is to solve the differential equations for the stress variables which are obtained by eliminating the strain variables between the stress–strain relations and the compatibility conditions.

† An infinitesimal strain is generally defined as a movement for which the space derivatives of the displacement functions in Cartesian coordinates are so small that their squares and products may be neglected; it is worth noting that this requires not only that the ratio of change of separation to separation of every pair of neighbouring particles shall be small, but also that the rotational movement of every material element shall be small; the translatory movement is not, of course, restricted.

[Quart. Journ. Mech. and Applied Math., Vol. IV, Pt. 1 (1951)]

Recently Weissenberg (**1**) and, independently, Green and Zerna (**2**), have shown that the fact that the Riemann curvature tensor field vanishes in Euclidean space can be used to derive the compatibility conditions in a form valid for large strains and for any coordinate system. In their general form the equations are non-linear in the strain components, and are so complicated that their use in most practical problems is likely to present formidable mathematical difficulties. Nevertheless, it seems worth while giving some discussion of the conditions.

In this paper we shall be concerned with two rather formal questions. We shall prove that the compatibility conditions as derived by Weissenberg are not only necessary but sufficient, and we shall prove a related theorem which states that whenever an initial configuration is given, a knowledge of the values of the strain components throughout the medium is sufficient to determine the corresponding final configuration to within an arbitrary translation and rotation of the medium as a rigid whole.

2. The description of strain

We consider two configurations of a continuous medium, one of which we shall call the initial configuration and the other the final configuration. We suppose not only that the medium is continuously distributed in space but that either configuration can be obtained from the other by a continuous motion, in the sense given below. (This restriction is physically important, for it means that any two particles which are infinitesimally near to one another in one configuration are infinitesimally near to one another in the other configuration, so that movements which, for example, involve diffusion of certain particles through the rest of the medium are excluded from the discussion.)

It is perhaps simplest in the first instance to suppose that the medium is of infinite extent, covering the whole of space; it is possible to see, however, that the arguments given below hold good for any region of medium of finite extent provided that this region can be regarded as a continuous part of a medium of infinite extent which moves continuously in going from either configuration to the other.

Let us take any coordinate system (not necessarily Cartesian) fixed in space, and let us describe the position of particles of the medium in terms of coordinates referring to this system. Let (x^1, x^2, x^3) and (X^1, X^2, X^3) denote the coordinates of the positions occupied by a typical particle in the initial and final configurations respectively. Since one and only one particle occupies one and only one position in a configuration, the functional relations

$$X^i = F^i(x) \quad (i = 1, 2, 3) \quad \text{(say)} \tag{2.1}$$

which exist between the two sets of coordinates must be one-valued and possess a one-valued inverse

$$x^i = f^i(X) \quad (i = 1, 2, 3) \quad \text{(say)}. \tag{2.2}$$

We have here used x as an abbreviation for x^1, x^2, x^3, and X as an abbreviation for X^1, X^2, X^3. Since the medium is continuously distributed in space, the variables x, X take on continuous ranges of values.

By requiring either configuration to be obtainable from the other by a continuous movement we mean not only that the functions F^i, f^i shall be continuous but that all their partial derivatives up to at least the third order shall exist and be continuous.

Let us now suppose that the initial configuration is given, so that any particle can be recognized by the values of x, and let us regard the final configuration as capable of being varied. It is clear that a knowledge of the functions F^i in (2.1) suffices to determine the final configuration completely. In particular, the final configuration of any infinitesimally small region of the medium is determined by the functions F^i. The movement of such a region from one configuration to the other can, however, be resolved into a translation and rotation involving no change in separation of particles of the region and a strain, which does involve such changes; the possibility of performing this resolution arises from the differentiability of the functions F^i. When stresses are set up in a moving material, they are primarily related to changes in separation of the particles and are not directly affected by rigid movements, so it is convenient to have some mathematical expression which describes the strain alone; it is clear that the functions F^i, for example, will not serve this purpose. There is in fact an unlimited number of possible expressions for describing strain, and several are in current use; it is generally the case that some are mathematically more convenient than others in a given context; the form of the compatibility conditions will, of course, depend on the expression chosen. We shall choose an expression which bears a close resemblance to the components of a metrical tensor field and which in consequence allows us to derive the compatibility conditions very readily by making use of certain known results; we shall indicate how the forms of the compatibility conditions appropriate to other expressions can be obtained.

Let $g_{ij}(x)$ denote the components of the metrical tensor field referred to the given coordinate system. The initial and final separations of a pair of neighbouring particles are then given by the expressions

$$(ds)^2 = g_{ij}(x)\, dx^i dx^j, \tag{2.3}$$

$$(dS)^2 = g_{ij}(X)\, dX^i dX^j, \tag{2.4}$$

where x, $x+dx$ are the initial positions, and X, $X+dX$ are the final positions. Here and elsewhere we use the summation convention with dummy suffixes taking values 1, 2, and 3.

We may now use (2.1) to express X in terms of x; substituting the result in (2.4) we obtain the final separation expressed in terms of the initial coordinates, viz.

$$(dS)^2 = h_{ij}(x)\,dx^i dx^j, \tag{2.5}$$

where

$$h_{ij}(x) = g_{\alpha\beta}\{F(x)\}\frac{\partial F^\alpha}{\partial x^i}\frac{\partial F^\beta}{\partial x^j}. \tag{2.6}$$

It is clear from (2.5) that, the initial configuration being given, a knowledge of the functions $h_{ij}(x)$ suffices to determine the separations of all pairs of neighbouring particles in the final configuration, and, moreover, that if the final configuration be varied, the values of $h_{ij}(x)$ change only when at least some of the separations change. Thus the functions $h_{ij}(x)$ may be used to describe the strain. (We note that $h_{ij}(x)$ are the components of a symmetric covariant tensor field, and so also are $h_{ij}(x)-g_{ij}(x)$; when $h_{ij}(x) = g_{ij}(x)$, the whole medium has moved rigidly in going from the initial to the final configuration.)

3. The compatibility conditions

In going over from the functions $F^i(x)$ to the functions $h_{ij}(x)$ we have achieved the desired result of finding expressions which are affected only by changes in separation of particles of the medium; we note, however, that the number of apparently independent functions has increased from three to six. This increase can only be apparent and not real because the six functions $h_{ij}(x)$ are completely determined once the three functions $F^i(x)$ are known, the precise relations between them being given in equations (2.6) above (the $g_{ij}(x)$ may be regarded as given once and for all with the coordinate system). By eliminating the functions F^i between these equations and such of their derived equations as may be necessary we should expect to be able to obtain certain equations for the $h_{ij}(x)$ and their derivatives which will effectively decrease the 'functional degrees of independence' of the $h_{ij}(x)$ from six to three. These are in fact the compatibility conditions for the strain components $h_{ij}(x)$.

To carry out the required elimination directly would be so tedious as to be hardly practicable. Fortunately, exactly the same mathematical problem occurs in Riemannian geometry (in connexion with the conditions which a given set of functions $g_{ij}(x)$ must satisfy in order to be components of a metrical tensor field in a three-dimensional Euclidean space) and the solution is well known; we shall be content to assume the truth of the required geometrical results and to show that they can be applied in our circumstances, not only to derive the compatibility conditions, but to show

that these are sufficient and to prove the related theorem mentioned in the introduction. From this point of view, the present paper is nothing but a translation of certain results from language familiar to geometers into language familiar to rheologists.

The theorem we require is attributed to Christoffel, but it seems better for our purpose to quote it in the form given subsequently by Eisenhart (**3**), whose proof is readily accessible.

THEOREM (3.1). *A necessary and sufficient condition that a quadratic differential form* $g_{ij}(x)\,dx^i dx^j$ $(i = 1, 2, 3)$ *be reducible to a form with constant coefficients is that the components of the Riemann tensor field constructed from the coefficients* $g_{ij}(x)$ *vanish; the transformation involves six arbitrary constants.*

Eisenhart proves the theorem for the general case of an n-dimensional quadratic form; we have put $n = 3$ corresponding to space being three-dimensional. An inspection of the text shows that 'reducible' means reducible by a transformation of variables having the properties of one-valuedness, differentiability, and reversibility which we have assigned to the transformation $x \to X = F(x)$ in section 2 above; we shall call such transformations 'allowable transformations'.

We shall now use the first part of the theorem to derive the compatibility conditions for $h_{ij}(x)$. Let us suppose that two configurations are given and that $h_{ij}(x)$ are the corresponding strain components. Equations (2.4) and (2.5) show that an allowable transformation $x \to X$ exists which transforms the quadratic form $h_{ij}(x)\,dx^i dx^j$ into the quadratic form $g_{ij}(X)\,dX^i dX^j$. Space being Euclidean, we know that $g_{ij}(X)\,dX^i dX^j$ is reducible to a quadratic form with constant coefficients (by a change of coordinate system, in fact). Since the result of performing two allowable transformations in succession is itself an allowable transformation, it follows that the quadratic form $h_{ij}(x)\,dx^i dx^j$ is reducible to a form with constant coefficients. Hence, by the theorem, the components of the Riemann tensor field constructed from the coefficients $h_{ij}(x)$ necessarily vanish. Using the expressions for these components in the form given by Eisenhart (**4**), we obtain the following equations:

$$\frac{\partial}{\partial x^\mu}\left(\frac{\partial h_{\nu j}}{\partial x^k} - \frac{\partial h_{\nu k}}{\partial x^j}\right) - \frac{\partial}{\partial x^\nu}\left(\frac{\partial h_{\mu j}}{\partial x^k} - \frac{\partial h_{\mu k}}{\partial x^j}\right)$$
$$= 2h^{\alpha\beta}\left\{\left(\frac{\partial h_{\alpha\nu}}{\partial x^k} + \frac{\partial h_{\alpha k}}{\partial x^\nu} - \frac{\partial h_{\nu k}}{\partial x^\alpha}\right)\left(\frac{\partial h_{\beta\mu}}{\partial x^j} + \frac{\partial h_{\beta j}}{\partial x^\mu} - \frac{\partial h_{\mu j}}{\partial x^\beta}\right) - \right.$$
$$\left. - \left(\frac{\partial h_{\alpha\mu}}{\partial x^k} + \frac{\partial h_{\alpha k}}{\partial x^\mu} - \frac{\partial h_{\mu k}}{\partial x^\alpha}\right)\left(\frac{\partial h_{\beta\nu}}{\partial x^j} + \frac{\partial h_{\beta j}}{\partial x^\nu} - \frac{\partial h_{\nu j}}{\partial x^\beta}\right)\right\}$$
$$(\mu, \nu, j, k = 1, 2, 3). \quad (3.2)$$

Here $h^{\alpha\beta}$ are functions of the strain components $h_{ij}(x)$ defined by the equations

$$h^{i\alpha}h_{\alpha j} = \delta^i_j \quad (i; j = 1, 2, 3), \tag{3.3}$$

δ^i_j being the Kronecker symbol.

The equations (3.2) are the compatibility conditions for the strain components $h_{ij}(x)$ in the form given by Weissenberg. They are evidently non-linear relations between $h_{ij}(x)$ and their first- and second-order partial derivatives. Only six of the equations are independent (reference **3**, p. 21); an independent set is obtained by giving the indices $(\mu, \nu; j, k)$ the values $(a+1, a+2; b+1, b+2)$ $(a, b = 1, 2, 3)$, with the convention of regarding as equivalent two indices which differ by a multiple of three (**5**).

It is interesting to note that the metrical components $g_{ij}(x)$ do not occur in the equations, so they have the same form whether the coordinate system is Cartesian or not.

The terms on the left-hand side of (3.2) are of the first degree in the second-order derivatives of $h_{ij}(x)$; the remaining terms are of the second degree in the first-order derivatives. When the coordinate system is rectangular Cartesian and the strain is infinitesimally small, $h_{ij}(x) \doteqdot \delta_{ij}$, and therefore the terms on the right-hand side are negligible compared with those on the left-hand side; the equations so obtained have the well-known form. The possibility of obtaining the compatibility conditions in these restricted circumstances in this way has been pointed out by E. Trefftz (**6**).

That the equations (3.2) are sufficient as well as necessary also follows from the first part of theorem (3.1); to prove this we shall show that any set of twice-differentiable functions $h_{ij}(x) = h_{ji}(x)$ satisfying (3.2) can describe a state of strain or, more precisely, that such functions being given, two configurations exist which are related by an allowable transformation $x \to X = F(x)$, where the functions $F^i(x)$ are related to $h_{ij}(x)$ by equations (2.6).

Since the given functions $h_{ij}(x)$ satisfy (3.2), it follows from theorem (3.1) that $h_{ij}(x)\, dx^i dx^j$ is reducible to a quadratic form with constant coefficients. The metrical form $g_{ij}(X)\, dX^i dX^j$ is also reducible to a quadratic form with constant coefficients. Two quadratic forms with constant coefficients can clearly be transformed into each other by an allowable transformation. Combining the various transformations involved, it follows that an allowable transformation $x \to X = F(x)$ exists for which

$$h_{ij}(x)\, dx^i dx^j = g_{ij}(X)\, dX^i dX^j. \tag{3.4}$$

Since values can be assigned at will to either set of differentials in this equation, it follows on making the substitution $X = F(x)$ that the functions $F^i(x)$ and $h_{ij}(x)$ are related by equations (2.6). Further, since $x \to X = F(x)$

is an allowable transformation, we may take any continuous configuration of the medium and regard it as the initial configuration and then use this transformation to define the final configuration. The given functions $h_{ij}(x)$ then describe the corresponding strain. This completes the proof of the sufficiency of the conditions (3.2).

The form of the compatibility conditions given above is appropriate to the use of the functions $h_{ij}(x)$ as strain components; some other types of strain components which have been used are expressible in terms of $h_{ij}(x)$ and the metrical components $g_{ij}(x)$, and the form of conditions for these can be obtained at once from the conditions given above; for example, if we use $h_{ij}(x)-g_{ij}(x) \equiv e_{ij}(x)$ (say), we merely substitute $e_{ij}(x)+g_{ij}(x)$ for $h_{ij}(x)$ in (3.2), and thus obtain conditions for $e_{ij}(x)$. There are, however, strain components which cannot be expressed in terms of $h_{ij}(x)$ and $g_{ij}(x)$ alone. These arise when the separations of particles are described in terms of the coordinates of their final positions, instead of their initial positions as above; the two methods of describing changes in separations which arise in this way have been called (7) 'Eulerian' and 'Lagrangian' respectively. For some purposes the distinction between Lagrangian and Eulerian descriptions is important, but this is not the case for the questions discussed in the present paper; this follows from the fact that we consider only two configurations which are on an equal footing; although we have given preference to one configuration by describing strain in terms of the coordinates of initial positions, it can be seen that the whole treatment can equally well be carried through in terms of the coordinates of final positions. Thus if we introduce quantities $H_{ij}(X)$ such that $H_{ij}(X)\,dX^i dX^j$ is the square of the initial separation of particles finally at X, $X+dX$, a simple interchange of the words 'initial' and 'final' wherever they are applied to configurations in the arguments given above allows one to deduce that the compatibility conditions for $H_{ij}(X)$ have exactly the same form as the conditions given for $h_{ij}(x)$ in (3.2) above. Other Eulerian types of strain components are expressible in terms of $H_{ij}(X)$ and $g_{ij}(X)$, and the compatibility conditions are accordingly readily obtainable.

4. A property of the strain field

Let us suppose that a coordinate system and an initial configuration are given, so that the coordinates of the initial position of every particle of the medium are known. We shall now consider the extent to which a knowledge of the strain components $h_{ij}(x)$ allows us to determine the corresponding final configuration. Because this information allows us to determine the final separation of every pair of neighbouring particles, we should expect the final configuration to be determined to within a movement

which involves no change in the separation of neighbouring particles and therefore no change in the separation of any particles. The second part of the theorem quoted above enables us to show that this is in fact the case.

We have the same conditions as in the proof of the sufficiency of the compatibility conditions set out above where, given quantities $h_{ij}(x)$ satisfying (3.2) and an initial configuration, we established the existence of a final configuration for which $h_{ij}(x)\,dx^i dx^j$ gave the square of the final separation of particles initially at (x), $(x+dx)$; we now consider the uniqueness of this final configuration. Let us first consider the case in which the given coordinate system is rectangular Cartesian. Let X, $X+dX$ be the coordinates of the final positions of particles initially at x, $x+dx$. We then have $h_{ij}(x)\,dx^i dx^j = \sum (dX^i)^2$, where $x \to X$ is an allowable transformation; the second part of Theorem (3.1) applies, and shows that this transformation can involve at most six arbitrary constants. Consider the variables $\bar{X}^i$, defined in terms of the variables X^i by the equations

$$\bar{X}^i = A^i + B^i_j X^j \quad (i = 1, 2, 3), \tag{4.1}$$

where A^i and B^i_j are constants, and B^i_j are the components of an orthogonal matrix. Clearly $x \to \bar{X}$ is an allowable transformation, and

$$h_{ij}(x)\,dx^i dx^j = \sum (dX^i)^2 = \sum (d\bar{X}^i)^2,$$

so that $x \to \bar{X}$ defines another final configuration consistent with the given data. It is evident from (4.1) that this final configuration is obtainable from the other final configuration by a translation and rotation of the medium as a rigid whole. Moreover, since three of the constants B^i_j can be given values at will, the transformation $X \to \bar{X}$ and therefore $x \to \bar{X}$ involves six arbitrary constants, so that all final configurations consistent with the given data are obtainable in this way. Hence the strain components $h_{ij}(x)$ determine the final configuration to within an arbitrary movement of the medium as a rigid whole.

It is easily seen that the same result holds good when the coordinate system is not rectangular Cartesian. From the given data, $h_{ij}(x)\,dx^i dx^j$ is a scalar for arbitrary values of the differentials, and therefore $h_{ij}(x)$ are components of a tensor field; the compatibility conditions express the vanishing of the components of a tensor field; therefore the strain components induced in any other coordinate system by the given strain components $h_{ij}(x)$ will also satisfy compatibility conditions of exactly the same form as those satisfied by $h_{ij}(x)$. In particular, we may transform to a rectangular Cartesian coordinate system, and the arguments given in the preceding paragraph can then be applied.

Acknowledgment

I would like to thank Dr. K. Weissenberg for many helpful discussions and for permission to refer to unpublished results. I would also like to thank the Council and the Director of Research of the British Rayon Research Association for permission to publish this paper.

REFERENCES

1. K. Weissenberg, private communication.
2. A. E. Green and W. Zerna, *Phil. Mag.*, Ser. 7, **41** (1950), 313.
3. L. P. Eisenhart, *Riemannian Geometry* (Princeton, 1926), p. 25.
4. —— ibid., equations (7.1) and (8.9).
5. T. Levi-Civita, *The Absolute Differential Calculus* (Blackie, 1947), p. 198.
6. E. Trefftz, *Handbuch der Physik* (Springer), vi. 64.
7. F. D. Murnaghan, *American J. Math.* **59** (1937), 235.

CONTACT STRESS AND DEFORMATION IN A THIN ELASTIC LAYER

By MARGARET HANNAH

(*Dept. of Textile Industries, University of Leeds*)

[Received 4 July 1950]

SUMMARY

The rollers used in drafting textile fibres are disk-shaped, the lower one made of steel, the upper with a metal centre and a fairly thin elastic cover. The length over which the rollers are in contact, and the pressure distribution over this length, are factors which affect their performance as drafting agents. The purpose of this paper is to show how these quantities vary with the material and thickness of the cover, the pressure between the rollers, and the roller size. The effect of allowing slippage at the inner boundary is also considered.

The system can be considered mathematically as one of generalized plane stress in an elastic layer, with given displacement conditions on its inner boundary (the interface between metal and cover will be termed the 'inner boundary' of the cover) and subject to pressure by a body of given shape on its free face. The layer is sufficiently thin for the inner boundary conditions to affect the stresses in the contact zone.

The analysis of contact stresses was first carried out by Hertz (**1**), and quoted in Love (**2**). The application to the two-dimensional case is given by Thomas and Hoersch (**3**)—their results, which are for plane strain, may be converted by the usual modification of the Poisson's ratio to those of generalized plane stress. These analyses, however, only hold if the contact stresses are the only effective forces over the contact zone

The effect of the boundary conditions on the solution for a single isolated force may be found straightforwardly by a method given in Coker and Filon (**4**). The displacement due to any pressure distribution over the contact zone can then be determined, and the actual pressure distribution may be found by imposing the condition of known displacement over this zone. It has been found most convenient, in practice, to determine the difference between the pressure distributions for an infinite and finite thickness; this difference can be expressed as a Fourier series, and a sufficient number of the coefficients can be found to give any desired accuracy.

Solution for infinite thickness

If the free face is the plane $y = 0$ and the y-axis is measured vertically downwards, then it is known that the displacement v in a semi-infinite plate due to a downward force W at the origin is given by

$$v = -\frac{2W}{\pi E}\log r + \text{constant}, \tag{1}$$

where E is the Young's modulus of the material, and $r^2 = x^2+y^2$.

It can be shown from this that, when an elastic disk of diameter D_1 is pressed against a hard disk of diameter D_2 with a force W, contact is over a length $2h$, where

$$h^2 = \frac{2WD}{\pi E} \quad \text{and} \quad 1/D = 1/D_1 + 1/D_2. \tag{2}$$

It is assumed in the derivation that h is small in comparison with D_1 and D_2.

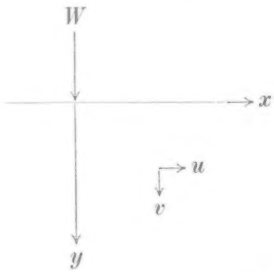

The pressure distribution over this contact length is given by

$$P(x) = \frac{2W}{\pi h}(1 - x^2/h^2)^{\frac{1}{2}} \quad (-h \leqslant x \leqslant h), \tag{3}$$

where $P(x)$ is the force per unit length at x. These results may be derived from those given by Thomas and Hoersch (**3**) (with a slightly different notation).

The displacement function for the idealized (and non-physical) isolated force contains an inevitable logarithmic term giving a non-physical infinite displacement at the origin. However, the physical separation $G(x)$ between the two surfaces at points outside but near to the contact zone may be found. We have

$$G(x) = v(x) + x^2/D - v(h) - h^2/D,$$

i.e.

$$G'(x) = v'(x) + 2x/D \quad \text{and} \quad G(h) = 0. \tag{4}$$

By using (3) and (1) and integrating over the contact zone,

$$v'(x) = -\frac{4W}{\pi^2 Eh}\frac{d}{dx}\int_{-h}^{h} (1 - x'^2/h^2)^{\frac{1}{2}} \log(x - x')\, dx',$$

which, from (2), becomes

$$v'(x) = -2h/D\{x/h - (x^2/h^2 - 1)^{\frac{1}{2}}\} \quad \text{for} \quad |x| > h,$$

and so

$$G(x) = 2h/D \int_{h}^{x} (x^2/h^2 - 1)^{\frac{1}{2}}\, dx$$

$$= h^2/D\{(x/h)(x^2/h^2 - 1)^{\frac{1}{2}} - \cosh^{-1} x/h\}. \tag{5}$$

Isolated force on a thin elastic layer

A solution for the stress function following the methods of Coker and Filon (**4**) with some slight changes of notation, is

$$X = \int\limits_0^\infty \frac{\cos mx}{2m^2}[\{\phi_1(m)+my\,\phi_2(m)\}\cosh my+\{\phi_3(m)+my\,\phi_4(m)\}\sinh my]\,dm, \tag{6}$$

which can be made to satisfy four sets of boundary conditions.

Coker and Filon give the solution appropriate to an isolated force W on the free face, with an inner boundary in contact with a smooth plane so that there is no shear and no vertical displacement there. This solution is

$$\phi_1(m) = \frac{2W}{\pi}, \qquad \phi_2(m) = \left(\frac{4W}{\pi}\right)\frac{\sinh u}{2u+\sinh 2u},$$

$$\phi_3(m) = -\left(\frac{4W}{\pi}\right)\frac{\sinh^2 u}{2u+\sinh 2u}, \qquad \phi_4(m) = -\left(\frac{4W}{\pi}\right)\frac{\cosh u}{2u+\sinh 2u}, \tag{7}$$

where $u = mb$, and b is the thickness of the layer. A constant term,

$$\frac{2W}{\pi}\int\limits_0^\infty \frac{1}{2m^2}\,dm$$

must be subtracted to give convergence at $m = 0$. The corresponding vertical displacement of points on the free boundary is

$$v(x) = -\frac{2W}{\pi E}\int\limits_0^\infty \frac{(\cosh z-1)\cos zx/2b}{z(z+\sinh z)}\,dz, \tag{8}$$

where $z = 2u$.

Proceeding on similar lines, the solution for an isolated force W and an inner boundary having no horizontal or vertical displacement has been found by the present writer to be

$$\phi_1(m) = 2W/\pi,$$

$$\phi_2(m) = -\phi_3(m) = -\left(\frac{2W}{\pi}\right)\frac{\{(3-4\sigma)\cosh u\sinh u-u\}}{u^2+(1-2\sigma)^2+(3-4\sigma)\cosh^2 u},$$

$$\phi_4(m) = \left(\frac{2W}{\pi}\right)\frac{(1-2\sigma+\cosh^2 u)}{u^2+(1-2\sigma)^2+(3-4\sigma)\cosh^2 u}, \tag{9}$$

where $\sigma = \eta/(1+\eta)$, η being Poisson's ratio. The same constant term as in

the above solution, $\left(\frac{2W}{\pi}\right)\int\limits_0^\infty \frac{1}{2m^2}\,dm$, must be subtracted to give convergence. The corresponding vertical displacement of points on the free boundary is

$$v(x) = -\frac{2W}{\pi E}\int\limits_0^\infty \left\{\frac{(3-4\sigma)\sinh z - z}{\frac{1}{2}z^2+(3-4\sigma)\cosh z+5-12\sigma+8\sigma^2}\right\}\cos\left(\frac{zx}{2b}\right)\frac{dz}{z}. \tag{10}$$

These solutions are for a straight layer on a horizontal plane. They may, however, be applied to an annular layer if the thickness is small relative to the diameter, i.e. if b is small relative to D_1.

Determination of contact stresses

Equations (8) and (10) give the displacements for an isolated force with two different sets of boundary conditions, in the form

$$v(x) = -\frac{2W}{\pi E}\int\limits_0^\infty Q(z)\cos\left(\frac{zx}{2b}\right)dz.$$

The displacement due to a pressure distribution $P(x)$ over $-h \leqslant x \leqslant h$ is

$$v(x) = -\frac{2}{\pi E}\int\limits_{-h}^{h} P(x')\,dx'\int\limits_0^\infty Q(z)\cos\left\{\frac{z(x-x')}{2b}\right\}dz,$$

and it is required to determine $P(x)$ so that this shall represent the given displacement, $d-x^2/D$, over the contact zone $-h \leqslant x \leqslant h$, d being the deflexion at the midpoint of the zone. Because of the logarithmic infinity, the condition has to be differentiated with respect to x; such differentiation is permissible under the integral sign. Thus it becomes

$$2x/D = \frac{1}{b\pi E}\int\limits_{-h}^{h} P(x')\,dx'\int\limits_0^\infty zQ(z)\sin\left\{\frac{z(x-x')}{2b}\right\}dz \quad (-h \leqslant x \leqslant h),$$

or, inverting the order of integration,

$$2x/D = \frac{1}{b\pi E}\int\limits_0^\infty zQ(z)\,dz\int\limits_{-h}^{h} P(x')\sin\left\{\frac{z(x-x')}{2b}\right\}dx' \quad (-h \leqslant x \leqslant h). \tag{11}$$

Assume now, by analogy with (3), that

$$P(x) = w\left\{(1-x^2/h^2)^{\frac{1}{2}}+\sum_{n=1} a_n\cos\frac{(2n-1)x\pi}{2h}\right\} \tag{12}$$

an even function, which makes the pressure zero at $x = \pm h$. Then

$$W = \int_{-h}^{h} P(x)\,dx = wh\left[\tfrac{1}{2}\pi + \sum_{n=1} (-1)^{n-1}\left\{\frac{4a_n}{(2n-1)\pi}\right\}\right]. \tag{13}$$

And

$$\int_{-h}^{h} P(x')\sin\left\{\frac{z(x-x')}{2b}\right\} dx'$$

$$= 2b\pi w\left[(1/z)J_1(zh/2b)+(h/2b)\sum_{n=1} (-1)^n \frac{a_n(2n-1)\cos(zh/2b)}{(hz/2b)^2-\{(2n-1)\frac{1}{2}\pi\}^2}\right]\sin zx/2b,$$

where $J_1(x)$ is the Bessel function of the first order. Writing $h/2b = K$, $x/h = X$, $(2n-1)\frac{1}{2}\pi = \psi_n$ the relationship (11) becomes

$$X/D = (w/Eh)\int_0^{\infty} zQ(z)\left\{J_1(Kz)/z+K\sum (-1)^n \frac{a_n(2n-1)\cos Kz}{K^2z^2-\psi_n^2}\right\}\sin KXz\,dz$$

$$\text{for} \quad -1 \leqslant X \leqslant 1. \tag{14}$$

Putting

$$\left.\begin{aligned} J_1(x)/x &= F(x) \\ (-1)^n \frac{(2n-1)\cos x}{x^2-\psi_n^2} &= F_n(x) \end{aligned}\right\} \tag{15}$$

(14) becomes

$$X/D = (w/Eh)\int_0^{\infty} zQ(z)\left\{F(Kz)+\sum_{n=1} a_n F_n(Kz)\right\}K\sin KXz\,dz \quad (-1 \leqslant X \leqslant 1). \tag{16}$$

And we have also, from equation (4),

$$(1/h)G'(x) = -(2w/Eh)\int_0^{\infty} zQ(z)\left\{F(Kz)+\sum_{n=1} a_n F_n(Kz)\right\}K\sin KXz\,dz+2X/D$$

$$(|X| > 1). \tag{17}$$

By inspection of (8) and (10) $zQ(z) \to 1$ as $z \to \infty$ in both cases, so that it is convenient to consider first

$$\left.\begin{aligned} H_0(X) &= \int_0^{\infty} F(Kz)K\sin KXz\,dz \\ \text{and} \qquad H_n(X) &= \int_0^{\infty} F_n(Kz)K\sin KXz\,dz. \end{aligned}\right\} \tag{18}$$

These are known integrals, whose values are

$$H_0(X) = X \qquad\qquad (-1 \leqslant X \leqslant 1)$$

and

$$= X-(X^2-1)^{\frac{1}{2}} \ (|X| > 1) \tag{19}$$

$$H_n(X) = \frac{(-1)^{n-1}}{\pi}\begin{Bmatrix} \cos(1-X)\psi_n \operatorname{Si}(1-X)\psi_n - \cos(1+X)\psi_n \operatorname{Si}(1+X)\psi_n \\ -\sin(1-X)\psi_n \operatorname{Ci}(1-X)\psi_n + \sin(1+X)\psi_n \operatorname{Ci}(1+X)\psi_n \end{Bmatrix}, \tag{20}$$

where

$$\operatorname{Si}(x) = \int\limits_0^x \frac{\sin u}{u}\,du, \qquad \operatorname{Ci}(x) = \int\limits_\infty^x \frac{\cos u}{u}\,du,$$

as usual.

From (19) it can be seen that, as b, the layer thickness, tends to infinity, condition (14) becomes

$$X/D = (w/Eh)\Big\{X + \sum_{n=1} a_n H_n(X)\Big\} \quad (-1 \leqslant X \leqslant 1).$$

The solution of this and equation (13) is $a_n = 0$, all n, $w = 2W/\pi h$, and $h^2/D = 2W/\pi E$, which agrees with the previously obtained solution, as quoted in (2), (3), for this case. Define

$$\left.\begin{aligned} L_0(K, X) &= \int\limits_0^\infty \{1-zQ(z)\}F(Kz)K \sin KXz\,dz, \\ L_n(K, X) &= \int\limits_0^\infty \{1-zQ(z)\}F_n(Kz)K \sin KXz\,dz. \end{aligned}\right\} \tag{21}$$

Then (16) becomes

$$X/D = (w/Eh)\Big[H_0(X) - L_0(K, X) + \sum_{n=1} a_n\{H_n(X) - L_n(K, X)\}\Big]$$
$$(-1 \leqslant X \leqslant 1). \tag{22}$$

Equation (22) can now be used with (13) to determine values of w, h, and a_n for any given K. The a_n are first determined by eliminating (wD/Eh); then using these

$$\frac{h^2}{D} = \left[\frac{H_0(1) - L_0(K, 1) + \sum_{n=1} a_n\{H_n(1) - L_n(K, 1)\}}{\frac{1}{2}\pi + \sum_{n=1} (-)^{n-1}\{4a_n/(2n-1)\pi\}}\right]\frac{W}{E}. \tag{23}$$

And when $K = 0$, from (2),

$$\frac{h^2}{D} = \frac{2W}{\pi E}.$$

Thus, for the same loading, the contact length is smaller for a thin layer in the ratio

$$C_1(K) = h_K/h_0, \tag{24}$$

where

$$C_1(K) = \left[\frac{H_0(1)-L_0(K,1)+\sum_{n=1} a_n\{H_n(1)-L_n(K,1)\}}{1+\sum_{n=1}(-)^{n-1}\{8a_n/(2n-1)\pi^2\}}\right]^{\frac{1}{2}}. \tag{25}$$

Similarly the loading required to give the same contact length is given by

$$W_K = C_1^{-2} W_0. \tag{26}$$

The contact pressure at any point, $P(X)$, may be compared with the average pressure over the zone, $W/2h$, to give a non-dimensional function $R(X)$; when $K = 0$ this function is $(4/\pi)(1-X^2)^{\frac{1}{2}}$. From (12) and (13), its value in the general case is

$$R(X) = \frac{2hP(X)}{W} = \frac{2\left[(1-X^2)^{\frac{1}{2}}+\sum_{n=1} a_n \cos\frac{1}{2}(2n-1)X\pi\right]}{\frac{1}{2}\pi+\sum_{n=1}(-)^{n-1}\{4a_n/(2n-1)\pi\}},$$

so that

$$R(X) = C_2(K,X)R_0(X), \tag{27}$$

where

$$C_2(K,X) = \frac{(1-X^2)^{\frac{1}{2}}+\sum_{n=1} a_n \cos\frac{1}{2}(2n-1)X\pi}{\left[1+\sum_{n=1}(-)^{n-1}\{8a_n/(2n-1)\pi^2\}\right](1-X^2)^{\frac{1}{2}}}. \tag{28}$$

$C_2(K,0)$ will be written simply as $C_2(K)$ in what follows. The ratio of the actual contact pressures at $X = 0$, the midpoint of the zone, for the same contact length $2h$, is then

$$C_3 = C_2/C_1^2. \tag{29}$$

Further, from (17), using (18), (19), and (21), we find

$$G'(X) = -\frac{2wh}{E}\left[X-(X^2-1)^{\frac{1}{2}}-L_0(K,X)+\sum_{n=1} a_n\{H_n(X)-L_n(K,X)\}\right]+\frac{2Xh^2}{D}. \tag{30}$$

Write

$$\int_1^X H_n(X)\,dX = I_n(X) \quad (n \geqslant 1); \qquad \int_1^X (X^2-1)^{\frac{1}{2}}\,dx = N_0(X) \tag{31}$$

$$\int_1^X L_n(K,X)\,dX = M_n(K,X), \quad \text{all } n.$$

From (5),

$$\{G(X)\}_{K=0} = (2h_0^2/D)\int_1^X (X^2-1)^{\frac{1}{2}}\,dX = (2h_0^2/D)N_0(X). \tag{32}$$

Then, if the loading is such that the contact lengths are the same, using (30), (31), and (32)

$$G(X) = C_4(K,X)G_0(X), \tag{33}$$

where $$C_4(K,X) = \frac{1}{2N_0(X)}\left\{X^2-1-\left(\frac{C_3}{1+\sum\limits_{n=1} a_n}\right)A(X)\right\} \tag{34}$$

and

$$A(X) = X^2-1-2N_0(X)-2M_0(K,X)+2\sum_{n=1} a_n\{I_n(X)-M_n(K,X)\}. \tag{35}$$

It is found that, using the term in a_1 only, equation (22) can be satisfied to within 3 per cent. over the whole range of X for $K = 1$, which is the worst case. As a check on the adequacy of this approximation in the rest of the work, a_2 and a_3 were also obtained for $K = 1$ by working out H_2, H_3, L_2, L_3 at $X = 0{\cdot}25$, $0{\cdot}75$ and solving the four equations given by (22) at $X = 0{\cdot}25$, $0{\cdot}5$, $0{\cdot}75$, 1. The values found were $a_1 = 0{\cdot}413$, $a_2 = 0{\cdot}0$ $a_3 = -0{\cdot}002$, as compared with $a_1 = 0{\cdot}511$ from the first approximation. It was found that the values for C_1 and C_2 (equations (25) and (28)) for the two approximations differed only in the third decimal place, while C_3 (equation (29)) differed by one in the second decimal. The results in Tables I and II were worked out on the more approximate formula, and so are given to two decimal places only, and the values for C_3 have been corrected. The results should then be reliable to this order. Figures are given for C_1, C_2, and C_3 for a fixed inner boundary, $\eta = 0$, and a range of values of K; for comparison values have also been found, for $K = 1$ only, when $\eta = \frac{1}{2}$ and also when there is sideways slip at the inner boundary. Values of $R(X)$ have also been calculated for X between 0 and 1, for $K = 0$ and $K = 1$, and are compared in Fig. 1.

C_1, C_2, and C_3 all refer to properties within the contact zone, while C_4 is a measure of the deformation outside, but near to this zone. Here it is found that the first approximation is inadequate, when $K = 1$: the comparative figures for $C_4(1, 2)$ are, from the first approximation, $1{\cdot}242$, and from the second, $1{\cdot}165$. The labour of extending this for the other values of K was not thought worth while for present purposes, since C_4 is the least important of the ratios calculated. The second value, $1{\cdot}17$, for $C_4(1, 2)$, may still be in error by two or three in the second decimal, and should be regarded as showing only the order of the effect.

The solution appropriate to any given layer thickness and given loading is found by using (2) to get, for the given conditions, the contact length $2h_0$ for an infinitely thick layer. Then the value of h for a finite thickness b must satisfy the two relations (14) and (24),

$$h = 2bK,$$

$$h = C_1(K)h_0,$$

so that K is defined by the relation

$$C_1(K) = (2b/h_0)K. \tag{36}$$

The other quantities can then be found from the table.

Details of computation

For small values of KX, $L_0(K,X)$, $L_n(K,X)$ are best evaluated by Simpson's Rule in the usual way. If KX is large, however, the rapid oscillations of $\sin KXz$ would require a very small length interval for z, and in this case it is better to use a different integration formula which will now be derived.

By fitting a parabola to $q(x)$ through the points $q(n\pi)$, $q\{(n+\frac{1}{2})\pi\}$, $q\{(n+1)\pi\}$, it can be shown that

$$\int\limits_{n\pi}^{(n+1)\pi} q(x)\sin x\,dx = (-)^n\left[\frac{\pi^2-8}{\pi^2}q(n\pi)+(16/\pi^2)q\{(n+\tfrac{1}{2})\pi\}+\frac{\pi^2-8}{\pi^2}q\{(n+1)\pi\}\right]$$

$$= (-)^n(0{\cdot}189q_n+1{\cdot}624q_{n+\frac{1}{2}}+0{\cdot}189q_{n+1}) \tag{37}$$

with an error of $0{\cdot}0562q^{\text{iv}}$, q^{iv} being, as usual, the value of the fourth differential at some point in the range $[n\pi, (n+1)\pi]$. This is more accurate than the corresponding Simpson formula, with strip length $\frac{1}{2}\pi$, whose error is $0{\cdot}1063q^{\text{iv}}$.

Any number of such strips can clearly be combined, and, because of the alternating sign, the end-values of each disappear, so that

$$\int\limits_{n\pi}^{N\pi} q(x)\sin x\,dx = (-)^n[0{\cdot}189q_n+1{\cdot}624\{q_{n+\frac{1}{2}}-q_{n+\frac{3}{2}}+\dots+$$
$$+(-)^{N-n-1}q_{N-\frac{1}{2}}\}+(-)^{N-n-1}0{\cdot}189q_N]. \tag{38*}$$

In the computations for L_0, L_n, the integrand is of the form $q(z)\sin pz$, where $p = KX$, and $q(z) \to 0$ as $z \to \infty$. Taking y as the largest value of z for which $q(z)$ is appreciable,

$$\int\limits_0^y q(z)\sin pz\,dz = \frac{1}{p}\int\limits_0^{py} q(z/p)\sin z\,dz,$$

which can be evaluated by the formula (38) using py/π strips, and so with a maximum cumulative error of

$$\frac{0{\cdot}0562yq^{\text{iv}}}{\pi p^4} = 0{\cdot}0179yq^{\text{iv}}p^{-4}.$$

* It has been pointed out to me that this formula is a special case of a general formula derived by Filon (**5**) for evaluating integrals of this type. He deals with strips of width θ, and obtains an expression in terms of sums of odd and even ordinates of the function $q(x)\sin x$; he gives numerical values of the coefficients which occur for values of θ between 0 and 45°. Formula (38) above corresponds to $\theta = \frac{1}{2}\pi$ in this notation. It may still, however, be of interest in itself, in that it involves only sums of ordinates of $q(x)$, and so is easier to evaluate than the more general case which brings in $q(x)\sin x$.

Similarly, using Simpson's Rule with a length interval h, and an error per strip of $q^{iv}h^5/90$, the cumulative error is $0{\cdot}0056yq^{iv}h^4$. Thus Simpson's Rule is better only so long as

$$p^4h^4 < 3{\cdot}218,$$

i.e.

$$ph < 1{\cdot}34.$$

In the computations $h = 1$, and Simpson's Rule was used for values of KX up to 1·2, replaced by formula (38) for larger values.

Results of computations

TABLE I

$\eta = 0$, *inner boundary fixed*

K	0	0·2	0·4	0·6	0·8	1·0
a_1	0	0·00841	0·0788	0·211	0·357	0·511
C_1	1	0·96	0·88	0·80	0·73	0·67
C_2	1	1·0016	1·01	1·03	1·05	1·08
C_3	1	1·09	1·32	1·63	1·97	2·37

TABLE II

$K = 1$

	$\eta = \frac{1}{2}$, *inner boundary fixed*	*Slip at inner boundary*
a_1	0·586	0·532
C_1	0·65	0·67
C_2	1·08	1·08
C_3	2·58	2·43

Considering first the set of results for $\eta = 0$, it can be seen that the effect of thickness on the deformation is quite considerable. The length of the contact zone is reduced to nearly two-thirds for the same loading, as K increases from 0 to 1; or if the same contact length is produced, the total loading has to be more than doubled. The deformation outside the contact zone is also considerably changed, so that the separation between the two surfaces, under conditions giving the same contact length $2h$, is 10–20 per cent. greater for the thin layer, $K = 1$, than for the infinite layer, at a distance h from the nip.

The pressure at the midpoint of the contact zone is very greatly increased when a thinner layer is loaded to give the same contact length. This is mainly because of the increase in total load, but the values given for C_2 show that a slightly larger proportion of the load is effective towards the centre of the contact zone, as the layer becomes thinner. This effect can be seen more clearly in Fig. 1, which compares the pressure distribution over the contact zone for $K = 0$ and $K = 1$.

Poisson's ratio can be seen to have little effect; the maximum possible change, from $\eta = 0$ to $\eta = \frac{1}{2}$, produces, at $K = 1$, a 4 per cent. decrease in contact length, or an 8 per cent. increase in load for a given contact length, with a corresponding 9 per cent. increase in pressure at the mid-point of the contact zone.

The results for a layer which can slip at the inner boundary lie between

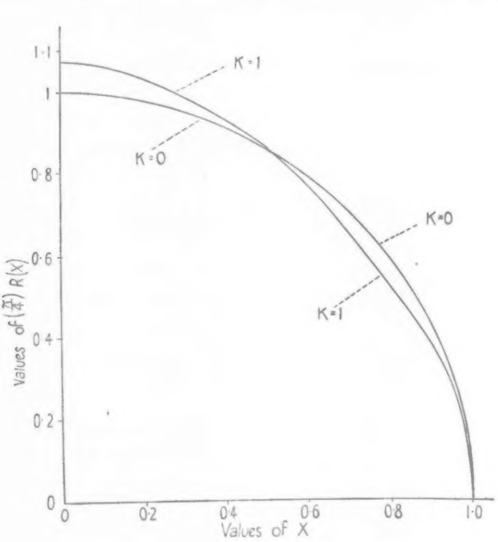

FIG. 1.

those for $\eta = 0$ and $\eta = \frac{1}{2}$, and are very near to the former set. This is to be expected, since the freeing of the inner boundary obviously has a much smaller effect on a substance with less tendency to spread sideways.

Conclusions

Next to the roller diameter, and elastic modulus, the layer thickness is the most important factor determining the relation between loading and deformation for this type of roller. A greater load is necessary to produce the same contact length, and even then the gap between the two rollers near the contact zone is much larger, for a thinner elastic layer; this last property results from a smaller vertical deflexion, i.e. a smaller approach of the roller centres. The pressure distribution over the contact zone is only slightly affected by layer thickness.

A change in Poisson's ratio makes an appreciable difference to the loading necessary for a given contact length, but has very little effect

otherwise; slipping at the inner surface gives results very similar to those with fixed inner surface and a zero value of Poisson's ratio.

REFERENCES

1. H. HERTZ, *J. f. Math.* (Crelle), **92** (1881), 156–171.
2. A. E. H. LOVE, *Mathematical Theory of Elasticity* (Cambridge, 1927), 193.
3. H. R. THOMAS, and V. A. HOERSCH, *Univ. Ill. Eng. Exp. Sta. Bull.* **212**, 1930.
4. E. G. COKER, and L. N. G. FILON, *Photoelasticity* (Cambridge, 1931), 435–7.
5. L. N. G. FILON, *Proc. Roy. Soc. Edin.* **19** (1929), 38.

THE FIELD INDUCED BY AN OSCILLATING MAGNETIC DIPOLE OUTSIDE A SEMI-INFINITE CONDUCTOR

By A. N. GORDON (*Imperial College, London*)

[Received 14 March 1950]

SUMMARY

Formulae are given for the external field produced by an oscillating magnetic dipole located outside a uniform semi-infinite conductor. The normal component of the field induced by a circular alternating current filament at the surface of the conductor is also considered.

1. Introduction

IT has been suggested that information about the variation with depth of the earth's conductivity can be obtained by means of a large-scale local experiment over a suitable flat region of the earth's surface. In this experiment a plane circuit of sufficiently great extent carries an alternating current and the magnetic field due to currents thereby induced in the earth is mapped over the surrounding country.

A method whereby the conductivity at any depth can be deduced from a knowledge of the induced field at the surface has been given by Slichter (**1**), but it is felt that this is not practicable and that it is likely that interpretation of the experimental results will depend on comparison with the fields calculated for some simple laws of variation of conductivity. Methods for computing the field are derived here for a uniformly conducting earth when the circuit is so small that it can be regarded as a magnetic dipole. A circular current filament is then considered, attention being restricted to the vertical component of the induced field, this component being the one which would be measured in practice.

2. The field induced by an oscillating magnetic dipole

For a magnetic dipole whose moment M varies sinusoidally with period $2\pi/p$, located at the point $(0, 0, h)$ outside a semi-infinite conductor of unit permeability and conductivity k, the inducing potential at the point whose polar coordinates are (ρ, ϕ, ζ) is

$$\Omega = M\frac{\partial}{\partial\zeta}\left(\frac{1}{R}\right),$$

where $R^2 = \rho^2+(h-\zeta)^2$.

Using the well-known result

$$\frac{1}{R} = \int_0^\infty e^{-\lambda(h-\zeta)} J_0(\lambda\rho)\, d\lambda \quad (\zeta < h),$$

this can be expressed in the form

$$\Omega = M \int_0^\infty e^{-\lambda(h-\zeta)} J_0(\lambda\rho)\lambda\, d\lambda.$$

It follows from equation (9.8) of (**2**) that since $J_0(\lambda\rho)$ satisfies equation (6.11) there, the induced potential will be

$$\Omega_i = M \int_0^\infty \frac{\theta-\lambda}{\theta+\lambda} e^{-\lambda(h+\zeta)} J_0(\lambda\rho)\lambda\, d\lambda \quad (\zeta > 0),$$

where $\theta^2 = \lambda^2 + 4\pi ikp/c^2$.

Writing $M_0 = \alpha^2 M$, $z = \alpha(h+\zeta)$, $r = \alpha\rho$, $\lambda = \alpha u$, where $\alpha^2 = 4\pi kp/c^2$, this becomes

$$\Omega_i = M_0 \int_0^\infty \frac{\sqrt{(u^2+i)}-u}{\sqrt{(u^2+i)}+u} e^{-uz} J_0(ur)u\, du. \tag{1}$$

When the oscillating dipole is at the surface we obtain for the magnetic field components at the surface

$$H_z = \alpha M_0 \int_0^\infty \frac{\sqrt{(u^2+i)}-u}{\sqrt{(u^2+i)}+u} J_0(ur)u^2\, du, \tag{2}$$

$$H_r = \alpha M_0 \int_0^\infty \frac{\sqrt{(u^2+i)}-u}{\sqrt{(u^2+i)}+u} J_1(ur)u^2\, du, \tag{3}$$

corresponding to an inducing field whose components at the surface are

$$H_z = \frac{\alpha M_0}{r^3}, \qquad H_r = 0.$$

3. Evaluation of the integrals (2) and (3)

Consider first the integral

$$I = \int_0^\infty \frac{\sqrt{(u^2+b^2)}-u}{\sqrt{(u^2+b^2)}+u} J_0(ur)\, du,$$

where b is to be regarded as real and positive. We have successively

$$I = \frac{1}{b^2}\int\limits_0^\infty \{2u^2+b^2-2u\sqrt{(u^2+b^2)}\}J_0(ur)\,du$$

$$= \frac{1}{r}-\frac{2}{b^2}\int\limits_0^\infty \{\sqrt{(u^2+b^2)}-u\}uJ_0(ur)\,du,$$

since

$$\int\limits_0^\infty J_0(ur)\,du = \frac{1}{r}.$$

Using

$$(u^2+b^2)^{\frac{1}{2}}-u = b\int\limits_0^\infty e^{-ux}J_1(bx)\frac{dx}{x},$$

(**3**, p. 386), changing the order of integration, and integrating with respect to u, we find

$$I = \frac{1}{r}+\frac{2}{b}\int\limits_0^\infty J_1(bx)\frac{\partial}{\partial x}\{(x^2+r^2)^{-\frac{1}{2}}\}\frac{dx}{x}$$

$$= \frac{1}{r}+\frac{2}{b}\frac{1}{r}\frac{d}{dr}\int\limits_0^\infty \frac{J_1(bx)}{(x^2+r^2)^{\frac{1}{2}}}\,dx$$

$$= \frac{1}{r}+\frac{2}{b}\frac{1}{r}\frac{d}{dr}\{I_{\frac{1}{2}}(\tfrac{1}{2}br)K_{\frac{1}{2}}(\tfrac{1}{2}br)\}$$

(**3**, p. 435), which can be written

$$I = \frac{1}{r}+\frac{2}{b}\frac{1}{r}\frac{d}{dr}\left(\frac{1-e^{-br}}{br}\right). \tag{4}$$

The restriction that b is real can now be removed by analytic continuation, provided only that its real part is positive.

Finally, writing Bessel's equation in the form

$$u^2J_0(ur) = -\frac{1}{r}\frac{d}{dr}\left\{r\frac{d}{dr}J_0(ur)\right\},$$

we can derive H_z from the integral I, giving

$$H_z = -\alpha M_0\frac{1}{r}\frac{d}{dr}\left[r\frac{d}{dr}\left\{\frac{1}{r}+\frac{2}{b^2r}\frac{d}{dr}\left(\frac{1-e^{-br}}{r}\right)\right\}\right], \tag{5}$$

where $b = i^{\frac{1}{2}}$, that root being taken for which the real part is positive.

Performing the differentiations we can also write

$$H_z = -\alpha M_0\left\{\frac{1}{r^3}-\frac{18}{b^2r^5}+\frac{2be^{-br}}{r^2}\left(1+\frac{4}{br}+\frac{9}{(br)^2}+\frac{9}{(br)^3}\right)\right\}. \tag{6}$$

For small values of r (up to unity, say) it is more convenient to use the series expansion

$$H_z = 2\alpha M_0 b^3 \sum_{n=0}^{\infty} (-1)^n \frac{(n+1)^2(n+3)}{(n+4)!} (br)^{n-1}. \tag{7}$$

The form of H_z given by (6) shows that when r is large enough the vertical component of the induced field is effectively equal and opposite to the inducing field. This is likely to be of importance in the experiment referred to in section 1 since it is true irrespective of the shape of the inducing circuit (which can be regarded as a dipole distribution) and also appears to be true for the case of variable conductivity.

The evaluation of H_r proceeds in a similar manner. We have

$$H_r = -\alpha M_0 \frac{\partial \Phi}{\partial r},$$

where
$$\Phi = \int_0^\infty \frac{(u^2+b^2)^{\frac{1}{2}}-u}{(u^2+b^2)^{\frac{1}{2}}+u} u\, J_0(ur)\, du$$

$$= 2\int_0^\infty e^{-ux} J_2(bx) \frac{dx}{x} \int_0^\infty u J_0(ur)\, du,$$

using (**3**), p. 386. Therefore,

$$\Phi = -2\int_0^\infty J_2(bx) \frac{d}{dx}\{(x^2+r^2)^{-\frac{1}{2}}\} \frac{dx}{x}$$

$$= \frac{-2}{r}\frac{d}{dr}\int_0^\infty \frac{J_2(bx)}{(x^2+r^2)^{\frac{1}{2}}}\, dx$$

$$= \frac{-2}{r}\frac{d}{dr}\{I_1(\tfrac{1}{2}br)K_1(\tfrac{1}{2}br)\}$$

using (**3**), p. 435. Hence

$$H_r = \alpha M_0 2 \frac{d}{dr}\left[\frac{1}{r}\frac{d}{dr}\{I_1(\tfrac{1}{2}br)K_1(\tfrac{1}{2}br)\}\right], \tag{8}$$

where $b = i^{\frac{1}{2}}$.

Performing the differentiations and using the recurrence relations for I and K (**3**, p. 79) we can also write

$$H_r = \alpha M_0 \left\{\frac{16}{r^3} I_1 K_1 - \frac{4b}{r^2}(I_0 K_1 - I_1 K_0) - \frac{b^2}{r}(I_0 K_0 - I_1 K_1)\right\}, \tag{9}$$

the functions involved being Kelvin's 'ber' and 'bei' functions, etc., which are tabulated.

For very small values of r it is more convenient to use a series expansion in ascending powers of r, which can be derived from the result given by Watson (**3**, p. 441),

$$I_1(z)K_1(z) = \frac{2}{\pi}\int_0^{\frac{1}{2}\pi} K_0(2z\sin\theta)\cos 2\theta\, d\theta,$$

by expanding $K_0(2z\sin\theta)$ and integrating term by term. The same series is also obtained by putting $\mu = 0$ in (12) (see later).

The values in Table I were computed by means of the above formulae, the factor αM_0 being omitted throughout.

TABLE I

r	*Inducing field* H_z	*Induced field* $-H_z$	$-H_r$
0·2	125·0	$0{\cdot}1646+1{\cdot}0625i$	$0{\cdot}0313+1{\cdot}2403i$
0·4	15·625	$0{\cdot}1429+0{\cdot}4402i$	$0{\cdot}0455+0{\cdot}6061i$
0·6	4·630	$0{\cdot}1231+0{\cdot}2361i$	$0{\cdot}0534+0{\cdot}3894i$
0·8	1·953	$0{\cdot}1054+0{\cdot}1372i$	$0{\cdot}0576+0{\cdot}2777i$
1·0	1·000	$0{\cdot}0896+0{\cdot}0808i$	$0{\cdot}0593+0{\cdot}2087i$
1·5	0·296	$0{\cdot}0576+0{\cdot}0149i$	$0{\cdot}0569+0{\cdot}1130i$
2·0	0·125	$0{\cdot}0347-0{\cdot}0083i$	$0{\cdot}0497-0{\cdot}0641i$

4. Evaluation of the integral (1)

Consider the integral

$$I_1 = \int_0^\infty e^{-uz}J_0(ur)\frac{du}{\sqrt{(u^2+b^2)}} \quad (b \text{ real}).$$

This can be written

$$\begin{aligned} I_1 &= \frac{1}{\pi}\int_0^\pi d\phi \int_0^\infty e^{-u(z+ir\cos\phi)}\frac{du}{\sqrt{(u^2+b^2)}} \\ &= \frac{1}{\pi}\int_0^\pi d\phi \int_0^\infty e^{-u(z+ir\cos\phi)}\, du \int_0^\infty e^{-ux}J_0(bx)\, dx, \\ &= \frac{1}{\pi}\int_0^\pi d\phi \int_0^\infty \frac{J_0(bx)}{x+\kappa}\, dx, \end{aligned}$$

where $\kappa = z+ir\cos\phi$.

The second integral is known (**3**, p. 436, (7)), so that

$$I_1 = \tfrac{1}{2}\int_0^\pi \{H_0(b\kappa)-Y_0(b\kappa)\}\, d\phi.$$

It follows that

$$I_2 = \int\limits_0^\infty (u^2+b^2)^{\frac{1}{2}} e^{-uz} J_0(ur)\, du \tag{10}$$

$$= \left(\frac{d^2}{dz^2}+b^2\right) I_1$$

$$= \left(\frac{d^2}{d\kappa^2}+b^2\right) I_1$$

$$= \tfrac{1}{2} \int\limits_0^\pi \frac{b}{\kappa} \{H_1(b\kappa)-Y_1(b\kappa)\}\, d\phi \tag{11}$$

using the recurrence relations for H and Y. This can be written

$$\frac{b^2}{\pi} \int\limits_0^\pi F\{b(z+ir\cos\phi)\}\, d\phi,$$

where

$$F(x) = \frac{x}{1.3} - \frac{x^3}{1.3^2.5} + \frac{x^5}{1.3^2.5^2.7} - \dots +$$

$$+\frac{1}{x^2} - \frac{1}{x} J_1(x) \log x + \frac{1}{2} \sum_{m=0}^\infty (-1)^m C_m \frac{(\frac{1}{2}x)^{2m}}{m!(m+1)!},$$

$$C_m = \frac{1}{1} + \frac{1}{2} + \dots + \frac{1}{m} + \frac{1}{2(m+1)} - \gamma + \log 2,$$

$$C_0 = \tfrac{1}{2} - \gamma + \log 2,$$

and γ is Euler's constant. Now

$$R^n P_n(\mu) = \frac{1}{\pi} \int\limits_0^\pi (z+ir\cos\phi)^n\, d\phi,$$

$$R^{-(n+1)} P_n(\mu) = \frac{1}{\pi} \int\limits_0^\pi (z+ir\cos\phi)^{-(n+1)}\, d\phi,$$

where $R^2 = z^2+r^2$ and $\mu = z/r$, so that the integral (10) becomes

$$I_2 = b^3 \frac{R.P_1}{3} - b^5 \frac{R^3.P_3}{3^2.5} + b^7 \frac{R^5.P_5}{3^2.5^2.7} + \dots +$$

$$+\frac{P_1}{R^2} + \frac{1}{2} \sum_{m=0}^\infty (C_m - \log b)(-1)^m \frac{b^{2m+2} R^{2m} P_{2m}}{2^{2m} m!(m+1)!} -$$

$$- \sum_{m=0}^\infty \frac{(-1)^m b^{2m+2}}{2^{2m+1} m!(m+1)!} \frac{1}{\pi} \int\limits_0^\pi (z+ir\cos\phi)^{2m} \log(z+ir\cos\phi)\, d\phi.$$

Since both sides still converge when b is complex, we can remove the restriction that b is real.

The function

$$F_n = \frac{1}{\pi}\int\limits_0^\pi (z+ir\cos\phi)^n \log(z+ir\cos\phi)\,d\phi = \frac{d}{dn}\{R^n P_n(\mu)\},$$

is a special solution of Laplace's equation (**4**, p. 172). It has the value

$$R^n P_n(\mu)\log\frac{R+z}{2} - 2R^n\left\{\frac{2n-1}{1.2n}P_{n-1} - \frac{2n-3}{2(2n-1)}P_{n-2} + \dots + (-1)^n\frac{P_0}{n(n+1)}\right\}.$$

The required potential (1), omitting the factor M_0, is thus

$$\Omega_i = \frac{1}{b^2}\int\limits_0^\infty \{2u^2+b^2-2u(u^2+b^2)^{\frac{1}{2}}\}e^{-uz}J_0(ur)u\,du$$

$$= \frac{P_1(\mu)}{R^2} + \frac{12P_3(\mu)}{b^2R^4} - \frac{2}{b^2}\frac{\partial^2}{\partial z^2}\int\limits_0^\infty (u^2+b^2)^{\frac{1}{2}}e^{-uz}J_0(ur)\,du.$$

Now

$$\frac{\partial}{\partial z}\{R^n P_n(\mu)\} = nR^{n-1}P_{n-1}(\mu),$$

$$\frac{\partial}{\partial z}\{R^{-(n+1)}P_n(\mu)\} = -(n+1)R^{-(n+2)}P_{n+1}(\mu),$$

and

$$\frac{\partial}{\partial z}\{F_n\} = nF_{n-1} + R^{n-1}P_{n-1}(\mu).$$

Hence, finally

$$\Omega_i = 2\left\{\frac{2}{3.5}b^3RP_1 - \frac{4}{3^2.5.7}b^5R^3P_3 + \frac{6}{3^2.5^2.7.9}b^7R^5P_5 \dots - \right.$$

$$- \sum_{m=1}^\infty (C_m - \log b)(-1)^m \frac{2m(2m-1)}{2^{2m}m!(m+1)!}b^{2m}R^{2m-2}P_{2m-2} +$$

$$\left. + \sum_{m=1}^\infty \frac{(-1)^m b^{2m}}{2^{2m}m!(m+1)!}\{2m(2m-1)F_{2m-2} + (4m-1)R^{2m-2}P_{2m-2}\right\}. \quad (12)$$

This formula is suitable for the calculation of the fields for values of R not substantially greater than 2.

Proceeding in the same manner and using the asymptotic expansion for $H_1(z) - Y_1(z)$ (**3**, p. 333 (2)), we arrive at the formula

$$\Omega_i = \frac{P_1}{R^2} + \frac{12P_3}{b^2R^4} + 2\sum_{n=0}^\infty (-1)^n \frac{(2n)!(2n+2)!}{(2n-1)2^{2n}n!\,n!}\frac{P_{2n+2}}{b^{2n+1}R^{2n+3}},$$

which is suitable for values of R not substantially less than 10. In order

to compute the field components for intermediate values of R numerical integration must be performed from $u = 0$ to u ($= 2$, say), the integral from x to ∞ being expanded into a series of integrals of the form

$$I_s = \int\limits_x^\infty J_0(ur)e^{-uz}\frac{du}{u^s}, \qquad K_s = \int\limits_x^\infty J_1(ur)e^{-uz}\frac{du}{u^s}.$$

These can be linked with I_0 and I_1, by means of reduction formulae, where I_0 and I_1 are given by

$$I_0 = \int\limits_x^\infty J_0(ur)e^{-uz}\,du = \frac{1}{R} - \sum_{n=0}^\infty (-1)^n \frac{x^{n+1}}{(n+1)!} R^n P_n(\mu),$$

$$I_1 = \int\limits_x^\infty J_0(ur)e^{-uz}\frac{du}{u}$$

$$= \log 2 - \gamma - \log x - \log(z+R) - \sum_{n=1}^\infty (-1)^n \frac{x^n}{n\,.\,n!} R^n P_n(\mu).$$

5. The circular current filament

The simple form of H_z in equation (5) enables the same component to be calculated in the case of a circular wire of radius d which carries an alternating current cI. For such a circuit, whose centre is at $(0, 0, h)$ and whose plane is parallel to the bounding face of the conductor, the inducing potential is

$$\Omega = 2\pi Id \int\limits_0^\infty e^{-\lambda(h-\zeta)}J_1(\lambda d)J_0(\lambda\rho)\,d\lambda \quad (\zeta < h).$$

In terms of the reduced units introduced in section 2, and with $a = \alpha d$, the induced potential is found to be

$$\Omega_i = 2\pi Ia \int\limits_0^\infty \frac{\sqrt{(a^2+b^2)}-u}{\sqrt{(a^2+b^2)}+u} e^{-uz}J_1(ua)J_0(ur)\,du,$$

where $b^2 = i$, so that

$$H_z = -\frac{\partial\Omega_i}{\partial\zeta} = 2\pi Ia\alpha \int\limits_0^\infty \frac{\sqrt{(a^2+b^2)}-u}{\sqrt{(a^2+b^2)}+u} e^{-uz}J_1(ua)J_0(ur)u\,du;$$

this can also be expressed in the form

$$H_z = -2\pi I\alpha a\frac{\partial}{\partial a}\int\limits_0^\infty \frac{\sqrt{(a^2+b^2)}-u}{\sqrt{(a^2+b^2)}+u} e^{-uz}J_0(ua)J_0(ur)\,du$$

$$= -I\alpha a\frac{\partial}{\partial a}\int\limits_0^{2\pi} d\phi \int\limits_0^\infty \frac{\sqrt{(a^2+b^2)}-u}{\sqrt{(a^2+b^2)}+u} e^{-uz}J_0(uR)\,du,$$

where $R^2 = a^2 - 2ar\cos\phi + r^2$.

In the special case $z = 0$ we have

$$H_z = -I\alpha a \frac{\partial}{\partial a} \int_0^{2\pi} d\phi \int_0^{\infty} \frac{\sqrt{(u^2+b^2)}-u}{\sqrt{(u^2+b^2)}+u} J_0(uR)\, du$$

$$= -I\alpha a \frac{\partial}{\partial a} \int_0^{2\pi} \left\{\frac{1}{R} + \frac{2}{b}\frac{1}{R}\frac{d}{dR}\left(\frac{1-e^{-bR}}{bR}\right)\right\} d\phi, \tag{13}$$

as in (4),

Expanding the integrand in ascending powers of R and performing the differentiation with respect to a,

$$H_z = -I\alpha \sum_{n=1}^{\infty} (-1)^n \frac{n(n+2)}{(n+3)!} b^{n+1}\{(a^2-r^2)X_{n-2}+X_n\}, \tag{14}$$

where $$X_n = \int_0^{2\pi} R^n\, d\phi.$$

These integrals can be computed from the tabulated elliptic integrals X_{-1} and X_1, using the results

$$X_0 = 2\pi, \qquad X_2 = 2\pi(r^2+a^2),$$

together with the reduction formula

$$(n+2)X_{n+2} = 2(n+1)(r^2+a^2)X_n - n(r^2-a^2)^2 X_{n-2}.$$

The expression (14) is suitable for computations involving small values of r and a. For larger values an alternative expansion can be derived as follows. We write (13) in the equivalent form

$$H_z = -\alpha I a \frac{\partial}{\partial a} \int_0^{2\pi} \left[\frac{1}{R} - \frac{2}{b^2R^3} - \frac{2}{bR}\frac{d}{dR}\left\{\sqrt{\frac{2}{\pi}}\frac{K_{\frac{1}{2}}(bR)}{(bR)^{\frac{1}{2}}}\right\}\right] d\phi$$

$$= -\alpha I a \frac{\partial}{\partial a} \int_0^{2\pi} \left[\frac{1}{R} - \frac{2}{b^2R^3} + 2b\sqrt{\frac{2}{\pi}}\frac{K_{\frac{3}{2}}(bR)}{(bR)^{\frac{3}{2}}}\right] d\phi.$$

To evaluate this integral we note that

$$\frac{K_{\frac{3}{2}}(bR)}{(bR)^{\frac{3}{2}}} = \sqrt{\tfrac{1}{4}\pi}\left(\frac{2}{b^2ar}\right)^{\frac{3}{2}} \sum_0^{\infty} (2n+3)C_n(\cos\phi)K_{n+\frac{3}{2}}(ba)I_{n+\frac{3}{2}}(br) \quad (a > r),$$

where $$(1-2h\cos\phi+h^2)^{-\frac{3}{2}} = \sum_{n=0}^{\infty} h^n C_n(\cos\phi),$$

(**3**, p. 365, 8), and interchange of I and K should be made when $a < r$.

The value of
$$I_n = \int_0^{2\pi} C_n(\cos\phi)\,d\phi$$
which is required, can be obtained from the recurrence relation
$$I_n - I_{n-2} = (2n+1)\int_0^{2\pi} P_n(\cos\phi)\,d\phi,$$
$$= \frac{\{1.3...(2n-1)\}^2}{2^{2n}n!\,n!}(2n+1)2\pi,\ n \text{ even},$$
$$I_n = 0,\ n \text{ odd}.$$

REFERENCES

1. L. B. Slichter, *Physics*, **4** (1933), 411.
2. A. T. Price, *Quart. J. Mech. and Applied Math.* **3** (1950), 385.
3. G. N. Watson, *Theory of Bessel Functions*, 2nd edn. (Cambridge, 1944).
4. E. W. Hobson, *Spherical and Ellipsoidal Harmonics* (Cambridge, 1931).

ELECTROMAGNETIC INDUCTION IN A UNIFORM SEMI-INFINITE CONDUCTOR

By A. N. GORDON (*Imperial College, London*)

[Received 30 May 1950]

SUMMARY

A systematic treatment of the problem of the induction of currents in a uniform semi-infinite conductor by external magnetic or electric fields is given, attention being drawn to the complementary nature of the magnetic and electric cases. A one-dimensional heat flow analogue is then derived which enables the familiar methods developed in connexion with heat conduction to be applied directly to the solution of corresponding problems in electromagnetic induction.

1. Introduction

THIS paper should be regarded as a sequel to a recent contribution by A. T. Price (**1**). Since the method of approach is rather different, however, it has been considered advisable to develop the subject afresh, without reference to Price's work.

With the usual notation, when displacement currents are neglected, Maxwell's equations for the electromagnetic field inside a uniform source-free medium of conductivity κ and permeability μ are

$$\operatorname{curl}\mathbf{E} = -\frac{1}{c}\frac{\partial\mathbf{B}}{\partial t}, \tag{1.1}$$

$$\operatorname{curl}\mathbf{B} = \frac{4\pi\mu\kappa}{c}\mathbf{E}, \tag{1.2}$$

$$\operatorname{div}\mathbf{E} = 0, \tag{1.3}$$

$$\operatorname{div}\mathbf{B} = 0. \tag{1.4}$$

Elimination of $\mathbf{E}$ yields for $\mathbf{B}$ the equation

$$\nabla^2\mathbf{B} = \frac{4\pi\mu\kappa}{c^2}\frac{\partial\mathbf{B}}{\partial t}, \tag{1.5}$$

while elimination of $\mathbf{B}$ leads to the same equation for $\mathbf{E}$.

2. Solution of (1.5) subject to (1.4)

In rectangular coordinates, the most general solution of (1.5) is

$$\mathbf{B} = \mathbf{i}W_1+\mathbf{j}W_2+\mathbf{k}W_3, \tag{2.1}$$

where $\mathbf{i}$, $\mathbf{j}$, $\mathbf{k}$ are unit vectors along the axes and W_1, W_2, W_3 are arbitrary solutions of the scalar equation

$$\nabla^2 W = \frac{1}{\alpha}\frac{\partial W}{\partial t}, \tag{2.2}$$

where
$$\alpha = c^2/4\pi\mu\kappa. \tag{2.3}$$

The additional requirement (1.4) imposes the condition
$$\frac{\partial W_1}{\partial x}+\frac{\partial W_2}{\partial y}+\frac{\partial W_3}{\partial z} = 0, \tag{2.4}$$
so that only two of the scalars W_1, W_2, W_3 are independent. Since there is no loss of generality in replacing W_1, W_2 by $\partial W_1/\partial z$, $\partial W_2/\partial z$, it follows from (2.4) that
$$W_3 = -\left(\frac{\partial W_1}{\partial x}+\frac{\partial W_2}{\partial y}\right).$$
Strictly speaking an arbitrary function of x, y, and t should be included in W_3, but this special type of solution, which leads to fields independent of z, will not be considered here. Equation (2.1) then becomes
$$\begin{aligned}\mathbf{B} &= \left(\mathbf{i}\frac{\partial W_1}{\partial z}-\mathbf{k}\frac{\partial W_1}{\partial x}\right)+\left(\mathbf{j}\frac{\partial W_2}{\partial z}-\mathbf{k}\frac{\partial W_2}{\partial y}\right),\\ &= -\operatorname{curl}(\mathbf{j}W_1)+\operatorname{curl}(\mathbf{i}W_2).\end{aligned}$$

Since W_1 and W_2 are independent, it follows that the most general solution can be obtained by combining simple solutions of the form $\operatorname{curl}(\mathbf{i}W)$ and $\operatorname{curl}(\mathbf{j}W)$, to which may be added, by symmetry, $\operatorname{curl}(\mathbf{k}W)$. However, using the identity
$$\operatorname{curl}\operatorname{grad} W = \operatorname{curl}\left(\mathbf{i}\frac{\partial W}{\partial x}+\mathbf{j}\frac{\partial W}{\partial y}+\mathbf{k}\frac{\partial W}{\partial z}\right) = 0,$$
any one of these types can be expressed in terms of the other two. Further, since
$$\operatorname{curl}\operatorname{curl}(\mathbf{k}W) = \operatorname{curl}\left(-\mathbf{j}\frac{\partial W}{\partial x}+\mathbf{i}\frac{\partial W}{\partial y}\right),$$
two independent solutions are
$$\operatorname{curl}(\mathbf{k}W); \quad \operatorname{curl}\operatorname{curl}(\mathbf{k}W), \tag{2.5}$$
the second of which can also be written
$$\operatorname{grad}\left(\frac{\partial W}{\partial z}\right)-\frac{1}{\alpha}\frac{\partial W}{\partial t}\mathbf{k},$$
in virtue of (1.5).

Equations (1.1) and (1.2) indicate that if $\mathbf{E}$ is identified with either of the solutions (2.5) then $\mathbf{B}$ corresponds to the other. This reciprocity is merely the degenerate case of the same feature in the solution of the electromagnetic wave equation (see, for example, Stratton (**2**), pp. 27, 28).

3. Application to the semi-infinite conductor

Suppose that the region $z > 0$ is occupied by conducting material while an external magnetic inducing system is confined to the region $z < -h$,

where h is positive. The equations to be satisfied by the magnetic field are

$$\nabla^2\mathbf{B} = \frac{1}{\alpha}\frac{\partial\mathbf{B}}{\partial t} \quad (z > 0),$$

$$\nabla^2\mathbf{B} = 0 \qquad (-h < z < 0),$$

$$\operatorname{div}\mathbf{B} = 0 \qquad (-h < z < \infty),$$

subject to the usual boundary conditions that B_z, H_x, and H_y are continuous across $z = 0$.

When a suitable solution has been obtained, the electric field inside the conductor follows uniquely from (1.2). Outside the conductor we must use (1.1), which leaves $\mathbf{E}$ indeterminate to the extent of the gradient of some scalar potential function.

To solve the equations we must first find a suitable solution of (2.2). If we seek solutions of the form

$$W = Z(z,t)P(x,y) \quad (z > 0), \tag{3.1}$$

$$= Z_1(z,t)P(x,y) \quad (z < 0),$$

the boundary conditions (which apply over $z = 0$ for all values of t) will involve only the functions Z and Z_1, and substitution of (3.1) into (2.2) indicates that

$$\frac{\partial^2 P}{\partial x^2}+\frac{\partial^2 P}{\partial y^2}+\lambda^2 P = 0, \tag{3.2}$$

$$\frac{\partial^2 Z}{\partial z^2}-\lambda^2 Z = \frac{1}{\alpha}\frac{\partial Z}{\partial t}, \tag{3.3}$$

where λ is a positive parameter.

Outside the conductor corresponding solutions of the same form are obtained by putting $\kappa = 0$ (i.e. $\alpha = \infty$), giving

$$W = Ce^{\pm\lambda z}P(x,y), \tag{3.4}$$

where C is a function of t only.

4. Solutions of magnetic type

Taking $\mathbf{B} = \operatorname{curl}\operatorname{curl}(\mathbf{k}W)$, where W is defined by (3.1) or (3.4), we get

$$\mathbf{B} = \left(\frac{\partial Z}{\partial z}\frac{\partial P}{\partial x}, \frac{\partial Z}{\partial z}\frac{\partial P}{\partial y}, \lambda^2 ZP\right) \quad (z > 0), \tag{4.1}$$

$$\mathbf{B} = Ae^{-\lambda z}\left(\frac{\partial P}{\partial x}, \frac{\partial P}{\partial y}, -\lambda P\right) + Be^{\lambda z}\left(\frac{\partial P}{\partial x}, \frac{\partial P}{\partial y}, \lambda P\right),$$

$$= \operatorname{grad}(Ae^{-\lambda z}+Be^{\lambda z})P \quad (z < 0), \tag{4.2}$$

where A and B are functions of t only.

Corresponding values of the electric field, derived from (1.2) and (1.1) respectively, are

$$\mathbf{E} = -\frac{1}{c}\frac{\partial Z}{\partial t}\left(\frac{\partial P}{\partial y}, -\frac{\partial P}{\partial x}, 0\right) \quad (z > 0), \tag{4.3}$$

$$\mathbf{E} = \frac{1}{c\lambda}\left(\frac{dA}{dt}e^{-\lambda z} - \frac{dB}{dt}e^{\lambda z}\right)\left(\frac{\partial P}{\partial y}, -\frac{\partial P}{\partial x}, 0\right) + \operatorname{grad}\psi \quad (z < 0), \tag{4.4}$$

where ψ is an arbitrary potential function.

The boundary conditions for H_x, H_y, B_z at $z = 0$ yield

$$A(t)+B(t) = \frac{1}{\mu}\left(\frac{\partial Z}{\partial z}\right)_0, \tag{4.5}$$

$$A(t)-B(t) = -\lambda(Z)_0 \tag{4.6}$$

and, eliminating $B(t)$,

$$\frac{1}{\mu}\left(\frac{\partial Z}{\partial z}\right)_0 - \lambda(Z)_0 = 2A(t). \tag{4.7}$$

Examination of (4.2) indicates that the term with exponent $(-\lambda z)$, which tends to zero as z tends to infinity, may be interpreted as an inducing magnetic field, the term with exponent λz being the induced field. For a given problem, where $A(t)$ is a known function of t, (4.7), together with the physical requirement that Z tends to zero as z tends to infinity, may be regarded as leading to a unique solution of (3.3). It also follows that (4.6) ensures the continuity of E_x, E_y at $z = 0$, provided that there $\operatorname{grad}\psi$ has at most a normal component and hence corresponds to some electric charge distribution in equilibrium on the boundary. Apart from this case, which corresponds to a superimposed electrostatic problem, ψ can be taken as zero.

In order to solve a given induction problem by the method described above it is first necessary to express the inducing potential in the form of a sum (or integral) of expressions of the type

$$Ce^{-\lambda z}P(x,y).$$

This can always be done, in principle, at least, by means of Fourier analysis. For example, the potential of a unit pole can be expressed in this form by means of the well-known result

$$(z^2+r^2)^{-\frac{1}{2}} = \int\limits_0^\infty e^{-\lambda z}J_0(\lambda r)\,d\lambda.$$

5. Solutions of electric type

In exactly the same way, starting with $\mathbf{E} = \operatorname{curl}\operatorname{curl}(\mathbf{k}W)$,

$$\mathbf{E} = \left(\frac{\partial Z}{\partial z}\frac{\partial P}{\partial x}, \frac{\partial Z}{\partial z}\frac{\partial P}{\partial y}, \lambda^2 ZP\right) \quad (z > 0), \tag{5.1}$$

$$\begin{aligned}\mathbf{E} &= Ae^{-\lambda z}\left(\frac{\partial P}{\partial x}, \frac{\partial P}{\partial y}, -\lambda P\right) + Be^{\lambda z}\left(\frac{\partial P}{\partial x}, \frac{\partial P}{\partial y}, \lambda P\right) \\ &= \operatorname{grad}\{(Ae^{-\lambda z}+Be^{\lambda z})P\} \quad (z < 0),\end{aligned} \tag{5.2}$$

the corresponding values for the magnetic field being

$$\mathbf{B} = \frac{c}{\alpha} Z\left(\frac{\partial P}{\partial y}, -\frac{\partial P}{\partial x}, 0\right) \quad (z > 0), \tag{5.3}$$

$$\mathbf{B} = \frac{1}{c\lambda}\left(-\frac{dA}{dt}e^{-\lambda z}+\frac{dB}{dt}e^{\lambda z}\right)\left(\frac{\partial P}{\partial y}, -\frac{\partial P}{\partial x}, 0\right)+\operatorname{grad}\psi \quad (z < 0) \tag{5.4}$$

where ψ is an arbitrary potential function.

In deriving (5.4), in order to maintain the symmetry between the two types of solution, the accurate equation

$$\operatorname{curl}\mathbf{B} = \frac{1}{c}\frac{\partial \mathbf{E}}{\partial t}$$

has been used in place of $\operatorname{curl}\mathbf{B} = 0$.

The boundary conditions for both **E** and **B** are all satisfied if we take $\psi = 0$ and

$$A(t)+B(t) = \left(\frac{\partial Z}{\partial z}\right)_0, \tag{5.5}$$

$$\frac{dA}{dt}-\frac{dB}{dt} = -4\pi\lambda\kappa(Z)_0. \tag{5.6}$$

This second type of solution is seen to correspond to the induction of currents by an external electric field. Since κ is large, equation (5.6) indicates that $(Z)_0$ is very small and (5.5) then indicates that under ordinary circumstances $A(t) \sim -B(t)$.

The associated electric surface charge is given by

$$\frac{d\sigma}{dt} = -i_z = -\kappa E_z = -\kappa\lambda^2(Z)_0 P, \tag{5.7}$$

where i_z and E_z are the normal components of the current and field inside the conductor at the surface $z = 0$.

6. Reduction to a problem in heat conduction

The formal resemblance of equation (1.5) to that governing heat conduction has often been noted and, in some simple cases, known solutions of heat conduction problems have been applied to those in electromagnetic induction, but in general the boundary conditions of an induction problem have no counterpart in heat conduction. For the type of solution considered in section 4, however, it will now be shown that a complete analogy does exist.

According to section 4, the currents in a conductor due to an inducing field which is derivable from a magnetic potential

$$\Omega = -Ae^{-\lambda z}P(x, y), \tag{6.1}$$

can be expressed in terms of a function $Z(z, t)$ which satisfies

$$\frac{\partial^2 Z}{\partial z^2} - \lambda^2 Z = \frac{1}{\alpha}\frac{\partial Z}{\partial t} \quad (z > 0), \tag{6.2}$$

while at the boundary $z = 0$,

$$\frac{\partial Z}{\partial z} - \mu\lambda Z = 2\mu A(t). \tag{6.3}$$

There is the further requirement that Z should tend to zero as z tends to infinity.

Making the substitution $\qquad Z = Ye^{-\lambda^2\alpha t}, \qquad (6.4)$

we have to satisfy

$$\frac{\partial^2 Y}{\partial z^2} = \frac{1}{\alpha}\frac{\partial Y}{\partial t}, \tag{6.5}$$

with

$$\frac{\partial Y}{\partial z} - \mu\lambda Y = 2\mu e^{\lambda^2\alpha t} A(t), \tag{6.6}$$

at $z = 0$.

Equations (6.5) and (6.6) have the same form as the corresponding ones in problems of heat flow in one dimension in a semi-infinite conductor, where the temperature T satisfies the equation

$$\frac{\partial^2 T}{\partial z^2} = \frac{1}{\kappa}\frac{\partial T}{\partial t},$$

κ being the diffusivity.

For radiation at the surface into a medium at temperature $f(t)$, there is the surface condition

$$\frac{\partial T}{\partial z} - hT = -hf(t),$$

where h is a constant related to the emissivity of the conductor. Solutions of a variety of problems of this type are known (see, for example, Carslaw and Jaeger (**3**)). It may also be noted, in passing, that the general question of heat conduction in a semi-infinite conductor (i.e. not limited to one-dimensional flow) can be treated by the methods described above.

A slightly different procedure will now be adopted which has the advantage that it can be modified to cover the electric case as well. Consider the function U defined by

$$U = \frac{\partial Y}{\partial z} - \mu\lambda Y. \tag{6.7}$$

This satisfies the same equation as Y, namely (6.5), throughout the conductor and its value is given over the boundary by (6.6). We can therefore identify U with the temperature of a conductor whose surface temperature is prescribed.

If we assume that there are no residual currents in the conductor other than those due to (6.1) we can now write down immediately

$$U = \frac{\partial Y}{\partial z} - \mu\lambda Y = \frac{4\mu}{\sqrt{\pi}} \int_0^\infty A\left(t - \frac{z^2}{4\alpha u^2}\right) e^{\alpha\lambda^2\{t-(z^2/4\alpha u^2)\}} e^{-u^2}\, du, \tag{6.8}$$

which is seen to satisfy all the requirements of the problem (cf. (**3**), p. 44, equation (1). The lower limit there is modified, however, since $A(t)$ is not necessarily zero prior to $t = 0$.)

An example of some interest is the sudden creation of a magnetic field outside the conductor. Taking Heaviside's unit function $H(t)$ for $A(t)$, (6.8) becomes, when use is made of (6.4),

$$\frac{\partial Z}{\partial z} - \mu\lambda Z = \frac{4\mu}{\sqrt{\pi}} \int_\beta^\infty e^{-u^2-(\lambda^2 z^2/4u^2)}\, du, \quad \text{where} \quad \beta = \tfrac{1}{2}z(\alpha t)^{-\frac{1}{2}}. \tag{6.9}$$

The evaluation of the current given by (4.3) is quite simple since it involves $\partial Z/\partial t$ only, and differentiation of (6.9) with respect to t gives for $\partial Z/\partial t$ the linear first-order equation

$$\frac{\partial}{\partial z}\left(\frac{\partial Z}{\partial z}\right) - \mu\lambda\left(\frac{\partial Z}{\partial t}\right) = \frac{2z}{\kappa c}\left(\frac{\mu\kappa}{t}\right)^{\frac{3}{2}} e^{-\lambda^2\alpha t-(z^2/4\alpha t)}. \tag{6.10}$$

7. Free decay of a 'magnetic' current system

In order to deal with the decay of a magnetic system of currents under the action of its own field it is necessary to put $A(t) = 0$ in (6.6). We require then the solution of

$$\frac{\partial^2 Y}{\partial z^2} = \frac{1}{\alpha}\frac{\partial Y}{\partial t}, \tag{7.1}$$

for which

$$\frac{\partial Y}{\partial z} - \mu\lambda Y = 0, \tag{7.2}$$

at $z = 0$. The heat analogue will be the decay of temperature in a semi-infinite conductor whose plane boundary is maintained at zero temperature.

The general solution of (7.1) subject to (7.2) is well known and is given by

$$\frac{\partial Y}{\partial z} - \mu\lambda Y = \int_0^\infty F(\phi)\sin(\phi z) e^{-\phi^2\alpha t}\, d\phi,$$

where $F(\phi)$ is arbitrary. Using (6.4) this becomes

$$\frac{\partial Z}{\partial z} - \mu\lambda Z = \int_0^\infty F(\phi)\sin(\phi z) e^{-(\phi^2+\lambda^2)\alpha t}\, d\phi. \tag{7.3}$$

Solving for Z, we obtain

$$Z = -\int\limits_0^\infty F(\phi)\frac{\phi\cos\phi z+\mu\lambda\sin\phi z}{\phi^2+\lambda^2\mu^2}e^{-(\phi^2+\lambda^2)\alpha t}\,d\phi, \tag{7.4}$$

the complementary function (which involves $e^{\lambda\mu z}$) being rejected since it increases indefinitely with increasing z. The free modes, defined by

$$Z = (\phi\cos\phi z+\mu\lambda\sin\phi z)e^{-(\phi^2+\lambda^2)\alpha t}, \tag{7.5}$$

are immediately evident.

The free decay of a current system, which is everywhere defined at $t = 0$, can now be investigated. Let the value of $Z(z,t)$ at $t = 0$ be denoted by Z_0. Then, according to (7.3), $F(\phi)$ is to be determined from the integral equation

$$\frac{dZ_0}{dz}-\mu\lambda Z_0 = \int\limits_0^\infty F(\phi)\sin\phi z\,d\phi.$$

Inverting this by Fourier's integral theorem we get

$$F(\phi) = \frac{1}{\pi}\int\limits_0^\infty\left(\frac{dZ_0}{dz}-\mu\lambda Z_0\right)\sin\phi z\,dz$$

$$= -\frac{1}{\pi}\int\limits_0^\infty(\phi\cos\phi z+\mu\lambda\sin\phi z)Z_0\,dz,$$

provided Z vanishes at $z = \infty$.

If, instead of Z, $\partial Z/\partial t$ is given at $t = 0$, we can proceed in exactly the same way.

It is instructive here to consider again the case of the sudden creation of a magnetic field outside the conductor. It is tacitly assumed in neglecting displacement current that the time rate of change of the fields is sufficiently small, since it is the term involving $\partial\mathbf{E}/\partial t$ that is neglected in equation (1.2). Sudden creation of fields violates this initial assumption and the sudden appearance of surface currents in the magnetic case and surface charges in the electric case is the price we have to pay. Once these surface distributions have come into being, however, they ensure that subsequent changes proceed sufficiently slowly for the initial assumptions to be valid. It should also be noted in this connexion that the parameter ϕ in (7.5) must not be too large and that in integrals like (7.4) we rely on their rapid convergence to make contributions from large values of ϕ relatively unimportant.

Consider then the inducing field

$$\mathbf{H} = e^{-\lambda z}\left(\frac{\partial P}{\partial x}, \frac{\partial P}{\partial y}, -\lambda P\right) \quad (t \geqslant 0),$$

suddenly applied at $t = 0$. It is well known that under these circumstances a surface current is instantaneously set up on the face of the conductor so as to completely shield the inside of the conductor from the applied field. The density per unit area of this current is given by

$$i_x = \frac{1}{2\pi}H_y; \qquad i_y = -\frac{1}{2\pi}H_x.$$

A much clearer picture of this process is obtained if the external field is regarded as approaching the conductor with a very large velocity in the form of a travelling discontinuity, on either side of which the magnetic field can be represented as the gradient of some scalar. Equation (1.1) then indicates that the electric field is everywhere zero except at the discontinuity, where it is infinite. It is this infinite electric field which produces the surface current on the conductor. Thereafter we can regard the field as completely reflected so as to set up the initial induced field

$$\mathbf{H} = e^{\lambda z}\left(\frac{\partial P}{\partial x}, \frac{\partial P}{\partial y}, \lambda P\right).$$

The surface current now diffuses into the conductor and we have a case of free decay. When the current has everywhere decayed to zero, however, there remains a stationary induced magnetic field

$$\mathbf{H} = \frac{1-\mu}{1+\mu}e^{\lambda z}\left(\frac{\partial P}{\partial x}, \frac{\partial P}{\partial y}, \lambda P\right)$$

outside the conductor, and a field

$$\mathbf{B} = \frac{2\mu}{1+\mu}e^{-\lambda z}\left(\frac{\partial P}{\partial x}, \frac{\partial P}{\partial y}, -\lambda P\right)$$

inside, so that ultimately

$$Z = -\frac{1}{\lambda}\frac{2\mu}{\mu+1}e^{-\lambda z},$$

and

$$\frac{dZ}{dz} - \lambda\mu Z = 2\mu e^{-\lambda z}.$$

Putting

$$\frac{\partial Z}{\partial z} - \lambda\mu Z = 2\mu e^{-\lambda z} + \int_0^\infty F(\phi)\sin(\phi z)e^{-(\phi^2+\lambda^2)\alpha t}\,d\phi, \tag{7.6}$$

and noting that at $t = 0$, Z vanishes identically throughout the conductor, we have

$$\int_0^\infty F(\phi)\sin\phi z\,d\phi = -2\mu e^{-\lambda z},$$

of which the solution is

$$F(\phi) = -\frac{4\mu}{\pi}\frac{\phi}{\phi^2+\lambda^2}.$$

Substituting this into (7.6) and solving for Z gives finally

$$Z = -\frac{1}{\lambda}\frac{2\mu}{\mu+1}e^{-\lambda z}+\frac{4\mu}{\pi}\int\limits_0^\infty \frac{\phi\cos(\phi z)+\lambda\mu\sin(\phi z)}{(\phi^2+\lambda^2)(\phi^2+\lambda^2\mu^2)}e^{-(\phi^2+\lambda^2)\alpha t}\phi\, d\phi.$$

If (7.6) is differentiated with respect to t, the equation (6.10) is again obtained after some reduction.

It has now been shown in this section that the decay of a given current system can be described in terms of a function $Z(z,t)$ whose initial value Z_0 is everywhere given. If

$$\frac{dZ_0}{dz}-\lambda\mu Z_0 = 0,$$

the process is straightforward since the magnetic field as well as the current system decays completely. Such a state of affairs could be brought about either by internal causes or by an external magnetic field which ceases to change as it passes through the value zero.

If, on the other hand,

$$\frac{dZ_0}{dz}-\lambda\mu Z_0 \neq 0,$$

there is a permanent residual magnetic field which must be taken into account in calculating the decay of the current system. This state of affairs can only correspond to an external field which ceases to change at $t = 0$, maintaining its non-zero value subsequent to $t = 0$. Sudden changes in the external field and the accompanying surface charge can be treated either by the methods of this section or as special cases in section 6.

Finally it will be pointed out that the free modes given by (7.5) also apply to a conducting slab occupying the region $0 < z < 2h$. In place of an unrestricted continuous range of values, however, ϕ is limited to the discrete set defined by

$$\phi\tan(\phi h) = \mu\lambda.$$

8. Induction of currents by external electric fields

Elimination of $B(t)$ from equations (5.5) and (5.6) indicates that, for the electric case, solutions of (3.3) are required subject to

$$\frac{\partial^2 Z}{\partial z\partial t}-4\pi\kappa\lambda Z = 2\frac{dA}{dt} \tag{8.1}$$

at the boundary $z = 0$. The surface charge given by (5.7) becomes, with the aid of (8.1),

$$\sigma = \frac{\lambda P}{2\pi}\left\{A(t)-\frac{1}{2}\left(\frac{\partial Z}{\partial z}\right)_0\right\}. \tag{8.2}$$

The method of section 6 leads to

$$\frac{\partial^2 Z}{\partial z \partial t} - 4\pi\kappa\lambda Z = \frac{4\mu}{\sqrt{\pi}} \int\limits_0^\infty A'\left(t - \frac{z^2}{4\alpha u^2}\right) e^{-(\lambda^2 z^2/4\alpha u^2)-u^2}\, du,$$

where the dash denotes differentiation with respect to t.

Since κ is large even for only moderately good conductors, for external fields which do not vary too rapidly, to a high degree of accuracy this reduces to

$$Z = -\frac{\mu}{\pi^{\frac{3}{2}}\kappa\lambda} \int\limits_0^\infty A'\left(t - \frac{z^2}{4\alpha u^2}\right) e^{-(\lambda^2 z^2/4\alpha u^2)-u^2}\, du, \tag{8.3}$$

with
$$\sigma = \frac{\lambda P}{2\pi} A(t). \tag{8.4}$$

Thus the electric field inside the conductor is very small, but this is not true of the current.

Equation (8.3) is unsuitable for dealing with sudden changes in the external electric field, which require special treatment. The remarks of section 7 in connexion with sudden changes in external magnetic fields are also applicable here. Introducing again the idea of a travelling electric field, the associated magnetic field is everywhere zero except at the electric wavefront, in which it lies. The penetration of the electric field alone into the conductor can only set up a finite current system and cannot lead to an instantaneous surface charge. On the other hand, in the infinite magnetic field carried along by the electric wavefront, we have an agent capable of producing the infinite current 'loops' at the surface necessary to bring such a charge into existence, and the arrival of the electric field is accompanied instantaneously by just that surface charge which prevents further penetration of the fields into the conductor. It is important to notice that the redistribution of surface charge which takes place is not due to a surface current, but to a system of current 'loops' confined to the surface layer of the conductor, the flow being normal at the surface. As such, this behaviour differs from that shown by equation (8.3), where there is appreciable current flow at a finite depth below the boundary.

Up to this point the electric and magnetic cases are completely complementary. In the magnetic case, however, the initial surface current diffuses into the interior of the conductor and, in due course, the incident magnetic field is able to penetrate. In the electric case, on the other hand, the surface charge remains, since a conductor cannot sustain an internal stationary electric field.

9. Free decay of an 'electric' current system

Putting $dA/dt = 0$ in (8.1), we find that the equation governing free decay is

$$\frac{\partial^2 Y}{\partial z^2} = \frac{1}{\alpha}\frac{\partial Y}{\partial t}, \tag{9.1}$$

subject to

$$\frac{\partial^2 Z}{\partial z \partial t} - 4\pi\kappa\lambda Z = 0, \tag{9.2}$$

at the boundary $z = 0$.

Proceeding as in section 7, the general solution can be written

$$\frac{\partial^2 Z}{\partial z \partial t} - 4\pi\kappa\lambda Z = \int\limits_0^\infty F(\phi)\sin(\phi z)e^{-(\phi^2+\lambda^2)\alpha t}\, d\phi, \tag{9.3}$$

or

$$Z = -\int\limits_0^\infty F(\phi)\frac{4\pi\kappa\lambda\sin(\phi z) - \beta\phi\cos(\phi z)}{\beta^2\phi^2 + (4\pi\kappa\lambda)^2} e^{-(\phi^2+\lambda^2)\alpha t}\, d\phi,$$

where $\beta = (\phi^2+\lambda^2)\alpha$.

The free modes of decay defined by

$$Z = \left(\sin(\phi z) - \frac{\beta\phi}{4\pi\kappa\lambda}\cos(\phi z)\right)e^{-\beta t},$$

are immediately evident.

To the same order of accuracy as was adopted in the magnetic case, the situation is much simplified, since a solution of (9.1) is required which vanishes at $z = 0$ (i.e. only the term $4\pi\kappa\lambda Z$ is retained in (9.2)). This can either be written down as a simple modification of (9.3), or can be exhibited in the equivalent form ((**3**), pp. 34 and 40),

$$Y = \frac{1}{\sqrt{\pi}}\int\limits_{-\infty}^{+\infty} F(z+2(\alpha t)^{\frac{1}{2}}u)e^{-u^2}\, du,$$

where $F(z)$ is an odd function of z. It is easy to verify that Y reduces to $F(z)$ when $t = 0$.

It follows that any choice of an odd function $F(z)$ will lead to some freely decaying system; for example,

$$F(z) = \sin(\phi z)$$

gives

$$Z = e^{-(\phi^2+\lambda^2)\alpha t}\sin(\phi z),$$

which corresponds to the free modes of decay.

Another example is $\quad F(z) = ze^{-\pi\mu\kappa b z^2/c^2},$

which leads to

$$Z = (1+bt)^{-\frac{3}{2}}e^{-\lambda^2 c^2 t/4\pi\mu\kappa}ze^{-\pi\kappa\mu b z^2/(1+bt)}.$$

At any time t, Z has a maximum at a depth given by

$$z = \left\{\frac{c^2(1+bt)}{2\pi\mu\kappa b}\right\}^{\frac{1}{2}},$$

which maximum moves progressively into the conductor.

The magnetic and electric cases have so far been considered separately. By expressing an arbitrary non-divergent current system in the form of a triple Fourier integral, it is not difficult to decompose it into constituent electric and magnetic parts, so that, in principle at least, its decay can be described by the above methods. If the separate parts do not automatically satisfy the necessary relations at the surface, the work will of necessity be complicated by possible surface charges and currents and permanent external fields.

10. Conclusion

Inducing fields that have already received fairly detailed treatment are those produced by (*a*) an infinite straight alternating current filament (Price (**1**)) and (*b*) an alternating magnetic dipole and a circular alternating current filament (Gordon (**4**)). In these, however, attention is mainly confined to the external induced field (the latter can be determined by means of (4.6) or (5.6) once $Z(z,t)$ has been found).

Another class of problems that can be solved fairly easily involves isolated magnetic poles or electric charges in uniform motion perpendicular or parallel to the surface of the conductor.

REFERENCES

1. A. T. Price, *Quart. J. Mech. and Applied Math.* **3** (1950), 385.
2. J. A. Stratton, *Electromagnetic Theory*, McGraw-Hill (1941).
3. H. S. Carslaw and J. C. Jaeger, *Conduction of Heat in Solids*, Oxford (1947).
4. A. N. Gordon, *Quart. J. Mech. and Applied Math.* preceding paper.

ely.
of
ent
be
ally
be
ent

are
nent
ting
inly
by

lves
ular

47).

THE QUARTERLY JOURNAL OF MECHANICS AND APPLIED MATHEMATICS

VOLUME IV PART 1 MARCH 1951

CONTENTS

CS

951

1

23

29

42

54

78

5

4

6

6